ABSTRACT

JETT, PAUL MICHAEL. A Comparison of Two Modeled Syngas Cleanup Systems and Their Integration with Selected Fuel Synthesis Processes. (Under the direction of Drs. Stephen Kelley and Hasan Jameel.)

Synthesis gas (syngas) cleanup is a required operation in most gas-to-liquids (GTL) processes. Cleanup typically involves removal of syngas tars, ammonia, and sulfur compounds such as H_2S. An ASPEN-modeled novel catalytic cleanup process from the Research Triangle Institute (RTI) was evaluated against traditional gas-cleanup operations utilized in the National Renewable Energy Laboratory's (NREL) thermochemical ethanol from indirect gasification of lignocellulosic biomass model.

In preparation for evaluation and comparison of the two cleanup technologies in question, the NREL thermochemical ethanol model was run in ASPEN Plus 2004.1 with a selection of ten biomasses to determine its robustness and response to a range of variable feedstock O/C ratios. The NREL model was able to run to completion with feedstocks varying in O/C ratio from 0.29 for lignite to 0.66 for sugarcane bagasse. Extensive examination of the NREL model revealed that while it was able to operate across a range of biomass feedstocks, its use as a predictive tool is limited due to the incorporation of empirical reaction yields and the lack of kinetic reaction modeling.

The catalytic tar reforming, quench, and amine scrubbing syngas cleanup section of the NREL model was converted to standalone operation and tested for response to variable

syngas feedstocks derived from the biomasses run in the gasifier section of the full NREL mixed alcohols model. An ASPENOne v7.1 model of the RTI Therminator cleanup process was modified to have input/output stream temperature and pressure conditions comparable to those of the NREL model, and also "exercised" with variable syngas compositions in a similar manner. Performance comparisons were made between the two cleanup systems, indicating that as modeled, the RTI Therminator technology is capable of tar, ammonia, and sulfur reduction similar to that of the baseline NREL system. The Therminator cleanup system did not reform lighter hydrocarbons such as methane or ethane, which resulted in a 10% and 74% lower CO and H_2 composition in the cleaned syngas respectively.

Subsequent fuel synthesis impacts from syngas treatment with the NREL and RTI cleanup technologies were evaluated as well, utilizing the catalytic mixed alcohols synthesis section isolated from the NREL model and a single-step catalytic dimethyl ether (DME) synthesis process modeled in ASPEN with Langmuir-Hinshelwood-Hougen-Watson (LHHW) kinetics. The LHHW reaction kinetics based DME synthesis model was evaluated against literature results for response to feed pressure, temperature, and reactant composition, and was found to have acceptable response.

The cleanup system material and energy impact evaluations were carried out with syngases derived from the default NREL biomass feedstock of hybrid poplar, treated with each cleanup technology, both with and without synthesis process recycle loops. Results from both synthesis pathways were similar, indicating that the reduced CO and H_2 composition of the RTI Therminator-cleaned syngas resulted in lower synthesis product

yields, a 33% and 48% reduction for mixed alcohols and DME respectively for non-recycle conditions. Methanol recycle in the mixed alcohols model and unreacted syngas recycle in the DME model generally narrowed the synthesis production penalty for reduced syngas H_2 from the RTI Therminator cleanup process. Process energy usage directly correlated with synthesis production.

A Comparison of Two Modeled Syngas Cleanup Systems and Their Integration with Selected Fuel Synthesis Processes

by
Paul Michael Jett

A thesis submitted to the Graduate Faculty of
North Carolina State University
in partial fulfillment of the
requirements for the Degree of
Master of Science

Forest Biomaterials

Raleigh, North Carolina

2011

APPROVED BY:

Dr. Richard Venditti

Dr. Stephen Kelley
Co-Chair of Advisory Committee

Dr. Hasan Jameel
Co-Chair of Advisory Committee

DEDICATION

This thesis is dedicated to my family. I am grateful for their unwavering love and support.

BIOGRAPHY

Paul Michael Jett was born in Raleigh, NC. He attended North Carolina State University, graduating in 1997 with a Bachelor of Science in Pulp and Paper Technology. After working in several paper mills in the southern US, he returned to NCSU in 2003 to work in the Cooperative Tree Improvement Program in the College of Natural Resources. In the fall of 2008, after 3 years of stay-at-home fatherhood, he returned to the NCSU Forest Biomaterials Department to pursue a Masters degree under the direction of Drs. Stephen Kelley and Hasan Jameel. Michael is currently living in Clayton, NC with his wife Janice, two children, and two cats.

ACKNOWLEDGEMENTS

I wish to express my sincere gratitude to my advisors Dr. Stephen Kelley and Dr. Hasan Jameel. Their patient guidance has been invaluable during my time in the Forest Biomaterials Department.

I would also like to thank Drs. Ranjeeth Kalluri, Atish Kataria, and David Dayton of the Research Triangle Institute for allowing me to work with them, and for providing crucial input on the Therminator process. Thanks also goes to Stephen Phillips of the National Renewable Energy Laboratory for his advice on the NREL thermochemical mixed alcohols model, and to Dr. William L. Luyben and Patrick Robinson of Lehigh University for elucidating LHHW kinetics in ASPEN.

Finally, thanks to my officemates for their humor and shared experiences.

TABLE OF CONTENTS

LIST OF TABLES

LIST OF FIGURES

CHAPTER 1

Gasification and Syngas Cleanup Background

1.1 Gasification History

Mankind has utilized fire and carbonaceous fuels for thousands of years for heating, whether for food, warmth, or altering other materials. In most parts of the world wood or coal are used daily as a source of heat or power in domestic and industrial applications. Historically, these solid fuels would be used in a direct combustion process, where the fuel materials would be completely oxidized in the presence of air to liberate heat, carbon dioxide, and water vapor.

This fundamental process changed in 1665 when it was realized that a gas could be produced from coal by heating it in an oxygen deficient atmosphere. (Ahrenfeldt and Knoef 2005) By the late 18^{th} century commercial coal gasification had been developed. Processing facilities called gasworks would indirectly heat (pyrolyze) coal in sealed coke ovens, yielding a medium-high energy density "producer gas" (20-23 MJ/m^3) suitable for lighting applications, and coke that could be used as solid fuel. (Reed 2002; Ahrenfeldt and Knoef 2005; Basu 2006; Higman, van der Burgt et al. 2008) Improvements in materials of construction led to higher temperature coke oven designs, and coupled with the introduction of steam to the coke furnace chamber, allowed for the wide spread production of a medium

energy density “blue water-gas” or “town gas”. Where the original producer gas contained hydrogen, carbon monoxide, and coal volatiles; the composition of town gas was very similar to the modern concept of syngas: primarily hydrogen and carbon monoxide, with an approximate energy content of 12MJ/m^3. Town gas derived from coal gasification was initially used for lighting and domestic cooking, and finally for space heating as technology improved and gas prices fell. (Higman, van der Burgt et al. 2008)

Experiments to operate spark ignition engines with producer gas were attempted around 1880, and small scale coal and biomass gasification units were used to fuel many types of engine operated equipment through World War II. The high demand, and subsequent scarcity of liquid transportation fuels during both World Wars led to a proliferation of smaller coal and biomass gasifiers. (LaFontaine and Zimmerman 1989; Ahrenfeldt and Knoef 2005) At the height of World War II, there were approximately one million biomass, charcoal, or coal gasifier powered motor vehicles in use in Europe. Axis controlled countries, among them Germany, Italy, and France, accounted for the majority of small-scale gasifier installations used in both motor vehicles and tractors. (Egloff and Van Arsdell 1943) Germany had over 75 years of research and experience in coal and biomass gasification by 1942. Between the world wars, Germany conducted a great deal of research into fuel and industrial chemical self-sufficiency. Significant reserves of coal in the Ruhr region of Germany, prevailing opinions in the 1920’s of crude oil’s imminent disappearance, and a self-sufficiency push from the Nazi government in the early 1930’s provided the impetus for the development of new technologies such as Winkler and Lurgi gasifiers. In

turn, these new processes created the need for innovative chemical engineering techniques including coal liquefaction and catalytic fuel synthesis. (Ludewig 1966; Steynberg and Dry 2004; Davis and Occelli 2007) Coke gasification became a significant feedstock for production of chemical products and intermediates, starting with dyestuff experiments in the gasworks of Badische Anilin und Soda Fabrik (now BASF) (Ludewig 1966), and with fuel synthesis experiments of Franz Fischer, Max Tropsch, Ruhrchemie A.G. and others through the 1920's and 30's. Synthetic motor fuels, lubricating oils, and an array of industrial chemicals were produced in Germany from coke gasification. (Golumbic 1946)

Germany's coal/coke gasification and fuel synthesis research was foundational to research and commercial develop efforts worldwide. The United States Bureau of Mines jumpstarted its previous research work by conducting thorough inspections of German gasification and synthesis facilities, as well as interrogations of technical personnel at the end of World War II. (Golumbic 1946; Weil and Lane 1948; Davis and Occelli 2007) In 1950, the Suid Afrikaanse Sinteriese Olie Limited (SASOL) Company was formed to realize the South African government's goal of fuel independence. SASOL employed coal gasification technology from Lurgi Gesellschaft, the Fischer-Tropsch gas-to-liquids processes from Ruhrchemie AG, and plant engineering from the US company M.W. Kellogg. (Mako 1984) SASOL's production of synthetic fuels, lubricants, and industrial chemicals from gasified coal began in 1955, expanding capacity over the years to a 2009 annual fuel production rate of 7.1 million tonnes. (Sasol 2009)

With the exception of SASOL, commercial interest in coal or biomass gasification for fuel synthesis was absent until the mid-1970's following the OPEC oil embargo. Texaco began research into coal gasification in 1948 and built a demonstration plant in 1957. It was not until 1978 that a pilot scale facility was brought online. (Schlinger 1984) In a manner similar to that around each World War, concerns of crude oil scarcity and political unrest prompted researchers and engineers to actively pursue new projects. Indeed, many demonstration, pilot, or small industrial scale coal gasifiers were brought online between the onset of the energy crisis in 1973 and the early 1980's. In addition to Texaco's pilot gasification plant, designs by Shell, Combustion Engineering, British Gas/Lurgi, Koppers/Babcock & Wilcox, Davy AG, Foster-Wheeler, and others came online as a response to global concerns about the availability and cost of petroleum. (Meyers 1984)

Although concerns over global energy stability led to a flurry of research and investment in the 1970's, by the mid 1980's a glut of low cost crude oil reduced all energy prices to the point that new gasification capacity was no longer being added. OPEC export revenues were at a minimum from 1986 until about 1999. (EIA 2010) Figure 1 illustrates the world's gasification capacity from the 1970's through the present, showing that during periods of low oil prices and revenues, there was minimal interest in investing in new gasification facilities.

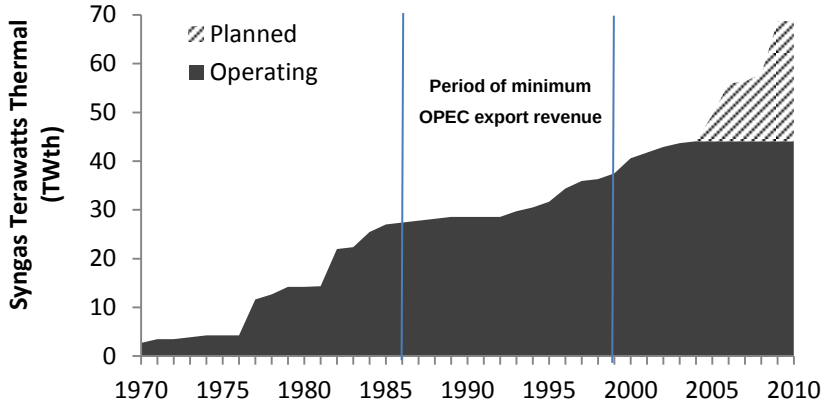

Figure 1. World gasification capacity, terawatts thermal. (Childress 2007)

Oil prices began to rise again in the late 1990's, and coupled with the uncertainty around Middle East stability following 9/11 and rapid industrialization of China and India, led to a renewed interest in gasification in the last decade. (Higman, van der Burgt et al. 2008) The spate of gasification technologies developed in the 70's and 80's that were halted at the demonstration phase are being reexamined following the sharp rise in oil and energy costs in advance of the 2008 economic downturn. Clean coal technologies have received significant political and public attention in recent years as a means to reduce the United States' energy independence. (DOE 2008) Integrated Gasification Combined Cycle (IGCC) plants are seen as a core technology for clean coal initiatives, as well as a more energy efficient means of power generation. (Basu 2006; Higman, van der Burgt et al. 2008) Additionally, when used for power production coal or biomass gasification also holds potential for carbon capture and storage. This in turn can serve to mitigate "carbon footprint" or life cycle analysis issues normally associated with combustion-based processes.

General Electric Energy acquired Texaco's gasification process in 2004, bringing together technologies that could foster IGCC large-scale commercial viability. (Basu 2006; Higman, van der Burgt et al. 2008) Similarly, gasification technology such as the entrained flow ConocoPhillips E-Gas system coupled with a GE Frame 7B gas turbine and suitable heat recovery steam generator (HRSG) offers the potential of state-of-the-art efficiency and cleaner coal-based energy. (Geosits and Schmoe 2005; ConocoPhillips 2010)

The Texaco gasification process has also been applied to industrial chemical synthesis from coal, exemplified by the Eastman Chemical Company of Kingsport, TN. (Zoeller 2009) Originally conceived following the 1970's petroleum shortage as a production pathway for their most energy intensive product, the Eastman "chemicals-from-coal" initiative utilized readily available Appalachian coal instead of natural gas and oil. (Eastman Company, Air Products and Chemicals 2003; Zoeller 2009) In 1983 two coal slurry-fired Texaco entrained flow gasifiers were brought online along with a Lurgi AG syngas-to-methanol plant and a rhodium-catalyzed acetic anhydride plant. (Zoeller, Agreda et al. 1992; Zoeller 2009) This production pathway proved to be reliable and financially sound enough to allow a facility expansion in 1991, and to date continues to produce high-value acetic anhydride product from coal-derived syngas. (Zoeller 2009)

1.2 Gasifier Technology Summary

Several hundred years of history has fostered the development of many different gasifier designs, following an evolution as process and engineering requirements necessitated improvements. Historic designs were simple modifications of existing furnace and boiler technology, with the development of improved materials, design, and control leading to more recent designs such as directly heated entrained flow or indirectly heated dual-circulating fluidized bed configurations. A brief summary of existing gasifier technologies, with attention to their designs and relative merits and applications follows.

1.2.1 Fixed Bed Gasifiers

Fixed bed gasifiers represent the original technology used for gasification (Ciferno and Marano 2002), and there are several variations that are differentiated by the location of oxidizer gas input and syngas extraction. Figure 2 shows some simple schematic representations of the two major fixed bed gasifier designs.

The updraft gasifier has the simplest reactor design, where fuel is introduced from the top and the product syngas travels up through the gasifier bed for top extraction. (Ahrenfeldt and Knoef 2005) The grate is placed at the bottom of the gasifier, with under-fire air to allow for combustion of the high carbon char residues at the grate level. Hot, slightly oxidative combustion gases travel countercurrently to the fuel, providing energy for gasification and pyrolysis reactions above the combustion zone. As the hot gases travel

toward the outlet the fuel bed is dried and preheated, allowing this gasifier design to more tolerant of wet biomass feedstocks. This flow pattern also allows gasification of high ash (high inorganic) feedstocks such as municipal solid waste (MSW), as any entrained ash particles tend to be filtered out traveling through the bed. (Ciferno and Marano 2002)

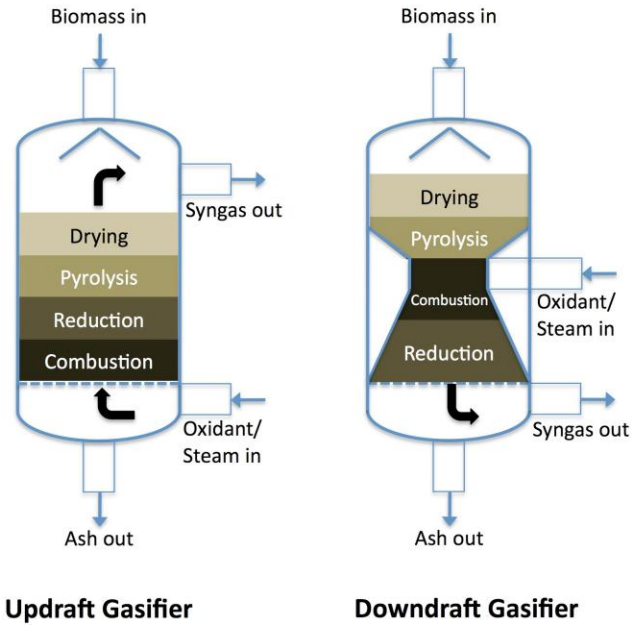

Figure 2. Schematic representation of the two major fixed bed gasifier designs. Based on diagrams from Baker 1986.

While the updraft gasifier gas flow allows for greater fuel flexibility, it comes at the expense of significantly increased tar production. Tars created during pyrolysis are swept out of the reactor without a chance to be cracked or combusted. The resulting tar content can constitute 10-20% by mass of the product syngas, and can require extensive cleaning, or constraint to direct combustion applications. (Ciferno and Marano 2002; Ahrenfeldt and

Knoef 2005) Lurgi or British Gas/Lurgi gasifiers are considered a variation of the updraft fixed bed design, modified for pressurization with lockhoppers on fuel inlet and ash/slag outlet, and scrubbers to capture tar. (NETL, Shelton et al. 2000; Lee, Speight et al. 2007)

Downdraft gasifiers were the next evolutionary step in design. The air inlet was placed nearer the middle of the reactor into an area of reduced diameter called the *throat*, and the syngas withdrawn underneath the bottom grate. (E4Tech 2009) The exothermic partial oxidation of the fuel occurs in the zone around the air inlet, leaving a char bed on the grate below in a reducing atmosphere suitable for gasification reactions. Because pyrolysis occurs above the air inlet and the syngas outlet, any tars generated are swept downward into the oxidizing zone and are cracked or combusted. As a result, the outlet syngas is much lower in tar and more suitable for use in engines or turbine combustion applications. (Reed 2002) The tradeoff for lower tar syngas is that ash created in the oxidation zone can be more easily entrained in the outlet syngas, possibly requiring downstream filtering to eliminate problems with ash deposition and corrosion. Furthermore, since there is little movement of heat upward through the feedstock, the downdraft design is less tolerant of wet fuel, and requires a feedstock of more consistent size. (Ahrenfeldt and Knoef 2005) As mentioned in the historical background section, downdraft gasifiers found widespread application during World War II, embodied in the French Imbert design. Modern downdraft gasifiers are still used in smaller installations for combined heat and power applications (CHP), and are even offered in micro scale for residential/hobbyist use. (Kwant and Knoef 2004; Babu 2005; Mason 2010)

Other specialized fixed bed gasifier configurations exist, including "open-core" downdraft and crossdraft. Open-core designs omit the throat restriction in the reactor, and are used with fine feedstocks that could pose bridging issues in typically constructed downdraft design. Crossdraft units are designed to utilize charcoal as a feedstock, and can be suitable for very small installations. (Ahrenfeldt and Knoef 2005)

1.2.2 Fluidized Bed Gasifiers

Due to their simplicity and modest capital and operating costs, fixed bed gasifiers are usually considered appropriate for relatively small-scale installations. (Maniatis 2008) Figure 3 provides a view of the relationship between gasifier design and the relative scales of different gasification technologies. For medium to large-scale coal or biomass gasification applications, fluidized bed gasifiers are typically employed. (Maniatis 2008)

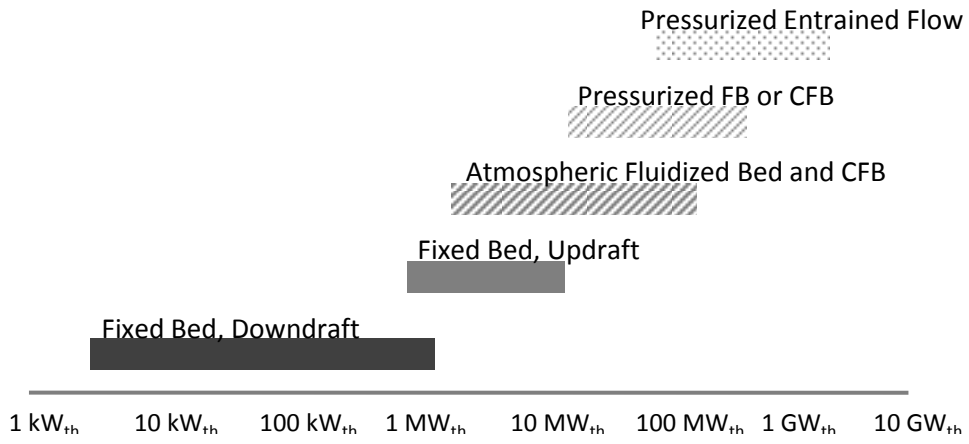

Figure 3. Approximate scale of fuel power for selected gasification technologies. Adapted from Rensfelt. (Rensfelt 2005)

Winkler of the I.G. Farbenindustrie AG company is credited with the development the first fluidized bed gasifier in 1922, for the gasification of coal. Winkler's design was capable of gasifying a wide range of coals, was scalable to large capacities, and over time was widely used, with approximately 70 commercial installations. (Bögner and Wintrup 1984; Basu 2006; Higman, van der Burgt et al. 2008) As effective as Winkler's fluidized bed design was, improvements were added over the years, yielding several different reactor technologies. While there are many subtle variations to the fluidized bed designs there are three relatively distinct classifications that can be identified. Descriptions of the differences between these classifications follow the overview schematics of fluidized and entrained flow gasifiers shown in Figure 4.

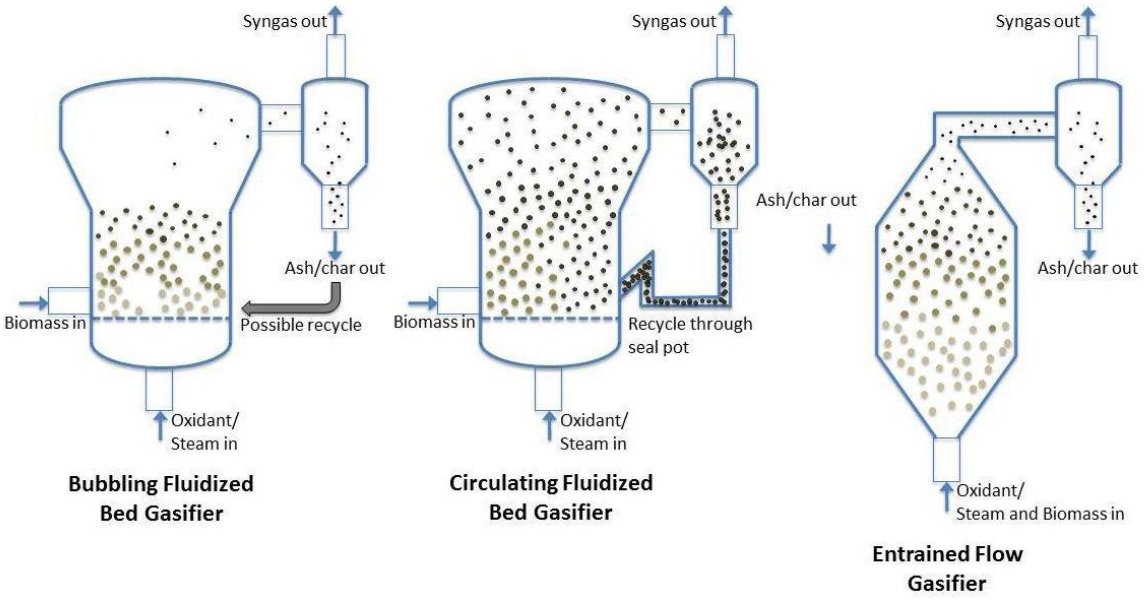

Figure 4. Simple schematic flow diagrams for fluidized and entrained flow gasifiers. Diagrams are modeled from Baker 1986 and Higman 2008.

Winkler's original coal gasifier is considered an atmospheric-pressure bubbling fluidized bed (BFB) system. The bubbling bed configuration utilizes a non-combustible, but not necessarily inert (olivine, for example, has some tar cracking catalytic activity) bed material to assist in maintaining rapid and uniform heat transfer. (Babu 2005; Basu 2006) Bed fluidization is typically accomplished by the input of air, oxygen, or steam into the bottom of the reactor through the bed grate. As the name suggests, a BFB configuration operates with a fluidizing velocity high enough to allow the bed to "boil," but not so high that the solids are swept out of bed and in the entrained in the product syngas. Typical fluidization velocities range between 1 to 3 m/s. (Basu 2006; Higman, van der Burgt et al. 2008) The utility of the bubbling bed design lies in its ability to gasify a wide range of fuels, with only moderate tar production and the potential for reliable operation. Reactor size requirements can be an issue with this technology, as reactor diameters must be sufficiently large enough to keep gas velocities below the point of entraining solids in the product gas. (Babu 2005; Basu 2006; Maniatis 2008) Furthermore, as some solids carryover is unavoidable, the amount of unreacted carbon in the ash can reach 20% on a feed basis depending on the type of fuel used. In order to mitigate carbon loss, the char-bearing ash can be reclaimed for use in an auxiliary boiler or recycled back to the fuel input of the fluidized reactor. Additionally, increasing the once-through carbon conversion in a BFB reactor by raising the operating temperature or pressure can reduce the amount of carbon loss. (Basu 2006; Higman, van der Burgt et al. 2008)

Where the Winkler gasifier operates at atmospheric pressure, high-pressure configurations up to 30 bar were introduced to realize carbon conversion improvements. (Higman, van der Burgt et al. 2008) The high-temperature Winkler (HTW) process operates at both elevated temperatures (>800˚C) and elevated pressures (10 bar). High temperature Winkler reactors require lockhoppers on the fuel feed and on the ash/char discharge to maintain elevated pressures. Further improvements in the HTW process were brought about by injecting the fluidizing medium both below the reactor grate and into the freeboard over the bed. The additional fluidizing gas added over-bed raises the temperature in that reactor zone to more selectively produce the desirable CO and H_2 products, rather than aliphatic hydrocarbons. Finally, high-pressure operation results in a pressurized syngas that should require less downstream compression energy for subsequent unit operations. (Basu 2006; Maniatis 2008)

Additional examples of the high-pressure bubbling fluidized bed processes are the Kellogg-Rust-Westinghouse (KRW) and the Institute of Gas Technology (IGT) U-Gas® (now Carbona RENUGAS®) processes. (Rollins, Reardon et al. 2002; Higman, van der Burgt et al. 2008) Internal construction of both the KRW and U-Gas reactors and the method of introduction of the fluidizing medium lead to internal recirculation of char and ash. (Lee, Speight et al. 2007) Ash agglomeration takes place during the circulation, allowing for easier removal. Carbon losses are minimized by separating carryover char and returning it to the bed. (Dominicis and Holt 1984)

Evolution in fluidized bed boilers led to the development of the circulating fluidized bed boiler (CFB) in the 1980's by Lurgi GmbH. At its most basic, the CFB configuration is similar to that of the bubbling bed gasifier, but with greater fluidization medium flow. By increasing the fluidization velocity to between 5 and 10 m/s, most solids are entrained in the furnace gas stream, separated in a cyclone, and returned via loop seal to the furnace grate. The increased bed and gas velocity leads to more thorough mixing and maximum heat transfer between solids and gases, generating high heating rates for incoming fuel. The higher the heat transfer rates, the lower the overall tar production, and the cleaner the resultant syngas. (Higman, van der Burgt et al. 2008)

Similarly to high pressure applications in fixed bed or bubbling fluidized bed gasifiers, CFB gasifiers can be operated at pressures of 10-25 bar through the use of isolating lockhoppers on fuel and ash. The increased complexity and expense of the pressurized fuel feeder and ash system is compensated for by a reduction in the amount of compression energy need downstream for turbine combustion or fuel synthesis reactions. As such, it is possible to directly feed a gas turbine with a pressurized gasifier. (Ahrenfeldt and Knoef 2005)

Circulating fluidized bed gasifiers are generally more tolerant of non-uniform sizes and shapes of fuels than other fluidized bed technologies. Coal gasifiers can utilize coal with diameters larger than 5 cm, if the unburnt fuel is captured in cyclones and returned for additional gasification. The fuel size tolerance possible with a CFB configuration is also particularly useful for the gasification of biomass, where the grinding energy is high and size

reduction processes yield a relatively wide distribution of particles. (Higman, van der Burgt et al. 2008)

In addition to better tolerance of non-uniform fuel, circulating fluidized bed gasifiers are considered reliable, mature technology at scales well beyond 100 MW_{th}. (Maniatis 2008) Current atmospheric and pressurized CFB designs are exemplified by installations from Foster-Wheeler (formerly Ahlstrom), Lurgi Energie and Entsorgung, TPS Termiska Processer AB, Carbona, and FERCO. (Kwant and Knoef 2004; Ahrenfeldt and Knoef 2005; Childress 2007; Higman, van der Burgt et al. 2008; Van Loo and Koppejan 2008) FERCO's SilvaGas process will be discussed in more detail in Section 1.4.

1.2.3 Entrained Flow Gasifiers

One final group of designs are entrained flow (EF) gasifiers, which are fundamentally different than the aforementioned fluidized processes. Many of the recent large coal gasifier installations are based on entrained flow designs, in large part due to the relative ease of building and operating systems greater than 100 MW_{th}. (Ahrenfeldt and Knoef 2005; Phillips 2006; Higman, van der Burgt et al. 2008) Several operational entrained gasifier installations exist with individual syngas output greater than 250 MW_{th}, with several more in planning stages as of 2007. (Childress 2007)

EF gasification does not utilize bed materials, rather the fuel is comminuted thoroughly so that effective mixing of the fine particles takes place in the gasifying medium and reaction mass transfer is very fast. Steam and/or oxygen are used to drive the

gasification reactions, with flow rates that result in very short fuel particle residence times (approximately 1 sec). (Lee, Speight et al. 2007) The operating temperature of entrained flow gasifiers is typically the highest of all of gasification technologies (1300-1600˚C), resulting in high rates of reaction, high single pass carbon conversion (around 90%), and agglomerated ash that slags out. (Lee, Speight et al. 2007) Such high operating temperatures also help limit tar and ammonia production to very low levels. (Ahrenfeldt and Knoef 2005)

Many entrained flow gasification technologies have been developed for coal feedstocks, starting with the Koppers-Totzek (KT) process in the 1940's. KT gasifiers are operated at atmospheric pressure, are considered robust in operation and tolerant of fuel characteristics (ash composition, ash fusion temperature, volatility, even phase). Finely pulverized solid fuel or liquid fuel is introduced into the bottom of the furnace along with steam and oxidant through a series of side mounted burner heads. As noted earlier, the high furnace temperatures minimize the outlet syngas hydrocarbon content, favoring production of CO and H_2. Furnace flow is upward, and can be water-quenched at the gas outlet to prevent molten ash from plugging the subsequent syngas cooler/HRSG. (Lee, Gogate et al. 1992; Higman, van der Burgt et al. 2008)

The Texaco coal gasification (TCG) process followed that of KT, and was developed in the late 1940's. The TCG process has some similar unit operations to KT, but the flow direction is reversed and furnace pressurized to between 20 and 85 bar. Rather than utilize lockhoppers to seal the fuel feed system, the coal is slurried and pumped into the furnace

under pressure. (Schlinger 1984) Like its predecessor, minimal hydrocarbon production is also a characteristic of TCG design.

Several additional entrained flow processes have been introduced as modifications to the original KT or TCG processes. Table 1 outlines the basic configuration details of eight entrained flow processes.

Table 1. General process configuration details for selected entrained flow gasification technologies, derived from Higman. (Higman, van der Burgt et al. 2008; NETL 2009; Uhde 2009)

Licensor	Process	Stages	Feed	Flow	Reactor wall	Syngas cooling	Oxidant
Koppers-Totzek	Koppers-Totzek	1	Dry	Up	Jacket	Syngas cooler	Oxygen
Royal Dutch Shell	Shell SCGP	1	Dry	Up	Membrane	Gas quench and syngas cooler	Oxygen
Uhde GmbH	PRENFLO	1	Dry	Up	Membrane	Gas quench and syngas cooler	Oxygen
Siemens	Siemens	1	Dry	Down	Membrane	Water quench and/or syngas cooler	Oxygen
GE Energy	Texaco	1	Slurry	Down	Refractory	Water quench or syngas cooler	Oxygen
ConocoPhillips	E-Gas	2	Slurry	Up	Refractory	Two-stage gasification	Oxygen
Mitsubishi Heavy Industries	MHI	2	Dry	Up	Membrane	Two-stage gasification	Air
J-Power	Eagle	2	Dry	Up	Membrane	Two-stage gasification	Oxygen

1.2.4 Gasifier Technology Summary

As noted, each gasification technology has an appropriate application, dictated by operating parameters and product syngas characteristics. A summary of the tar and ash production characteristics, as well as typical applications for each of the major gasification

technologies, is shown in Table 2. (Warnecke 2000; Rezaiyan and Cheremisinoff 2005; Bain 2006; Higman, van der Burgt et al. 2008)

Table 2. Syngas tar/particulate load and typical application for each of the major gasification technologies.

Gasifier Technology	Tar Loading	Particulate Loading	Application
Fixed Bed, Updraft	High	Low	Heating
Fixed Bed, Downdraft	Low	Low	Engine power
Bubbling Fluidized Bed	Moderate	Moderate	Large scale coal/biomass
Circulating Fluidized Bed	Moderate	Higher	Large scale coal/biomass
Entrained Flow	Low	Higher	Large scale coal

1.3 Biomass Gasification

Heretofore, a majority of the historical and technical background presented was based on coal as a feedstock. Historically coal has been utilized as the preferred feedstock due to its high energy-density and ease of handling. The first historical mention of coal gasification was between 371 and 287 BC by the Greek Theophrastus. (Mattusch 2008) As noted earlier, coal was being gasified on a research scale by the 17th century and on a commercial scale during the early 19th century. As coal became scarce during World War II, biomass was utilized as a fuel for many small-scale transportation gasifiers. (Ahrenfeldt and Knoef 2005) Ahrenfelt and Knoef note that while biomass enjoyed widespread use as a gasifier fuel during World War II, it was abandoned quickly because of the relative difficulty of using biomass as

feedstock. This highlights a problem that often accompanies the use of biomass as a feedstock: while being carbonaceous like coal, biomass is non-uniform and requires careful preparation for effective, reliable gasification. (Quaak, Knoef et al. 1999; Ahrenfeldt and Knoef 2005; Higman, van der Burgt et al. 2008)

A series of economic, environmental and national security drivers have led to renewed interest in carbon-neutral domestically produced biomass for energy generation, despite the well-known process difficulties. (Quaak, Knoef et al. 1999; Kumar, Jones et al. 2009) These difficulties can change the relative merits of the different gasifier designs and necessitate process changes to allow for appropriate biomass processing. Higman provides a good summary of the operational differences between biomass and coal gasification. (Higman, van der Burgt et al. 2008)

- Low melting point ash, with elemental components that react aggressively with typical refractory linings
- Fibrous nature of biomass, making comminution during feedstock preparation more energy intensive and the resulting particles less easily fed
- Relative high level of reactivity for biomass feedstock, which can allow for lower gasification temperatures
- Increased generation of tar from biomass gasification over that of coal
- Significant difference in the elemental composition, in particular the high oxygen content of biomass relative to coal, which changes the composition of the resulting syngas

These differences between coal and biomass effectively limit the choice of gasification technologies that are commercially viable for biomass. Despite widespread use

of entrained flow gasifiers for large-scale coal fed plants, there are no commercial-scale biomass fired EF units. The very fine particle size required for EF operation is not economically feasible with biomass as its fibrous nature significantly increases the energy required for comminution. (Maniatis 2008) Furthermore, the surface characteristics and hydrophilic nature of cellulosic of biomass limits the ability to create and feed slurries for pressured EF operation without additional pretreatments such as torrefaction. (van der Drift, Boerrigter et al. 2004).

Fixed bed reactors fair only marginally better. The inherently high amounts of tar from gasified biomass makes the use of fixed-bed updraft designs impractical except in "close-coupled mode," where the tar-laden syngas is used for direct combustion for heating applications. Indeed, in close-coupled configurations the inclusion of pyrolysis tars increases the heating value of the syngas. (Reed 2002; Maniatis 2008) Updraft gasifiers designed by Bioneer of Finland and PRM Energy Systems in the US exemplify small-scale close-coupled designs. Capacities of these gasifiers range between 1 and >50 MW_{th}, with a range of feedstocks from rice hulls to laminate floor production waste. (Ahrenfeldt and Knoef 2005)

Downdraft fixed-bed gasifier designs are capable of generating syngas that requires minimal tar removal, generating up to three orders of magnitude less tar per volume of syngas. (Ahrenfeldt and Knoef 2005) However, fibrous biomass with bridging tendencies could cause issues in the gasifier throat section. Downdraft gasifiers also require uniform heat around the oxidation zone to prevent tar slipstreams from escaping through the syngas outlet. Scale-up has been limited as larger diameter reactors can have cooler spots in the

oxidation zone. (Groeneveld and van Swaaij 1979) Such issues are lessened at small-scale (<1.5 MW_{th}), and downdraft gasifiers like those from the Belgian company Xylowatt are being installed on a limited basis as community combined heat and power (CHP) installations in the 300 kW_e/600 kW_{th} range. (Maniatis 2008; Xylowatt 2008)

Fluidized bed gasifiers are generally regarded as the most appropriate technology for commercial scale biomass gasification. (Quaak, Knoef et al. 1999; Ciferno and Marano 2002; Ahrenfeldt and Knoef 2005; Lee, Speight et al. 2007; Higman, van der Burgt et al. 2008; Maniatis 2008) The differing strengths and weaknesses between fixed bed (downdraft) gasifiers and fluidized bed (both bubbling and fluidized bed) gasifiers do not provide a clear technological winner at the medium scale of 15 MW_{th}, although fluidized bed designs have a higher throughput, smaller footprint, and better scaling abilities. (Warnecke 2000)

As mentioned earlier, fluidized bed gasifier processes can be broken into two major classifications: bubbling and circulating bed. Both technologies have been tested at the demonstration and commercial scale, and have proven reliabilities. (Kwant and Knoef 2004; Childress 2007; Maniatis 2008) Bubbling bed gasifiers are capable of handling a wide variety of biomass feedstocks from bark to municipal solid waste (MSW), with particle sizes up to 50mm. (Warnecke 2000; Ahrenfeldt and Knoef 2005) Several demonstration scale units have been successfully tested for technical assurance, and subsequently mothballed for financial considerations. A currently operating example of BFB biomass gasification is the Skive, Denmark plant utilizing a Carbona gasifier. This facility is utilizing wood pellets and chips to generate a maximum of 5.4 MW_e/11.5 MW_{th} when operating at full designed

capacity. (Salo and Horvath 2008; E4Tech 2009) As of 2009, several large-scale MSW fired bubbling bed gasifiers were in planning stages. (Salo and Horvath 2008; E4Tech 2009)

Circulating bed gasifiers, due to their ability to scale to larger facilities, have been more widely implemented in biomass gasification installations. Judging by database figures, the number of CFB gasifiers that have been commissioned and are still in operation indicates that circulating bed technology is preferred for large-scale projects. (Kwant and Knoef 2004; Childress 2007; Maniatis 2008) This is despite the moderate levels of syngas tar that circulating bed gasifiers inevitably generate, and the capital expense that subsequent gas cleanup will require. (Ahrenfeldt and Knoef 2005) The upper limit of biomass fuel particle size is 50mm for both the CFB and BFB units. As noted earlier, CFB gasifiers are tolerant of a wide distribution of particle sizes, since finely divided fuel is gasified during the first pass through the unit and larger particles/pieces are reduced in size during each subsequent recirculation. Because of this fuel tolerance, demonstration and commercial CFB units have been fed a wide variety of fuels, including sunflower seed hulls, wheat straw, bark, and wood chips. Currently operating units include Foster-Wheeler based designs in Finland, Sweden, and Portugal; and Lurgi based designs in Germany and the Netherlands. (Ahrenfeldt and Knoef 2005; Childress 2007)

A prime example of CFB gasifier implementation is the integrated gasifier system built by Readymix AG in Rüdersdorfer, Germany in 1996. Readymix AG is using a variety of biomass and waste materials such as wood wastes, refuse derived fuels (RDF), and waste plastics to fire a 100 MW_{th} Lurgi CFB gasifier. (Kwant and Knoef 2004) Lignite ash waste

is also added into the gasifier at the seal pot as an additional carbon source. Syngas from the solids recovery cyclone is sent untreated to fuel the cement plant's lime kilns, where tar and fine particulate matter do not pose a problem. Ash generated from the fuel blend is collected and included with the normal mineral inputs for the cement plant, leaving minimal waste from the gasification process. (Griel, Hirschfelder et al. 2002) This system also highlights the advantages of siting gasifiers adjacent to industrial operations that are compatible with the different residual streams.

A final example of circulating bed gasification technology applied to biomass, particularly relevant to the following chapters of this thesis, is the now mothballed Future Energy Resources Company (FERCO) dual CFB facility. The FERCO plant utilized the separate gasifier/combustor system developed by the Battelle-Columbus Laboratory in the 1980's. Figure 5 shows the general schematic for the dual-CFB configuration.

As the schematic outlines, the SilvaGas system has a separate gasification reactor and combustor. Following startup on natural gas, dried biomass is introduced into the steam-injected gasifier. A noncombustible bed material is used in both the gasifier and combustion sections to help facilitate the uniform and rapid heating of fuel. The original process research unit (PRU) at Battelle-Columbus utilized sand as the bed material (Feldmann, Paisley et al. 1988), but in-bed tar cracking could be incorporated by using an iron-bearing mineral such as olivine ($Mg_2(SiO_4)$ $Fe_2(SiO_4)$). (Corella, Toledo et al. 2004; Torres, Pansare et al. 2007)

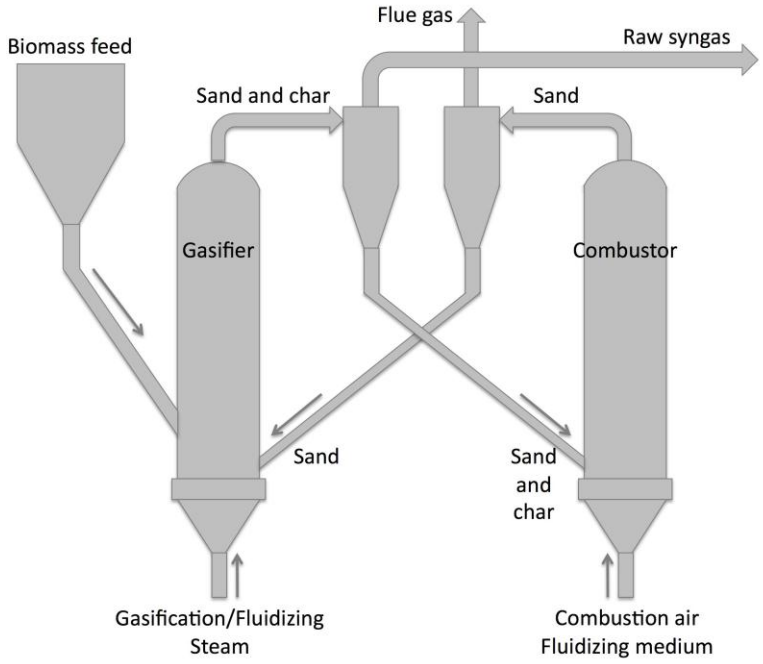

Figure 5. General flow schematic for SilvaGas/Battelle dual circulating fluidized bed gasification system. (Paisley, Overend et al. 2004)

Any remaining char from the gasification reactions and bed material is carried through the gasifier outlet and separated from the raw syngas via a cyclone. The char solids are completely burned in the air-injected combustor section. The now combustion-heated bed material is carried from the combustor bed and separated with another cyclone. Flue gas is directed to process heat exchanging and/or biomass drying. Hot bed material is recycled back to the gasifier section to provide the energy needed to drive the gasification reactions. (Paisley, Overend et al. 2004; Higman, van der Burgt et al. 2008)

The benefits of the dual bed system are considered by the process developers to be high biomass throughput and a medium-heating value, low nitrogen syngas (17-18 MJ/nm^3),

obtained without the use of oxygen. (Paisley, Overend et al. 2004) While the original Burlington, VT pilot-scale facility is offline, the current owner of the SilvaGas technology (Rentech, Inc., Los Angeles, CA) is planning to commission a new integrated biomass fed dual-CFB synthetic diesel refinery in 2012. (Rentech 2009) Finally, a related process, the fast internal circulating fluid bed (FICFB) gasifier developed by the Vienna University of Technology, is currently operating as a 2 MW_e/4.5 MW_{th} demonstration scale CHP plant in Güssing, Austria. (Higman, van der Burgt et al. 2008)

1.4 Syngas Cleanup Background

As early as the late 19th century, the concept of syngas cleanup was being considered around the use of "town gas" for illumination. The Fontana coal gasification process developed in 1780 to produce "blue water gas," which roughly equivalent to the modern definition of syngas as CO and H_2, burned with a blue flame. Such a blue flame was not suitable for the then widespread use of coal derived gases for street illumination, and it was realized that mixing tar laden coal gases with the "blue water gas" would yield a brighter flame. This was only effective if long chain hydrocarbons were removed, as their inclusion caused fouling of the distribution piping. Lowe invented the carbureted water gas process in 1872, passing the mix of blue water gas and "oil gas" through a reactor with white-hot checkerboard brickwork. The heated brickwork "packing" cracked the long chain and

aromatic components to light hydrocarbons, making syngas appropriate for lighting by rudimentary cleanup. (Shadle, Berry et al. 2000)

As alluded to in Section 1.3, the wide variety of modern gasification technologies and designs can exhibit a range of raw syngas quality, and the specific nature of the biomass feedstock also plays a role in the syngas quality. Updraft gasifiers, for example, tend to generate higher concentrations of tars in the product syngas. Downdraft fixed bed and any of the fluidized bed gasifiers tend to pass a higher concentration of fine particulate matter. Tar and particular matter are both considered contaminants, and must be removed for many, but not all downstream applications. With close-coupled (i.e. directly attached) gasifiers, combustors are not adversely affected by tar contamination; rather tars can actually improve the syngas heating value. Engine applications, on the other hand, are not tolerant of particulates or tars. Particulates can foul engine internals and accelerate wear throughout the system, and tars can condense within the fuel metering system leading to blockage. There are a multitude of gas cleanup strategies to deal with these various application-defined contaminants, and detailing each is outside the scope of this writing. Major cleanup technologies employed for a biomass to fuels pathway will be considered.

1.4.1 Particulate Removal

Relevant to biomass feedstocks, all appropriate gasification technologies have particulate loading in their outlet syngas streams. (Ahrenfeldt and Knoef 2005) These particulates are in the solid phase at the gasifier exit temperature, and can include entrained

ash, char, and bed materials (in the case of fluidized bed reactors). (Stevens 2001) The syngas end use will dictate the amount of solids that can be tolerated, for example applications such as direct syngas combustion in lime kilns are unaffected by solids loading. Combustion engine use requires syngas particulate loadings under 50 mg/m^3, although even at that concentration engine wear was reported to be up to five times greater than the gasoline baseline. (Baker, Brown et al. 1986) Gas turbines and chemical synthesis applications require a more complete solids removal. Gas turbines are particularly sensitive to alkali ash particles and vapors, which can be deposited on the relatively cool blades causing corrosion and wear problems. (Ahrenfeldt and Knoef 2005) Current alkali vapor/ash removal strategies involve cooling the syngas below the condensation temperature of the vapor-phase alkali materials, about 600˚C. Once cooled and condensed into fine solids, the alkali materials can be removed with conventional solids removal methods.

Stevens outlines four general types of particulate removal strategies: cyclone filters, barrier filters, electrostatic filters, and wet scrubbers. (Stevens 2001) The effectiveness of these different ash removal technologies are linked to the particle size and temperature requirements for the syngas end use. For example, direct syngas combustion in gas turbines requires clean and hot syngas, with minimal cooling, while gas-to-liquids processes are generally cooled during the intermediate process steps. (Ahrenfeldt and Knoef 2005)

Cyclonic filters are simple, easy to install and maintain, and can remove particles larger than 5 μm by inducing a circulating gas flow. Centrifugal forces act upon the particulates as the syngas stream circulates, causing them to spiral out of the bottom of the

cyclone unit while ejecting cleaner syngas from the top. (Stevens 2001) In fluidized bed gasification technologies entrained solids separators are an integral part of the process, returning char and bed material back to the reactor for further gasification. Due to their simple operation, lower pressure drop, and high temperature operation abilities, cyclone filtration is often used as the first gas treatment step regardless of the gasification technology. (Stevens 2001)

In order to remove particles in hot gas streams smaller than 5 μm, a barrier separation device such as a metal or ceramic candle filter is used. Candle filters are simple perforated metal or ceramic cylinders that are capable of removing dry solids from 0.5 to 100 μm. Some syngas cooling may be necessary with this cleanup technology, to prevent very hot entrained solids from sintering around and plugging candle pores. Bag filters and packed bed filters are also considered barrier devices, but may require much cooler syngas to prevent filter damage or bed agglomeration. Bag filters are typically constructed of woven metal or ceramic fibers and typically used at temperatures below 350˚C. They can easily remove particles smaller than 1 μm. Packed bed filters operate by forcing raw syngas through a bed of solid materials such as wood chips (LaFontaine and Zimmerman 1989) or activated charcoal. Accumulation of solids and tars eventually fouls the bed packing, requiring replacement. In this way, packed bed filter configurations are only feasible in micro to small-scale biomass gasification applications. Fouled combustible bed materials can be recycled as feedstock for the small-scale gasification process, ultimately providing an inexpensive option for concentrating and removing ash particulates along with tars in one

unit operation. (Stevens 2001; Ahrenfeldt and Knoef 2005) While candle filters and packed beds are capable of removing fine solids at elevated temperatures, the higher pressure drop of these devices can require implementation of a different technology.

Electrostatic filters are capable of removing a wide variety of solids depending on configuration and the charging voltages employed, while potentially operating up to 500˚C. Entrained solids are subjected to internal electrodes of opposite polarities, at first charging the particles with one polarity, and then attracting them out of entrainment for capture with another. Captured particles can be mechanically removed in dry precipitator units with shakers or rappers. Electrostatic precipitators, while being conventional, tested technology are typically used only for large-scale coal gasification operations due to their size and capital expense. (Stevens 2001)

Wet scrubbing is the last particulate removal unit operation to be discussed, as it can serve as a means of both particulate and tar removal. Wet scrubbing affects gas cleaning by impacting fluid droplets (typically water) with the entrained syngas solids. As water is typically the scrubbing medium, and must be in liquid phase for scrubbing to occur, the maximum operating temperature for a wet scrubbing system is typically 100˚C. (Ahrenfeldt and Knoef 2005) Syngas cooling prior to wet scrubbing is therefore required, either by heat exchanging/recovery, or by water quenching. (Stevens 2001; Rubin, Berkenpas et al. 2007) An additional consequence of syngas cooling under the dew points of tars is that some degree of tar removal will be affected by condensation and de-entrainment of tar droplets, as well as some reduction in water-soluble gaseous contaminants such as ammonia. (Stevens 2001)

Spray tower, impingement, packed bed, and venturi type wet scrubbers are utilized for both particulate and tar removal; with venturi scrubbing being the most commonly implemented technology. Venturi scrubbing removes entrained solids and condensed tars by introducing a scrubbing fluid into a venturi on the inlet side of the scrubber. In typical configurations, coalesced water droplets carrying up to 99% of entrained solids 1μm or larger are removed from the cleaned gas stream via cyclone. (Stevens 2001; Ahrenfeldt and Knoef 2005)

1.4.2 Tar Removal

Tars, generally considered complex mixtures of aromatic and poly-aromatic hydrocarbons with the possible inclusion of olefins (Milne, Evans et al. 1998), are produced to some extent in all biomass gasification processes. While some syngas end uses can tolerate tar contamination (notably close-coupled direct syngas combustion), most uses require the removal of at least some of the tars present in the syngas. Milne, et al. have thoroughly reviewed the impacts of tar contamination and the end use tolerances. (Milne, Evans et al. 1998) Generally, however, tar removal is necessary whenever syngas is to be cooled, compressed, or utilized in mechanical-based combustion systems. (Ahrenfeldt and Knoef 2005)

Two basic tar removal schemes are utilized. Syngas can be cooled, with tar droplets condensed and removed in a manner similar to entrained particulates. Alternatively, thermal

or catalytic tar destruction can also be employed, providing the energy to break bonds and ultimately reduce tars to CO and H_2.

Naturally, as condensed tars are sticky, some physical removal technologies are more effective than others, with wet scrubbing as the most promising candidate. (Milne, Evans et al. 1998) Wet scrubbing for tar removal is typically a two-step process, involving syngas cooling/quenching followed by venturi scrubbing with water. Scrubbing temperatures are in the range of 35-60˚C when water is used as the scrubbing liquid. Tar removal efficiencies between 50-98% have been reported utilizing water scrubbing technologies. (Milne, Evans et al. 1998) Scrubbing liquids other than water can be used, and systems such as the OLGA process from the Energy Research Centre of the Netherlands (ECN) or scrubbing system at the Güssing, Austria biomass gasification plant utilize oil solvents. (Ahrenfeldt and Knoef 2005) The OLGA process has a reported 99% tar removal efficiency, and is currently in four demo and commercial scale installations. (Zwart, Bos et al. 2008)

Wet electrostatic precipitation is another effective physical tar removal technique, working in a similar manner to ESP particulate removal. Wet ESP tar removal employs a wire and tube electrode configuration, applying an initial charge to incoming tar droplets, and subsequently attracting them to oppositely charged tubes. The tube electrodes are continuously washed down with water to collect any separated tars and prevent electrode fouling. Wet ESP operation for tar removal is temperature limited to a maximum of 150˚C, but is capable of 99% removal of tar particles smaller than 0.1μm.

Physical tar removal can generate an additional wastewater stream from a biorefinery process unless the removal technology allows for tar recycle back to the gasification unit. All physical tar removal operations require syngas cooling, which can represent a loss of sensible heat that must be regained for end use processes (Dayton 2002), as is the case of integrated gasification combined cycle (IGCC) energy generation or for most gas to liquids schemes.

Hot gas cleaning techniques such as catalytic or thermal tar destruction can eliminate the tar wastewater stream and return more calorific content to the syngas stream. (Dayton 2002) Catalytic tar removal or *conversion* is likely preferable over thermal destruction, as the temperatures required for straight thermal treatment range from 900 to 1200˚C, usually well above that seen in gasification outlet streams. Due to the attractiveness of hot gas catalytic tar conversion, a substantial amount of research has been carried out in that area, including work on non-metallic and metallic catalysts, and *in situ* (within the gasification reactor) and external conversion processes. (Stevens 2001)

Non-metallic catalysts such as dolomite, calcite, zeolite, or olivine have been used with moderate success for both *in situ* and external-reactor applications. (Corella, Toledo et al. 2004; Ahrenfeldt and Knoef 2005) These non-metallic catalysts are inexpensive, can have reasonable tar destruction (Stevens reports 95-98% tar removal for dolomite under laboratory conditions), and can also break down ammonia present in the syngas. In spite of these positive attributes, there are several significant limitations including attrition (physical breakdown of the catalysts due to turbulence in the process with the corresponding formation

of ash) and susceptibility to H_2S poisoning. (Stevens 2001; Corella, Toledo et al. 2004; Ahrenfeldt and Knoef 2005) Despite this, non-metallic catalysts have been utilized at least pilot scale for both the Battelle gasifier PDU and the FERCO/SilvaGas gasification facility. (Stevens 2001)

Metallic catalysts similar to those used in the petrochemical industry have also been applied to tar conversion. Nickel, cobalt, and molybdenum catalysts with supports have been tested extensively, and demonstrate effective tar removal at temperatures as low as 740˚C. Nickel catalysts particularly with a variety of support materials have been evaluated, and while effective in tar destruction, are susceptible to coke fouling and poisoning from chlorine, sulfur, and alkali metals. High temperature operations to mitigate coke fouling, or high regeneration temperatures to remove accumulated coke foul can also lead to sintering and nickel volatilization. (Stevens 2001; Dayton 2002; Yung, Jablonski et al. 2009) Nickel monolith tar removal catalysts have been used to successfully crack tars at the pilot scale in several installations. (Ahrenfeldt and Knoef 2005)

1.4.3 Light Hydrocarbons, Ammonia, and Acid Gas Removal

Similarly to ash and tar removal, the requirements for removal of light hydrocarbons, ammonia and sulfur are tightly linked to the final syngas end-use. Light hydrocarbons such as methane and ethane can serve as a diluent for fuel synthesis processes. Conversely, for IGCC and other combustion uses, non-condensable hydrocarbons help improve syngas heating value. Ammonia and H_2S in concentrations likely to be encountered in biomass-

derived syngas are also not an issue for combustion uses. (Ahrenfeldt and Knoef 2005) The majority of fuel synthesis applications have much more stringent requirements, as NH_3 and H_2S are considered catalyst poisons at ppm concentrations for methanol and Fischer-Tropsch synthesis processes, among others. (Baker, Brown et al. 1986). CO_2 can serve as reactant for methanol synthesis (Luyben 2010) and adds additional mass flow to syngas streams used in turbine applications, but must be excluded for ammonia synthesis. (Breckenridge, Holiday et al. 2000)

Catalytic hot syngas cleanup processes are often considered preferable, since some of the sensible heat of the gas stream is retained for downstream applications. Similar to the application of hot-gas conditioning for tar removal is removal or reforming of non-condensable hydrocarbons. Nickel based tar-reforming catalysts also display activity for cracking light hydrocarbons, so that a catalytic tar reformer can be used for hot-gas removal of a wide range of hydrocarbons. (Dayton 2002; Gerber 2007) Catalytic ammonia removal can also be accomplished with Ni-based materials, but NH_3 removal efficiency will be greatly reduced if syngas under cleanup has a high tar load. (Corella, Toledo et al. 2005) Pansare and workers have demonstrated that tungsten carbide and tungstenated zirconia catalysts have useful ammonia and tar cracking ability, provided suitable physical properties can be obtained. (Gangwal, Gupta et al. 1995; Pansare, Goodwin et al. 2008)

Higman divides the non-catalytic cleanup technologies into absorption, adsorption, and diffusion groups, although the absorption and adsorption processes show the greatest commercial potential. Absorptive technologies are characterized by the use of a liquid

solvent which is followed by a desorption process. Adsorption processes utilize solid material sorbents to remove contaminants from syngas. Diffusion systems exclude gaseous species by size to affect gas cleanup. (Higman, van der Burgt et al. 2008)

Absorption-based cleanup employs liquid solvents that wash acid-gas components (H_2S and CO_2) from the syngas, and operate and temperatures significantly lower than those in hot-gas conditioning. The contaminant bearing solvents are regenerated and recycled back to the absorption tower. Many of the commercial acid-gas cleanup strategies used for coal syngas can be classified as absorption process and include: amine scrubbing, Rectisol, Purisol, and Selexol processes. (Higman, van der Burgt et al. 2008) Wet scrubbing with water as a solvent is also considered an absorption-based cleanup technology, and can reduce ammonia, HCl, and CO_2 in the treated syngas stream. (Kumar, Jones et al. 2009)

Rectisol is a physical absorption commercial acid-gas cleanup system created by Lurgi AG and Linde AG concurrently with the development of Lurgi moving-bed coal gasifiers. It is based on the affinity of cold (-30 to -60˚C) methanol for CO_2 and H_2S. Acid-gas laden methanol is regenerated by flashing and stripping and/or reboiling. (Hochgesand 1970) Variations of the Rectisol process have been designed where the absorption of H_2S and CO_2 can be selectively controlled. Such a selective process is based on a two-absorber system, one operated at approximately -30˚C for H_2S removal, and the other at about -60˚C for CO_2 recovery. (Hochgesand 1970; Weiss 1997) While the Rectisol process is very effective, the very low operating temperatures lead to a significant cooling and reheating loads, and associated higher operating costs

Purisol is also a physical absorption cleanup process developed by Lurgi AG, but uses N-methyl-pyrrolidone (NMP) as the solvent. The Purisol process operates in a temperature range of 15-40˚C, and typically at high pressures. Besides the obvious difference in operating temperatures from Rectisol, the Purisol process allows more H_2S to pass through the clean-up process, but is also more selective in removing H_2S over CO_2. Applications that can tolerate ppm-range H_2S concentration syngas from the Purisol process can avoid the considerable costs associated with Rectisol methanol refrigeration. (Hochgesand 1970; Higman, van der Burgt et al. 2008) Selexol is quite similar to the Purisol process in terms of acid-gas removal and operating temperature, and utilizes dimethyl ethers of polyethylene glycol (DMPEG) as an absorption solvent. (Higman, van der Burgt et al. 2008)

Amine scrubbing is a reversible chemical absorption washing process for acid-gas removal, and dates from the 1930's. (Rochelle 2009) Amine scrubbing reduces syngas acid-gas contaminants by chemically binding CO_2 and H_2S with the amine solution in absorption columns. (Kohl and Nielsen 1997) The absorber is typically washed with a 30% solution, utilizing one of many possible amine washes. Monoethanoamine is frequently employed, but diethanoamine (DEA) and methyldiethanoamine (MDEA) are also common. (Rochelle 2009) A reboiling/stripping tower follows the adsorber, regenerating the amine wash. Hydrogen sulfide liberated from the amine reboiler is frequently converted to elemental sulfur via the Claus process, a thermal oxidation/catalytic conversion of H_2S to sulfur. The oxidative LO-CAT process based on regenerable chelated iron solution is also applied to sulfur recovery. (Higman, van der Burgt et al. 2008)

The final acid gas cleaning strategies to discuss are those that are classified as *adsorptive*, where syngas contaminants are adsorbed onto solid bed materials. Sorbent materials can be disposable or regenerable. Zinc oxide-copper oxide based sorbents are highly effective at removing H_2S from gas streams, but must be disposed of when exhausted as regeneration is difficult. Typical applications of ZnO/CuO sorbents are as guard beds upstream of sulfur sensitive, lower temperature catalytic reactions (Higman, van der Burgt et al. 2008) Zinc oxide sorbents, while extremely effective at sequestering sulfur, are subject to reduction or spalling which shortens the operating life. Improved ZnO derived sorbents that can be regenerated incorporate titanium or iron. Zinc ferrite or zinc titanate mixed-metal oxide sorbents are more tolerant of high temperature and with appropriate support and physical structure can be used in fluidized bed hot-gas desulfurization process to good effect. (Gangwal, Gupta et al. 1995)

CHAPTER 2

Exercising and Utility of the National Renewable Energy Lab (NREL) Mixed Alcohols Thermochemical Model

2.1 Introduction

Thermochemical conversion of biomass to syngas, and the subsequent conversion of syngas to power or fuels is an area of active research. There is a significant level of interplay between the gasification and gas clean-up processes and the fuel synthesis pathway. Despite this, the ability for gasification processes to convert biomass feedstock of almost any composition offers a tremendous advantage over traditional fermentative processes.

An examination of current research literature shows that many laboratory or pilot scale thermochemical biomass to fuels systems exist. However, the introduction into biomass gasification and synthesis gas cleanup provided in Chapter 1 is an indication of the complexity involved in scaling to a commercial-scale process.

One of the most promising ventures for integrated biomass to fuels production in United States, the Colorado-based Range Fuels, constructed an integrated gasification based biomass to alcohols facility in Soperton, GA.(RangeFuels 2011) The endeavor required millions of dollars in US Government grants and private investment. In January 2011, the Soperton, GA facility was shut down and its staff laid off. The only production scale thermochemical biomass-to-fuels facility in the US was shuttered after one production run of

ethanol. (Wang 2011) Carbo-V gasification technology, the basis of an alternative biomass-to-liquids (BTL) approach being developed by CHOREN Industries GmbH in collaboration with Volkswagen and Daimler AG, has also been slowed by technical barriers. (Luxmore 2007)

A biomass gasification platform, mixed alcohols production model was developed at the National Renewable Energy Laboratory (NREL) to simplify operational and financial analysis of commercial-scale integrated facilities. Such a comprehensive model can serve as a tool to test process sensitivities to feedstocks and equipment configurations, as well as economic sensitivities around areas such as raw material costs and fuel market prices, with the goal decreasing development costs and increasing the likelihood of technical success.

To this end, Phillips and workers at NREL developed an overall plant process model and associated techno-economic model in 2007. (Phillips, Aden et al. 2007) It owes much of its structure and methodology to previous research work in the areas of coal/biomass gasification and biochemical, fermentative biomass to ethanol conversion. The following sections present a brief model history, background, and a summary of basic model design elements. These sections are intended to help provide an understanding of how the model is assembled and how that assembly impacts the operation and predictive capability of the model. Finally, this chapter demonstrates the use of this NREL gasification model using a series of biomass feedstocks.

2.2 Model History

The National Renewable Energy Laboratory (NREL) has been researching the production of alcohols from biomass using both biochemical and thermochemical routes since its beginnings as the Solar Energy Research Institute in the late 1970's. Figure 6 outlines a simple lineage of gasification-related work performed at NREL.

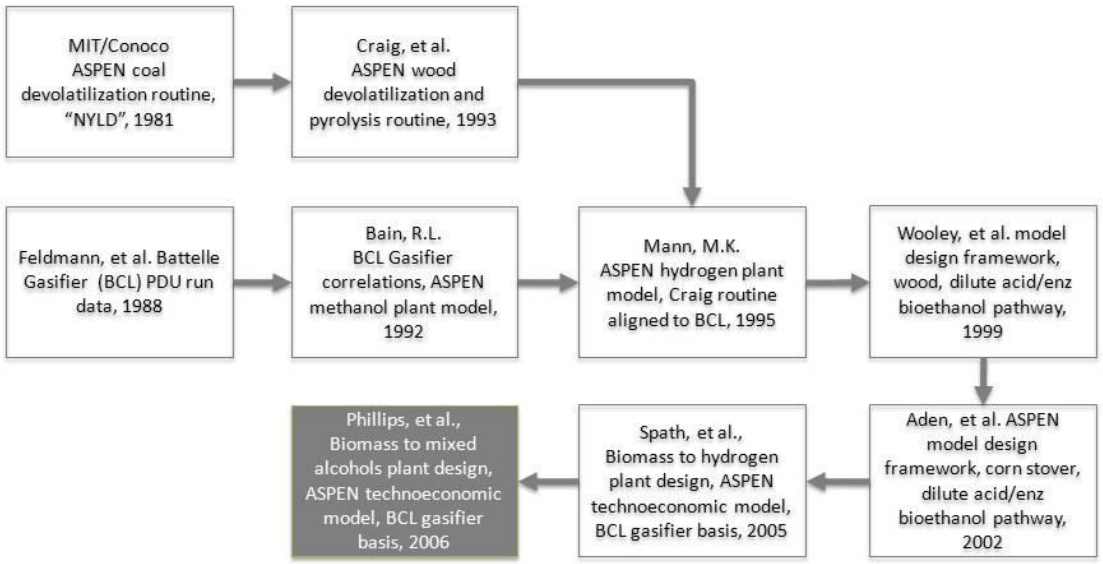

Figure 6. NREL mixed alcohols model lineage block diagram. Shaded block indicates model that was examined and exercised.

Bain brought the two research threads of biomass-derived alcohols and gasification together in 1992, designing Advanced System for Process Engineering (ASPEN) (AspenTech Inc., Burlington, MA) models to simulate the gasification systems from the Institute of Gasification Technology and the Battelle-Columbus Laboratory (BCL).

The BCL process demonstration unit (PDU) was a dual circulating fluidized bed system, with an indirectly heated gasifier coupled to a fluidized bed char combustor. Char generated in the pyrolyzer/gasifier by contact with hot sand was separated in a cyclone and burned in a secondary combustor. The hot sand leaving the combustor was separated with another cyclone, and sent back to the gasifier to provide heat for pyrolysis/gasification. The proof-of-concept gasifier was built with a 6-inch body, and the pilot scale gasifier with a 10-inch body.

The ASPEN models were then used to evaluate case studies utilizing the two gasification technologies to provide syngas feedstock to methanol synthesis unit operations. (Bain 1992) An integral part of the BCL model is a series of second order polynomial regression equations that correlate gasifier output syngas composition and char flow against operating temperature. These second order polynomials were based on a total of 37 sets of gasifier run data were analyzed using linear least squares (Bain 1992) from a set of 142 runs conducted by Feldmann and co-workers using both the 6 and 10 inch BCL gasifiers (Feldmann, Paisley et al. 1988). The original gasification runs were made with a variety of feedstocks including chips made from cherry (*Prunus* sp.), mixed oak *(Quercus* sp.), birch (*Betula* sp.), maple (*Acer* sp.), pine (*Pinus* sp.), and mixed hardwoods. (Feldmann, Paisley et al. 1988) The temperature-dependent correlations developed by Bain are shown in Table 3.

Bain's process models simulated all of the major unit operations of a biomass to methanol gasification plant. The gasifier was modeled as a simple ASPEN RYIELD reactor,

utilizing percent yield derivations at a fixed temperature built from the BCL conversion correlations.

Wood and char materials were simulated as non-conventional components, and utilized ASPEN's inherent coal ultimate, proximate, and sulfur analysis component attributes. A syngas preformer and reformer followed the gasifier. Tar and hydrocarbon cracking in the performer was simulated using an RSTOIC reactor, where balanced cracking reactions to methane were specified. An RSTOIC reactor block assumes that the specified reactions proceed to a given completion extent, with the concentration of products and remaining reactants dictated by given reaction stoichiometry and conversion. (Aspen Technology 2009)

Table 3. Second-order polynomial linear least squares regression correlations of Battelle-Columbus data by Bain. Form is $x = A + BT + CT^2$. Temperature is in degrees Fahrenheit.

Variable	Units	A	B	C	R^2
H_2O Conversion	lb/lb dry wood	2.8959E-01	-8.9048E-04	4.3384E-07	0.842
Dry Gas	SCF/lb dry wood	2.8993E+01	-4.3325E-02	2.0966E-05	0.938
Gas	lb/lb dry wood	1.5553E-01	-2.2057E-04	3.7617E-07	0.872
Tar	lb/lb dry wood	4.5494E-02	-1.9759E-05		0.998
Char	lb/lb dry wood	7.5503E-01	-3.0212E-04	-3.1178E-08	0.655
H_2	mole %	1.7996E+01	-2.6448E-02	1.8930E-05	0.918
CO	mole %	1.3346E+02	-1.0290E-01	2.8792E-05	0.397
CO_2	mole %	-9.5251E+00	3.7889E-02	-1.4927E-05	0.417
CH_4	mole %	-1.3820E+01	4.4179E-02	-1.6167E-05	0.693
C_2H_2	mole %	-4.3114E+00	5.4499E-03	-1.5610E-06	0.717
C_2H_4	mole %	-3.8258E+01	5.8435E-02	-1.9868E-05	0.876
C_2H_6	mole %	1.1114E+01	-1.1667E-02	3.0640E-06	0.852

Steam reforming was modeled using an ASPEN RGIBBS reactor, where the modeling engine attempts to minimize the Gibb's free energy of products from the methane

steam reforming reaction (Equation 1), Boudouard reaction (Equation 2), and water-gas shift reaction (Equation 3). The subsequent gas cleanup section of the model plant was non-rigorously simulated with simple split blocks. Finally, the methanol synthesis section of the Bain model is approximated using an ASPEN REQUIL reactor block, which estimates equilibrium concentrations of reactants and products based on calculated reaction equilibrium.(Aspen Technology 2009) The methanol reactor was based on the methanol synthesis reaction from carbon monoxide (Equation 4), and the water-gas shift reaction. ASPEN results were subsequently used for manual equipment sizing and a simple techno-economic model. (Bain 1992)

$$\mathbf{CH_4 + H_2O \rightleftharpoons CO + 3H_2} \quad \textbf{(1)}$$

$$\mathbf{C + CO_2 \rightleftharpoons 2CO} \quad \textbf{(2)}$$

$$\mathbf{CO + H_2O \rightleftharpoons CO_2 + H_2} \quad \textbf{(3)}$$

$$\mathbf{CO + 2H_2 \rightleftharpoons CH_3OH} \quad \textbf{(4)}$$

The first biomass to fuels model from Bain was the predecessor to a gasification-derived hydrogen plant model developed by Mann in 1995. (Mann 1995) Mann's gasifier model was also based upon the BCL gasifier correlations from Bain, but incorporated a FORTRAN user model to more rigorously account for temperature dependent material balances across the gasifier. This was in contrast to the original Bain model, which relied on user input for derived yields at a particular gasification temperature.

The user model utilized by Mann was originally based upon a coal devolatization routine built by the Massachusetts Institute of Technology (MIT). The "NYLD" devolatization routine was developed by MIT as part of a Lurgi slagging gasifier. (Stefano 1985) The non-kinetic algorithm of fixed yields to convert coal to char and organic and inorganic gases was coupled with elemental material balances based on the ultimate analysis of the feed material to match results from the gasifier design study. (Stefano 1985) Craig built a wood devolatization routine based upon MIT's NYLD model in 1993, and modified it to reflect the BCL gasifier correlations developed earlier. (Craig 1993) The resulting FORTRAN non-kinetic gasifier user routine was called "BATYD" and incorporated into Mann's hydrogen plant model. (Mann 1995)

In a similar manner to the preceding methanol plant design, a RGIBBS reactor block was used with a low temperature approach to simulate non-equilibrium reformer reaction results. Rather than incorporate water-gas shift activity into the reformer of the hydrogen plant model, two separate high and low temperature water-gas shift reactors were used, each as a RSTOIC reactor with fixed CO conversion extents. Simple SEP blocks modeled cleanup and hydrogen purification, just as was done in Bain's methanol model. (Mann 1995)

In 2005, Spath, et al. presented the successor to the hydrogen production plant model that Mann created in 1995. (Spath, Aden et al. 2005) Spath's hydrogen plant system was designed in a much more inclusive and rigorous way, modeled after the methodologies developed to thoroughly evaluate biochemical biomass to ethanol by Wooley, et al. in 1999 and Aden et al. in 2002. Spath's process design started with the generation of full process

flow diagrams (PFDs), informed by literature review and professional input from consulting engineering firms. The integrated PFDs were translated to ASPEN models, the subsequent material and energy balances used to size equipment and construct economic analyses. At the heart of the Spath hydrogen model was an updated version of the BATYD (BATYD4) gasification user routine, coupled with another FORTRAN user routine, "USRDC1." The USRDC1 user routine was designed as a coal decomposition routine by Stone at the Morgantown Energy Technology Center (METC), after MIT's Lurgi slagging gasifier model was transferred to the US Department of Energy (DOE). (Stone 1984) As used in the Spath thermochemical hydrogen model, the USRDC1 user routine is a means to decompose char solids from the pyrolysis section of the gasifier, based on the ultimate analysis of the char and any unburned wood. This routine, and the subsequent ASPEN RSTOIC reactor configured to generate combustion reactions formed the char combustor model for the indirectly heated BCL gasifier. (Spath, Aden et al. 2005)

In keeping with the philosophy of more realistic model treatment, syngas cleanup was simulated in a more commercial process engineering manner. Tar reforming was accomplished by an REQUIL reactor block configured with hydrocarbon cracking reactions, followed by a SEP block to model catalyst purge. Solids removal and tar reduction were accomplished by venturi scrubbing and quench system, respectively, using FLASH and SEP blocks, with an ASPEN design specification and calculator control. A LO-CAT liquid phase iron-catalyzed H_2S removal unit removed a large part of the syngas sulfur load, utilizing HEAT, SEP blocks, and a RSTOIC block with the final syngas H_2S concentration and the

LO-CAT oxidizer air being controlled by ASPEN calculators. Polishing removal of syngas H_2S in ZnO beds was modeled with RSTOIC reactor block, with the oxidizer controlled by a calculator, rounding out the thermochemical hydrogen model syngas post-processing.

2.3 Current Model Background

Phillips, Aden, Jechura, Dayton, and Eggeman developed NREL's Thermochemical Ethanol via Indirect Gasification and Mixed Alcohols Synthesis of Lignocellulosic Biomass model between 2006 and 2007. The focus of the model was to supply techno-economic information for the calculation of a minimum ethanol selling price (MESP) in an integrated biorefinery application at the target year of 2012. (Phillips, Aden et al. 2007) Previous NREL studies suggested that thermochemical processes (gasification and syngas to mixed alcohols, followed by ethanol recovery and recycling of other alcohols) could produce ethanol at a selling price of $1.07. In order to determine the feasibility of meeting the published MESP with a more detailed study, the Phillips model first drew upon the process design methods developed by Wooley in 1999, Aden in 2002, and Spath in 2005.

Again, the complete process flow diagrams were developed in cooperation with consulting engineering firms, utilizing a combination of current state of technology unit operations and aspirational technological goals deemed achievable by DOE in the target year. Indirect, low-pressure steam gasification was chosen as the appropriate technology for the gasifier primarily because of the aforementioned research done around the Battelle Columbus

indirect gasifier PDU. The complete PFDs were then used to design an ASPEN model. Just as was done in the work of Wooley, Aden, and Spath, the Phillips model was constructed using distinct process blocks. Figure 7 provides an overview of the model plant process blocks.

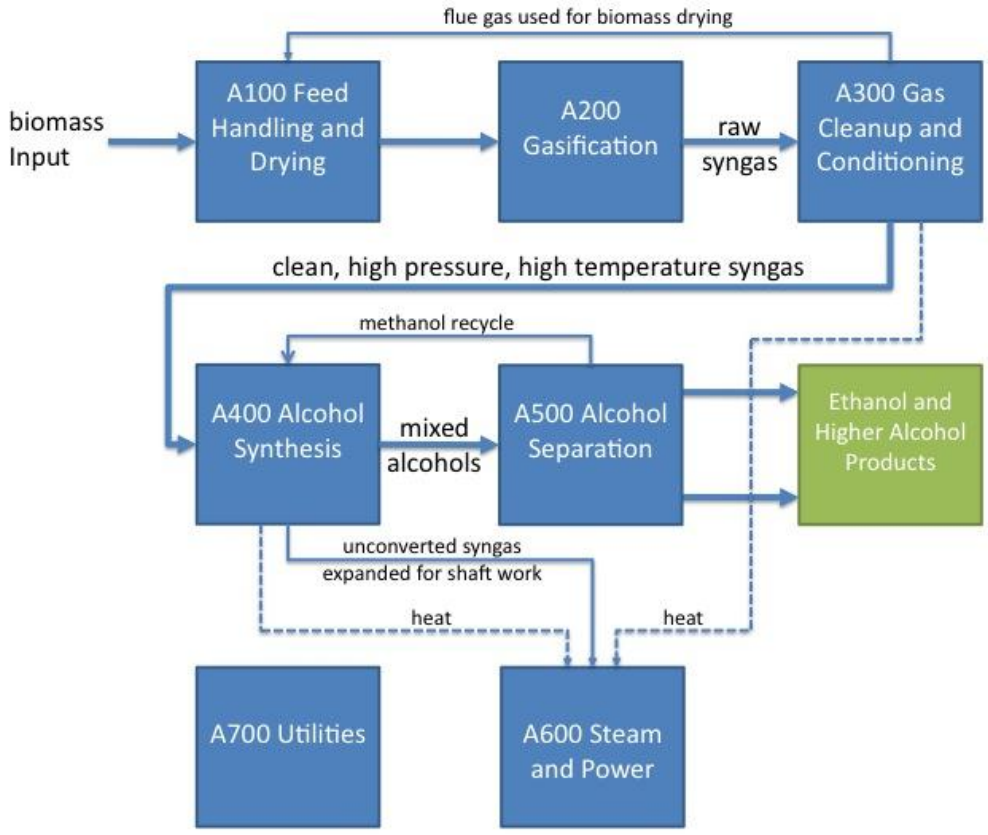

Figure 7. NREL mixed alcohols model process area overview.

The use of modular process blocks simplifies model management and navigation. A brief summary of the process blocks and their major design points follows. Appendix A presents a more detailed explanation of the ASPEN model for each process area.

2.3.1 Block 100, Feedstock Preparation

Block 100 encompasses the unit operations that are used to prepare the biomass feedstock for gasification. As modeled, only drying is included in this block. Drying is accomplished by flashing moisture from the wood, using heat supplied by flue gas from the gasifier in Block 200 and the tar reformer catalyst regenerator in Block 300. The final moisture of the wood fed into the gasifier is dictated by a user defined parameter, with a default value of 5%.

2.3.2 Block 200, Gasification

A two stage non-kinetic gasification model is employed in Block 200, based on the BATYD5 FORTRAN code, and physical design of the Battelle-Columbus Laboratory PDU gasifier introduced in Section 2.2. The gasifier (first stage) syngas outlet composition is temperature-dependent, and is completely controlled by temperature driven empirical correlations and subsequent elemental balances performed in the BATYD5 code. A feedback loop is established within the overall gasifier model, where initial temperature and feedstock characteristics yield a calculated amount of char to be burned in the char combustor (second stage). Combustion of the char liberates heat, which is applied back to the gasifier. Increasing gasification temperatures are correlated in BATYD5 to decreasing amounts of char, allowing the gasifier model to reach equilibrium. Raw product syngas is split into two major process streams, one which serves as an eventual feedstock to the Block 400 fuel synthesis section, and one which is combusted in Block 300 for heat and power. The

use of these temperature driven correlations is a limitation for the model as it cannot be used to independently evaluate the effects of changing the composition of the biomass feedstock while maintaining a controlled temperature.

2.3.3 Block 300, Syngas Cleanup

Raw syngas generated in the Block 200 gasifier is cleaned in preparation for catalytic fuel synthesis in Block A400. Tars present in the raw syngas pose a fouling hazard for downstream unit operations, and represent an opportunity to increase the yield of CO and H_2. An olivine ($Mg_2(SiO_4)$ $Fe_2(SiO_4)$) catalyzed tar reformer is modeled as a basic, non-kinetic yield controlled reactor, with tar, benzene, lower molecular weight hydrocarbons, and ammonia reforming extents defined by user parameters. A catalyst regenerator reactor is coupled with the tar reformer, and is modeled as a simple stoichiometric combustion reactor that utilizes a split stream of raw syngas and unreacted syngas from the synthesis block (A400) as a fuel source to supply heat to the tar reformer.

Any residual catalyst particulate matter, tar, or ammonia is removed in a syngas quenching and scrubbing step that follows reforming. Medium pressure compression to 430 psi (2.96 MPa) follows quenching and water scrubbing. A monoethanoamine scrubber is used to remove a majority of the H_2S from the pressurized syngas. Amine scrubbing is modeled by mathematically splitting a user-specified amount of H_2S from the syngas. Subsequent sulfur capture from the sour-gas waste stream is affected by a simulated LOCAT

sulfur oxidization process. LOCAT oxidation is carried out with a non-kinetic stoichiometric reactor.

2.3.4 Block 400, Mixed Alcohol Synthesis

Block 400 includes all unit operations need to feed clean syngas to a catalytic mixed alcohols synthesis reactor and perform the synthesis. Clean, medium pressure syngas from Block 300 is further pressurized and preheated in preparation for synthesis. Syngas is compressed to 1000 psi (6.89 Mpa) and heat exchanged with raw syngas until synthesis reactor feed is 570 °F (299 °C).

Alcohol synthesis is accomplished by a MoS_2 catalyzed reactor, modeled in two steps with a non-kinetic specified yield reactor and a water-gas shift reactor capable of calculating reaction equilibria. The non-kinetic synthesis reactor is controlled by series of reactions with user-defined extents, adjusted to give an aspirational first past CO conversion of 60%. Any unreacted syngas is decompressed to extract shaft work for use in other parts of the model and routed to Block 300 for fuel in the tar reformer catalyst regenerator.

2.3.5 Block 500, Alcohol Separation

Following alcohol synthesis, the product alcohol vapor is flashed and heat exchanged prior to being dehydrated with a molecular sieve. The molecular sieve is modeled with a simple separation block based on user-defined output component fractions. The resultant

dehydrated alcohol stream is processed with two distillation columns, the first separating off alcohols equal to or higher than propanol, and the second separating the product ethanol from methanol. Since one of the goals of the simulation was to maximize the yield of ethanol, the methanol vapor is compressed and recycled to the inlet of the synthesis reactor, as the synthesis catalyst is modeled as having methanol hydrocarbonylation activity. (Phillips, Aden et al. 2007)

2.3.6 Block 600, 700, and 900, Support Systems

An integrated boiler, turbine, condensate recovery, and boiler feedwater system is encompassed by Block 600. A formal boiler and steam drum system is not included in the model, rather an extensive heat balance is performed across all areas of the model to balance the needs of process heating and cooling. The heat balance controls the high pressure steam feed to the modeled condensing turbine, which in turn controls the amount of shaft work available. Both the heat and work balances throughout the model are open-loop. Heating and cooling equipment throughout the model is not directly connected to the steam system. Similarly, motors and compressors are not directly linked to the major sources of shaft work, the unreacted syngas decompressor and the main steam turbine.

Blocks 700 and 900 are support systems, with Block 700 providing basic modeling around cooling water systems and Block 900 a means to consolidate work streams. Work consumption/generation estimates are tabulated for each process area, and are summed together within Area 900 to calculate overall plant power requirements or surpluses.

2.4 Experimental

In order to evaluate the NREL thermochemical wood to mixed alcohols model, the most recent version (April 2007) was downloaded from the NREL extranet website, http://www.nrel.gov/extranet/biorefinery/aspen_models/. All necessary support files were included in this repository webpage. The following files shown in Table 4 were used for model evaluation:

Table 4. NREL mixed alcohols model files downloaded from NREL extranet

File Name	Purpose
sp0612m.bkp	Aspen backup file format of model
sp0612m.xls	VBA-enabled Excel™ techno-economic spreadsheet interface to model. Requires zetoolkit.dll from Aspen
sp0612m.sum	Aspen summary file containing all model run data. Model run April 17, 2006, with 2000 mt/day hybrid poplar feed
FortranMixedAlcohols.zip	Visual Fortran 6.6 compiled and linked .objs

Aspen Plus version 2006 without an outboard FORTRAN compiler was available for use from the NCSU Virtual Computing Lab (VCL) system. However, as the supplied linked object (.obj) files were compiled in the obsolete Compaq Visual Fortran 6.6, a new compiler was necessary to extend the basic capabilities of the NCSU VCL version of Aspen Plus 2006. Intel Visual Fortran Version 9.1 or higher was recommended by AspenTech as compatible with Aspen 2006, shown in Table 5. Intel Visual Fortran Version 11.1 was obtained to extend the useable application life with future versions of the Aspen environment.

Table 5. ASPEN environment and necessary compiler version matrix.

ASPEN Product Name	ASPEN Version Number	Appropriate Fortran Compiler
2004.x	13.2	Compaq Visual Fortran 6.6
2006.x	18	Compaq Visual Fortran 6.6, Intel Visual Fortran 9.1
V7.x	21 or higher	Intel Visual Fortran 9.1 or higher

As the VCL system is entirely virtual, and only accessible through Microsoft Remote Desktop, a new virtual computer image was required to include the requisite FORTRAN compiler. A new VCL image was constructed based on an existing image containing Microsoft Windows XP Service Pack 3, Aspen Plus 2006, and Intel Visual Fortran 11.1, and Excel 2003. The new image was configured to allow Aspen 2006 to properly access the new compiler, and placed into service.

Initial trials of the mixed alcohols model running under the Aspen Plus 2006 environment with recompiled BATYD5 and USRDC1 user subroutines indicated that the model would be more stable running under its native Aspen 2004.1 environment. An archived Aspen 2004.1 VCL image was located and reinstated. The compatible Compaq Visual Fortran 6.6 was included in the Aspen 2004.1 VCL image. Model operation under Aspen 2004.1 was more stable, and allowed exercise tests to move forward.

As will be further discussed in Chapter 2.5, modifications to the SETFEED calculator were necessary to allow intuitive changes to model feedstock parameters. Additionally, in order to obtain consistent model results in trials, the D505 RADFRAC block was replaced with an exact duplicate. An initial evaluation of the model operating window and its stability was carried out by starting with NREL's baseline hybrid poplar feedstock parameters, and

adjusting the ultimate analysis compositions to simulate more or less carbon content. Carbon mass percentage was started at the base 50.88%, and was decremented or incremented by 5% intervals, holding hydrogen, nitrogen, sulfur and ash constant. Oxygen was adjusted to keep the total elemental analysis equal to 100%. Proximate analysis was fixed at the NREL default percentages.

The final working evaluations of the effects of varying feedstocks composition reported here utilized experimental literature data for both ultimate and proximate analysis, serving as trial feedstock parameters for the mixed alcohols model. Table 6 shows the feedstock parameters supplied to the biorefinery model. All feedstock ultimate and proximate values were taken from Gaur and Reed, a compendium of biomass combustion data from several experimental sources. (Gaur and Reed 1998) The subset of feedstock materials was chosen with as wide a range of elemental carbon content as was possible, where the model was still deemed functional. Changes were made as necessary to model parameters to allow the biorefinery model to function. These modifications are also outlined in the Results and Discussion section.

To understand the variations in the composition of the different biomass feedstocks, all chosen feedstocks for the mixed alcohols model were plotted on a van Krevelen diagram, overlaid on experimental feedstock data from literature, shown in Figure 8. Van Krevelen diagrams were developed in the 1950's as a graphical method of characterizing coal structure and reactions. (van Krevelen 1950) The van Krevelen diagram provides a quick manner of evaluating where the chosen model feedstocks fall in a spectrum of possible solid biomass

fuels. Model reaction to dehydrated, lightly pyrolyzed wood, or *torrefied* wood, was of interest.

Table 6. Proximate analysis, ultimate analysis, and molar O/C ratio of feedstock survey biomass types.

	Proximate Analysis			Ultimate Analysis						
Biomass Type	FC	VM	Ash	C	H	N	S	O	Ash	O/C	H/C
Sugarcane bagasse	14.95	73.78	11.27	44.80	5.35	0.38	0.01	39.55	9.91	0.663	1.423
White Oak	17.20	81.28	1.52	49.48	5.38	0.35	0.01	43.13	1.65	0.654	1.296
Loblolly pine	12.76	86.83	0.41	50.25	5.97	0.00	0.00	43.34	0.44	0.647	1.416
Loblolly pine, 250°C torrefaction	11.80	87.70	0.50	50.73	6.21	0.12	0.00	42.44	0.50	0.628	1.459
NREL base poplar	15.29	83.84	0.87	50.88	6.04	0.17	0.09	41.90	0.92	0.618	1.415
Loblolly pine, 275°C torrefaction	16.40	83.00	0.60	52.27	6.13	0.15	0.00	40.85	0.60	0.587	1.398
Spruce	26.60	69.60	3.80	51.80	5.70	0.10		38.60	3.80	0.559	1.311
Loblolly pine, 300°C torrefaction	17.00	82.30	0.70	54.81	5.94	0.14	0.00	38.41	0.70	0.526	1.291
Peat	26.87	70.13	3.00	54.81	5.38	0.89	0.11	35.81	3.00	0.490	1.170
German Braunkole Lignite	46.03	49.47	4.50	63.89	4.97	0.57	0.48	24.54	5.55	0.288	0.927

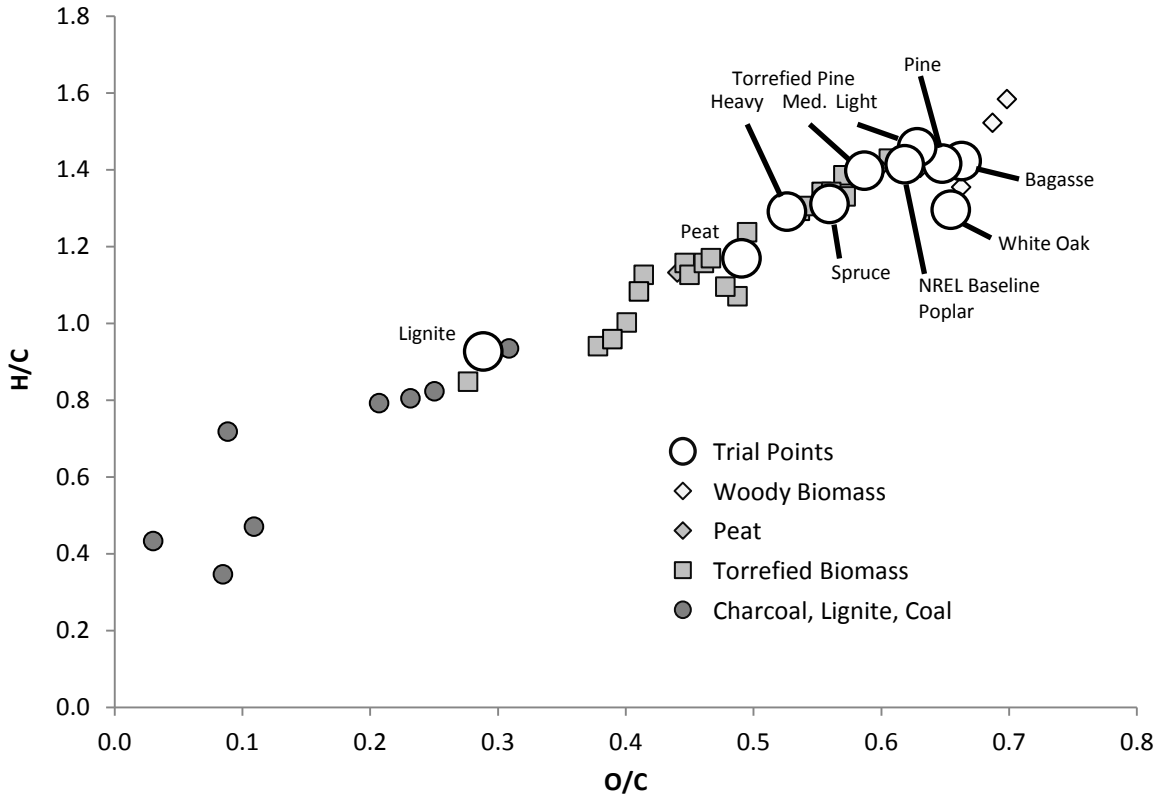

Figure 8. Van Krevelen plot showing O/C-H/C plots of the surveyed biomasses superimposed over representative types of biomass-derived fuels. (Bergman, Boersma et al. 2005)

2.5 Results and Discussion

Initial attempts to run the 2007 Phillip's model under the ASPEN 2006 environment yielded inconsistent results. Trial runs with the base model feedstock of hybrid poplar ended with severe ASPEN errors around the alcohol separation block, A500, and the overall heat balance calculator "QBALANCE." Troubleshooting uncovered extremely high reboiler and condenser heat duty values around the RADFRAC (distillation) block D505. Heat duty values in the range of 10^{35} BTU/hr were obviously incorrect and caused a cascade of errors in

the model. A workaround was implemented by noting all of the requiring engineering specifications for the D505 methanol/ethanol separation column, removing the original RADFRAC block from the model, and placing a new D505 block with identical specifications.

With the replacement of the D505 column, subsequent model runs went to completion without warnings or errors. Running the mixed alcohols model with the default biomass feed characteristics in the SETFEED calculator yielded the same output as that obtained by Phillips in 2007.

Figure 9 highlights general model inputs and outputs based upon the feedstock defaults provided by NREL.

Subsequent experimental runs varied feedstock conditions showed no obvious changes in model results at all points of the model. Following additional study, it was noted that the SETFEED calculator that was designed to specify the Stream 100 wood feed stream was not fully connected to the rest of the ASPEN model. The original SETFEED configuration allowed Stream 100 to have its wood and water components set at the initialization of the model. The calculator configuration did not allow the other necessary parameters to be exported back to the model feed stream. In order to make the operation of the SETFEED calculator more intuitive, the highlighted variable definitions shown in Table 7 were added.

Table 7. SETFEED calculator variable definitions.

Variable	Info. Flow	Definition
BDWOOD	Export	Mass-Flow Stream=100 Substream=NC Component=WOOD Units=lb/hr
XH2O	Export	Compattr-Var Stream=100 Substream=NC Component=WOOD Attribute=PROXANAL Element=1
WATFLO	Export	Mass-Flow Stream=100 Substream=MIXED Component=H2O Units=lb/hr
CAR	Export	Compattr-Var Stream=100 Substream=NC Component=WOOD Attribute=ULTANAL Element=2
HYD	Export	Compattr-Var Stream=100 Substream=NC Component=WOOD Attribute=ULTANAL Element=3
OXY	Export	Compattr-Var Stream=100 Substream=NC Component=WOOD Attribute=ULTANAL Element=7
NIT	Export	Compattr-Var Stream=100 Substream=NC Component=WOOD Attribute=ULTANAL Element=4
ASH	Export	Compattr-Var Stream=100 Substream=NC Component=WOOD Attribute=ULTANAL Element=1
SUL	Export	Compattr-Var Stream=100 Substream=NC Component=WOOD Attribute=ULTANAL Element=6
PFC	Export	Compattr-Var Stream=100 Substream=NC Component=WOOD Attribute=PROXANAL Element=2
PVM	Export	Compattr-Var Stream=100 Substream=NC Component=WOOD Attribute=PROXANAL Element=3
PASH	Export	Compattr-Var Stream=100 Substream=NC Component=WOOD Attribute=PROXANAL Element=4
SSULFT	Export	Compattr-Var Stream=100 Substream=NC Component=WOOD Attribute=SULFANAL Element=2

Predictable SETFEED calculator operation allowed for experimental model runs to evaluate the effects of feedstock change on model operation and results. Figure 10 illustrates the model's gasifier section operation relative to default hybrid poplar when presented with variable feedstock composition characteristics. Since the gasifier FORTRAN user model is directly based on the Battelle gasifier correlations developed by Bain, the gasifier outlet compositions are directly related to temperature. This is a limitation with the model since it does not allow for independent variation in the biomass composition, while holding the gasifier temperature constant.

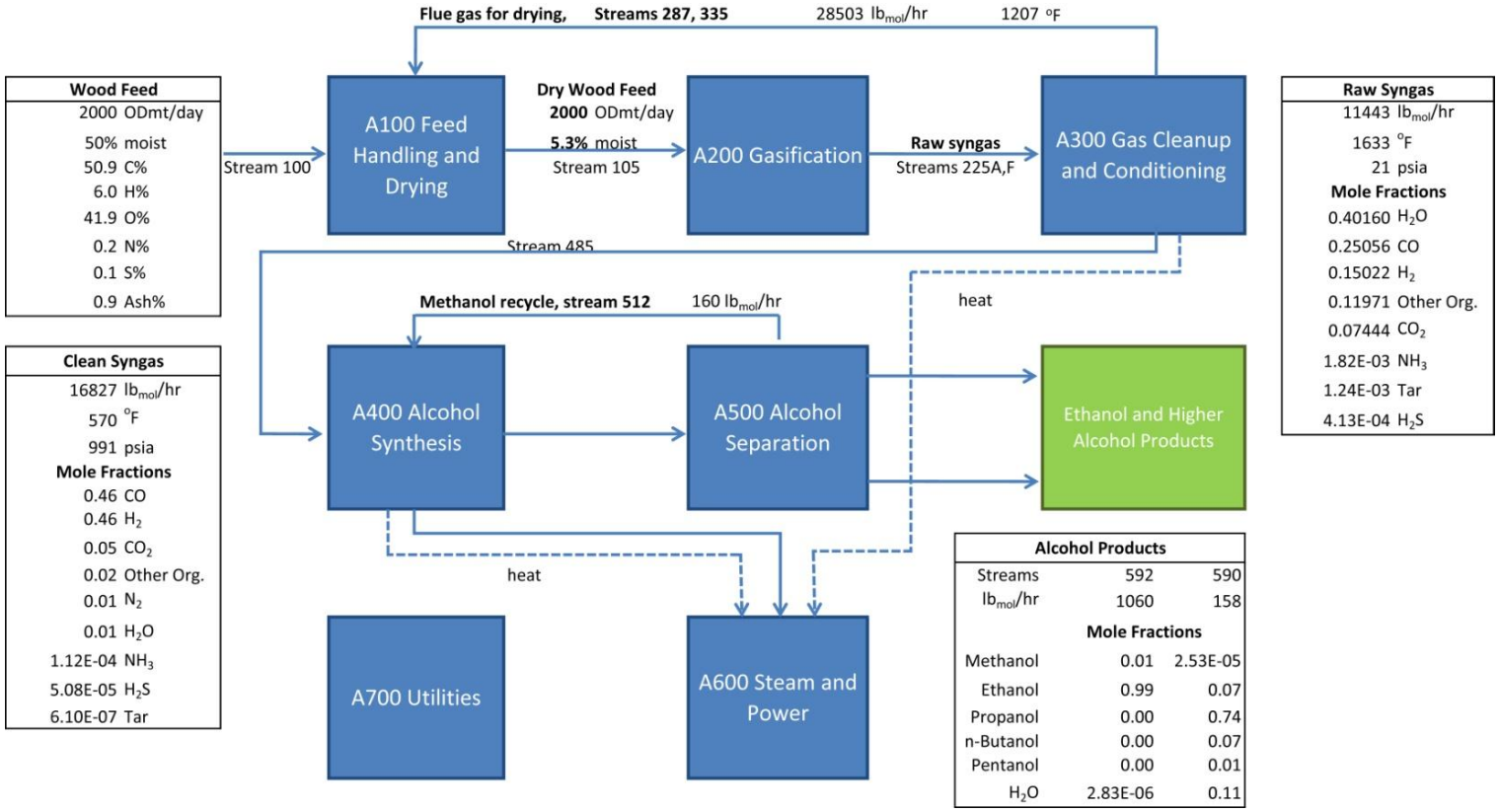

Figure 9. Phillips mixed alcohols model normal operation overview results.

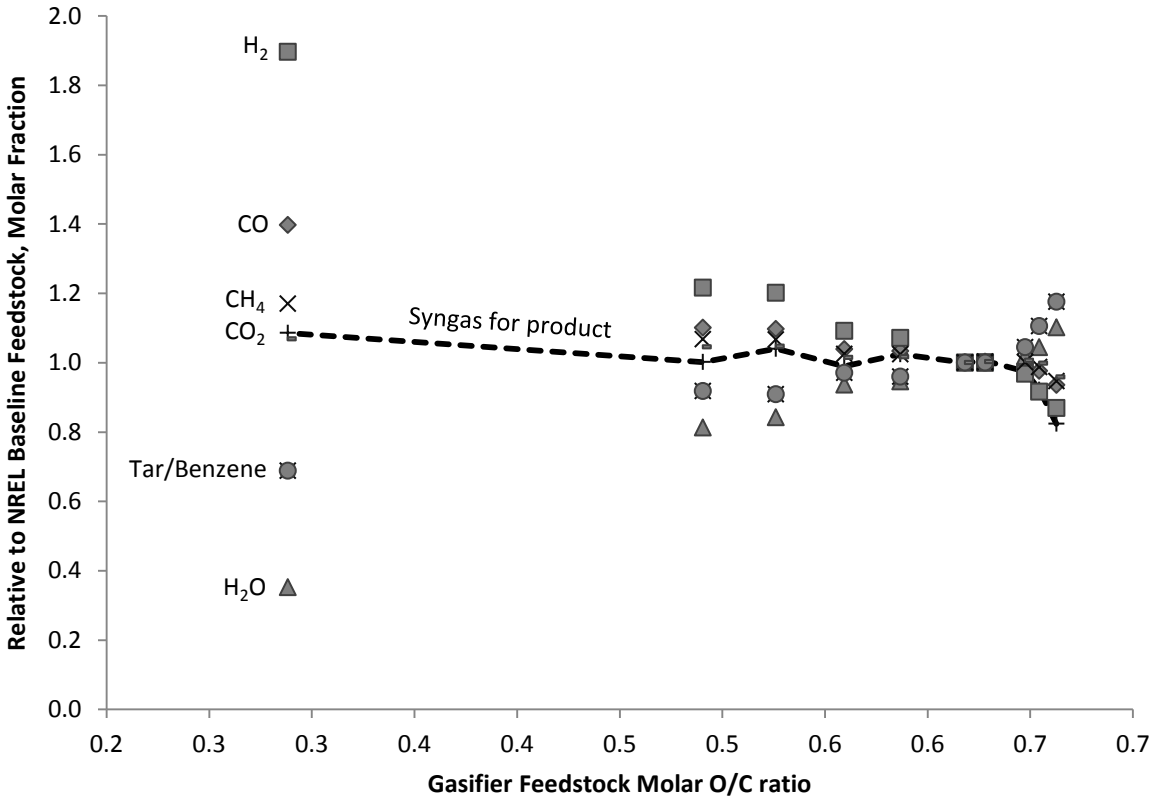

Figure 10. NREL mixed alcohols model gasifier outlet components with select biomass feedstocks.

Refer to Table 3 for outlet component-temperature correlations. Gasifier outlet temperatures presented in Stream 225 were assumed to be representative of the internal gasifier temperature. Graphing the temperature of Stream 225 with varying biomass feedstocks showed a strong negative trend between temperature and biomass O/C ratio. The ASPEN RYIELD block R201 approximates the pyrolysis section of BCL indirectly heated gasifier. The self-regulating feedback loop between the two units of the gasifier was demonstrated by examining the heat and material balances around R201 and the R202 char combustor. The

initial call for the R201 block and its associated BATYD5 user routine specifies the gasifier temperature of 1500 °F. After the BATYD5 routine determines the individual gaseous components in the outlet stream and calculates the overall char flow based on temperature, elemental balances are used to assign the remaining material to the char. The R202 RSTOIC reactor block modeling the char combustor section of the BCL gasifier unit showed response to variations in input char flow, ultimate analysis, and heating value. Generally, as outlined in Table 8, the enthalpy of olivine returning to the pyrolysis section increases as a function of feedstock carbon content.

Table 8. General heat and material flows around the R202 char combustor.

Feedstock	Feedstock O/C Ratio	Char Flow Kg/hr	Char MJ/kg	Olivine Enthalpy GJ/hr
Sugarcane bagasse	0.66	25057	16.90	2.258
White oak	0.65	19019	23.55	2.276
Loblolly pine	0.65	16728	29.19	2.320
Torrified loblolly pine, 250˚C	0.63	15235	33.16	2.351
NREL base poplar	0.62	15342	32.52	2.353
Torrified loblolly pine, 275˚C	0.59	15050	34.93	2.398
Spruce	0.56	17943	28.68	2.412
Torrified loblolly pine, 300˚C	0.53	16000	35.11	2.469
Peat	0.49	18375	29.53	2.475
Lignite	0.29	24508	30.28	2.792

Olivine sensible heat determines the operating temperature of the gasifier, and closes the feedback loop between the two gasifier sections. Char higher heating value (HHV) was estimated using ASPEN reported ultimate analyses and a HHV correlation equation for solid and liquid fuels. (Equation 5) (Channiwala and Parikh 2002) Gasifier temperature response is shown in Figure 11.

$$HHV = 0.3491C + 1.1783H + 0.1005S - 0.1034O - 0.0151N - 0.0211A \quad (5)$$

Where *C, H, S, O, N,* and *A* represent weight fractions of carbon, hydrogen, sulfur, oxygen, nitrogen, and ash respectively. HHV is returned in MJ/kg.

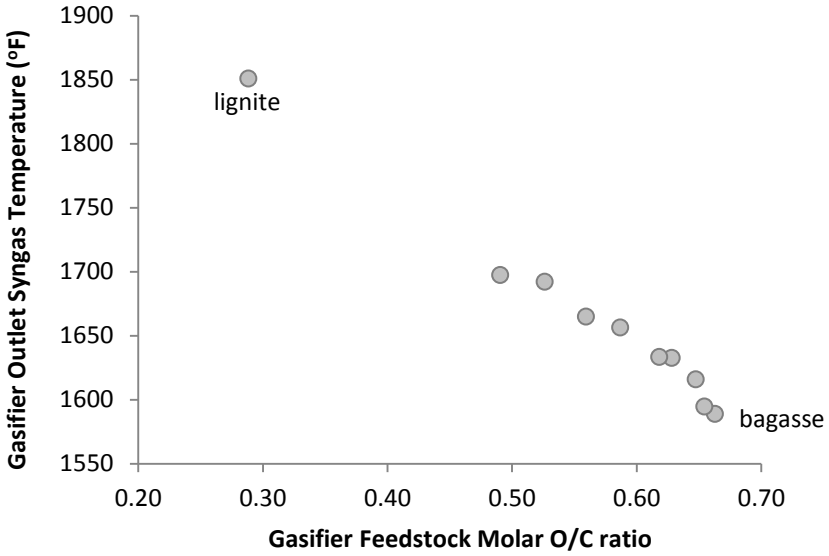

Figure 11. Gasifier outlet temperature as a function of feedstock O/C molar ratio.

As noted earlier, the model gasifier response shown in Figure 10 is entirely dictated by its internal temperature, as the yield of the output gases and tars are correlations based on gasifier temperature rather than chemical differences in the feedstocks. Model response of the gasifier directly follows literature results for the components CO, and H_2. A decrease in feedstock O/C ratio is linearly related to gasification temperature. Increased gasifier temperature should yield increased CO and H_2 concentrations as the Boudouard (refer back

to Equation 2) and water-gas reaction (Equation 6) are driven forward with the increase in temperature, (Basu 2006) resulting in increased concentrations of their respective products.

$$\mathbf{CO} + \mathbf{H_2O} \rightleftharpoons \mathbf{CO_2} + \mathbf{H_2} \quad \textbf{(6)}$$

Tar generation in pyrolysis is dependent upon the temperature regime. In the range below 900-1000˚C, tar formation increases as pyrolysis temperature increases. Above 1100˚C, product syngas tar composition is inversely proportional to gasification temperature, as long-chain hydrocarbons are comminuted with increased thermal energy input. (Kinoshita, Wang et al. 1994; Basu 2006) The modeled results of decreased tar production proportional to reduced O/C ratio, and hence increased pyrolysis/gasification temperature, generally follow these temperature regime rules-of-thumb. Reported literature results from air/steam gasified fluidized bed gasifiers are qualitatively similar to those seen in the NREL model. (Kinoshita, Wang et al. 1994; Li, Grace et al. 2004; Corella and Sanz 2005)

The model response observed in regards to syngas methane composition does not follow equilibrium predictions for the calculated process temperatures, but does show results to similar gasifier configurations results from literature. Basu indicates that the methanation reaction can take place under pyrolysis/gasification conditions. The methanation reaction shown in Equation 7 is exothermic, and therefore the production of methane should not be thermodynamically favored at higher temperatures. (Desrosiers 2002; Reed 2002; Basu 2006)

$$\mathbf{C + 2H_2 \rightleftharpoons CH_4} \quad \textbf{(7)}$$

However, model results show syngas methane composition to be directly proportional to gasifier temperature. As the R201 pyrolysis/gasifier block is controlled primarily by the BCL correlations developed by Bain, the methane response to temperature is probably tied to particular process configurations of the Battelle gasifier. The BATYD5 user routine also allows for mathematical adjustments to be made specifically for the correlation-derived syngas methane concentration against CO and CO_2 (Craig 1993), however those adjustments were not utilized during model exercise. Experimental results from other indirectly heated or circulating fluidized bed gasifiers show similar presence of methane (Kinoshita, Yue et al. 1991), indicating that the Battelle gasifier is not unique. The BCL gasifier experimental data (Feldmann, Paisley et al. 1988) for syngas methane concentration likely indicates that as the feedstock is being heated to gasification temperatures, it is subjected to thermal energies and heating rates that support fast pyrolysis. Substantial methane production can occur at pyrolysis temperatures (Milne 2002), and it should be noted that the title of the Battelle-Columbus gasifier project report from Feldmann, Paisley, et al. references "methane-rich" product gas. Feldmann and co-workers attribute the production of methane and ethane in the BCL gasifier, and hence the NREL mixed alcohols model, to pyrolysis. Additionally, the direct relationship between gasifier temperature and syngas methane concentration can be linked to the increasing amounts of tar cracking that take place at gasification temperatures. (Hanping, Bin et al. 2008)

Syngas water content results from the Phillips, et al. model appear be consistent with thermodynamic equilibrium trends and literature results for fast pyrolysis. Gasification/bed fluidization steam and feedstock biomass post-dryer moisture is held constant in the model. With the limited input of water with the biomass the water is reasonably predicted to come from the fast pyrolysis reactions. Demirbaş finds that yield of pyrolytic water decreases with the temperature of pyrolysis. (Demirbaş 2005) At the same time the water-gas and water-gas shift gasification reactions consume water at a rate that increases with increasing temperature. (Basu 2006) As hydrogen is a product of both reactions, we would expect to see the syngas hydrogen composition the inverse of water content. The combination of a diminishing source and increasing consumption of water produces an inverse relationship between gasifier temperature and syngas water content seen in the model results.

The model shows minimal temperature dependence on CO concentrations. Experimental results from literature are inconclusive about product syngas carbon dioxide concentrations. Lv et al. found no appreciable correlation between gasifier temperature and syngas CO_2 when evaluated in a low-pressure air/steam fluidized bed gasifier. (Lv, Chang et al. 2003) Other workers investigating air/steam fluidized bed gasifiers found experimental results that indicated a negative trend of CO_2 concentration with respect to gasifier temperature. (Wang and Kinoshita 1992; Hanping, Bin et al. 2008) A negative relationship between product syngas CO_2 concentration and reactor temperature would be expected considering the increased rate of the Boudouard reaction with increased temperature. In that scenario, CO_2 concentration would be the inverse of syngas CO composition. Zhou et al

noted similar results when gasifying biomass under Ar and pure O_2. (Zhou, Masutani et al. 2000) Again, it is possible that the process configuration of the Battelle gasifier is such that CO_2 consumed in the Boudouard reaction is offset by CO_2 produced from tar cracking and the water-gas shift reaction, with the offset positively correlated with temperature.

The tar reformer/gas cleanup system in the mixed alcohols model was also examined for response to changes in biomass feedstock supplied to the gasifier. Simulation results were driven by the syngas composition from the gasifier and the results of reactions modeled in the tar reformer section. CO, H_2O, CH_4, H_2, and tar/benzene concentrations from the cleanup section tracks their respective concentrations coming from the gasifier, with the exception of those modeled for the lowest O/C ratio feedstock – lignite. The syngas cleanup section model results are shown in Figure 12. The lower cleanup section H_2 concentration is of note as the gasifier outlet H_2 concentration is substantially higher for lignite. Due to the manner that tar reformer steam addition is calculated, no reformer steam is added in the model run for lignite. Furthermore, reformer syngas temperature is higher for lignite, and should drive forward the cracking/reformer reactions. A possible explanation for the reduced H_2 concentration may lie in the reactor modeling methodology used for the R303A REquil tar reformer. An REquil Aspen reactor block may have its reactions specified by a temperature approach method, or by a molar extent method. The mixed alcohols model recycles unconverted syngas from the synthesis reactor as well as purged alcohol streams back to the tar reformer. All alcohol conversions to H_2 and CO are specified by molar extent, and therefore simple fraction of possible extent of reaction. The lack of tar reformer steam

input may manifest itself in limiting alcohol reforming to H_2 and CO, leading to a reduction in clean syngas H_2 content relative to the one derived from the NREL baseline feedstock.

The mixed alcohols model was designed to calculate a yield of C_1 through C_5 alcohols in order to derive a reasonable estimate of MESP. The simulation output of the synthesis section was of particular interest as is contains some of the most tangible model results. As would be expected, the alcohol output of synthesis tracks carbon input to the gasifier. There is a direct, almost monotonic, relationship between feedstock carbon input and synthesis alcohol production, illustrated in Figure 13.

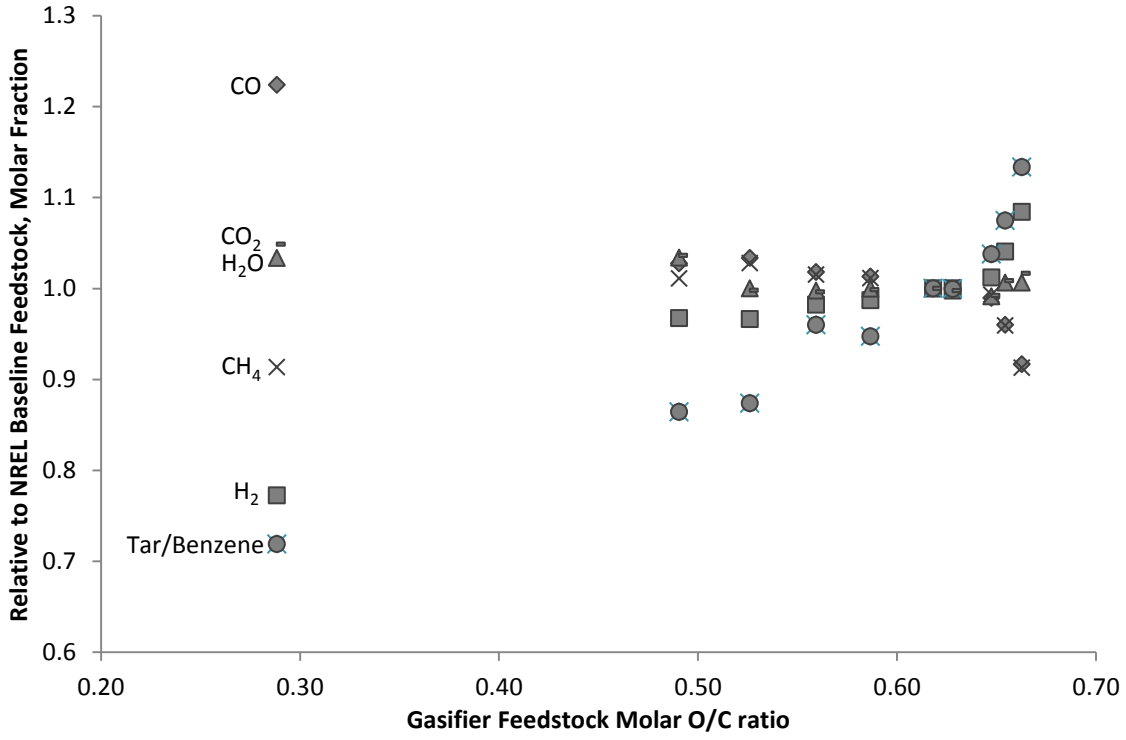

Figure 12. Cleanup section molar flows, relative to those obtained with the hybrid poplar baseline feedstock.

The non-linear response shown by the two data points of the feedstocks with the highest O/C ratio was interesting to note. In the process of examining the reduced alcohol production, it was realized that a source of run-to-run inconsistency had not been accounted for. The mixed alcohols model attempts to simulate an integrated plant, calculating steam and power requirements for each process section. Steam is generated by heat exchanging feedwater with heat sources like the tar reformer and the alcohol synthesis reactor.

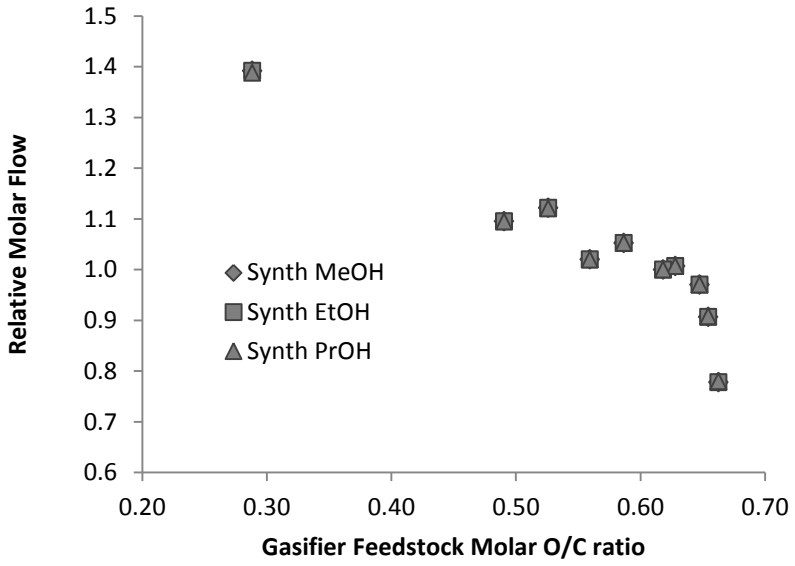

Figure 13. Product ethanol molar flows, relative to NREL model run with baseline feedstock.

One of the original project goals for the NREL model was that the plant would be energy self-sufficient. All heat and power would be generated onsite, at the expense of syngas production allocation for synthesis. The model therefore calculates a net work value for the plant, considering all heat and power required against all sources, with the intention of W_{net}

equaling zero. It was discovered that the syngas allocation between alcohol production and heat/power was not controlled. By design, in order to set the model plant's net work to zero, a manual adjustment of the tar reformer fuel-combustor reactor (R301B) temperature was necessary. The reactor temperature is adjusted in an Aspen design spec, R301BTEM, as a target. The design spec vary controls the raw syngas allocation for heat and power. Figure 14 shows the plant net work in horsepower if this reactor temperature is held constant at the default 1775.5 ˚F. Figure 15 shows the allocation of syngas to alcohol production, once W_{net} was zeroed for each model feedstock trial. The same non-linearity shown in Figure 13 is obvious in the syngas allocation figure. Finally, tracing back the two data points that showed the pronounced reduction in syngas allocation for synthesis revealed a combination of lower carbon ultimate analysis and significantly higher ash content. The two feedstock parameters together insured that less carbon was available for alcohol production.

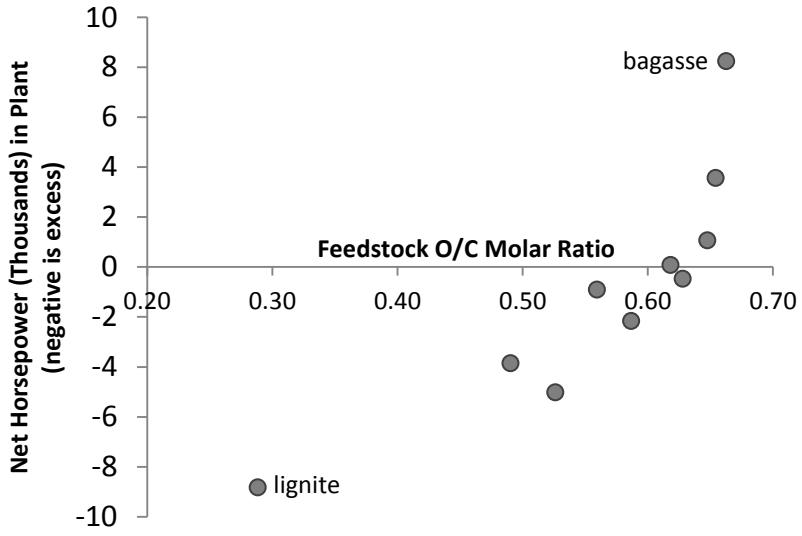

Figure 14. Feedstock O/C ratio effects on model energy closure. Basis is R301 temperature of 1775.5 °F.

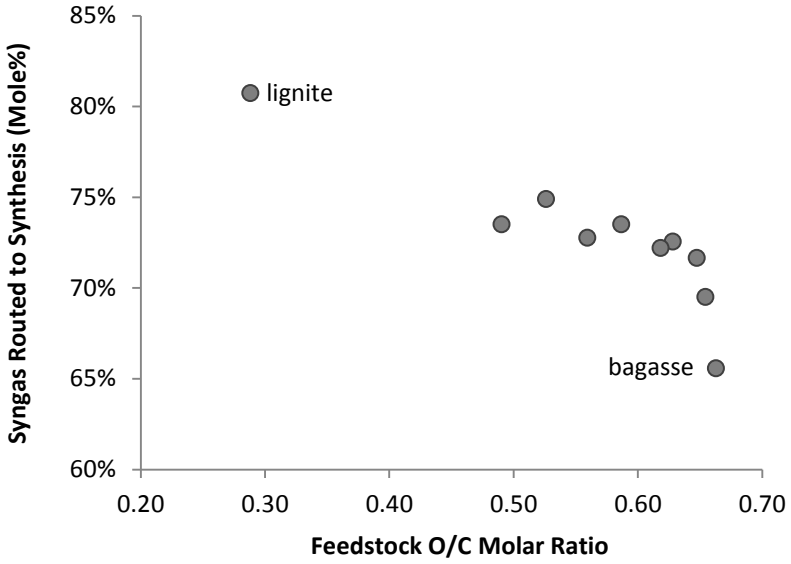

Figure 15. Energy closure effects on syngas diversion from the fuel synthesis pathway. W_{net} set to zero for each feedstock.

2.7 Conclusions

Thorough inspection and troubleshooting of the NREL thermochemical mixed alcohols model yielded a framework to perform operating window tests, establishing the utility of the model for applications beyond its original design. A straightforward experiment was conducted around the model to evaluate the effects varied feedstock characteristics would have on model operation and results. Experimental results using a series of biomass feedstocks with a wide range of carbon contents indicates that the NREL model can provide reasonable results for feedstocks with compositions other than the design hybrid poplar. The NREL model, with some simple modifications, can serve as a useful tool to explore the thermochemical biomass to mixed alcohols process.

Successful use of the NREL model was found to have several caveats. Feedstock characteristics are critically important, and range of carbon content or O/C ratio examined in the study represented the widest range in which the NREL model would yield meaningful results. The implementation of the gasifier, based on empirical results from a single PDU, may not accurately simulate real gasification equipment. Product syngas composition generated by the gasifier model should be a general indication of performance. Similarly, non-kinetic reactor model implementations for tar reforming and mixed alcohol fuel synthesis are likely only suitable for discerning major trends when the model is away from its design center.

CHAPTER 3

Comparison of Therminator[1] and Conventional Syngas Cleanup Technologies and Implications for Selected Synthesis Processes

3.1 Introduction

Syngas composition, in particular the ratio of CO to H_2, has been modified to improve its utility for different applications almost since its discovery. Nineteenth century engineers employed a rudimentary syngas tar cracking to clean street-lamp illuminating gas. In these early tar cracking units, hydrocarbon-laden syngas was passed over incandescent masonry reactor surfaces to breakdown tars which could foul gas distribution piping. (Shadle, Berry et al. 2000) Early twentieth century industrial processes such as Haber's ammonia, or Fischer and Tropsch's hydrocarbon wax synthesis sought to minimize iron catalyst poisoning by syngas sulfur and water removal. (Anderson 1984; Jennings and Ward 1989)

Through World War II, coal was the primary feedstock for gasification technologies. As such, cleanup technologies were designed to deal with issues specific to coal syngas: sulfur and heavy hydrocarbon contamination. However, limited wartime supplies of coal led to the increased use of biomass as a gasification feedstock, particularly for civilian applications. While cheap fossil fuel availability for 30-40 years post-war curtailed

[1] The Therminator system is an experimental syngas cleanup technology developed by the Research Triangle Institute, Research Triangle Park, NC.

investment into both coal and biomass syngas development, the 1970's fuel crisis renewed research interest into biomass as a potentially renewable fuel and chemical building block. (Ahrenfeldt and Knoef 2005)

Syngas derived from biomass gasification can pose greater tar loading issues than coal (Higman, van der Burgt et al. 2008), while still potentially introducing similar sulfur contamination. Syngas cleanup technologies, then, are just as important for an "environmentally green" feedstock such as biomass as they were for coal.

A cursory examination of gasification literature indicates that a substantial amount of research has been conducted just around biomass syngas tar cleanup. A cleanup technology such as catalytic tar cracking offers a solution for destroying a contaminant that can adversely affect many subsequent applications, while keeping the tar's chemical and thermal energy in the syngas stream. (Dayton 2002) Gas cleanup, therefore, represents a critical process area within a gasification-based biorefinery and a major area of concern for potential investors. (Bridgwater and Bolhàr-Nordenkampf 2005)

The syngas cleanup technologies considered in this research encompass more established processes as those modeled by Phillips, et al for the National Renewable Energy Laboratory's (NREL) thermochemical bioethanol report (Phillips, Aden et al. 2007), and a novel single catalytic reactor cleanup process proposed by the Research Triangle Institute (RTI, Research Triangle Park, NC). Both approaches are catalyst-based solutions. The RTI Therminator is targeted to remove similar syngas contaminants, ideally with less equipment and therefore lower investment capital. This modeling study was conducted to compare the

efficacy of the Therminator syngas cleanup system against conventional technologies and to evaluate any potential major fuel synthesis process implications.

3.2 Background of Comparison Cleanup Technologies

3.2.1 Overview of NREL Conventional Cleanup Technology

A detailed discussion of NREL's biomass to fuels research programs is presented in Section 2.2. NREL research in this area spans almost 30 years, and includes both extensive process modeling and pilot-scale gasification trials. Wooley and coworkers developed a rigorous techno-economic modeling framework in 1999 by incorporating experimental data, ASPEN process models, and equipment sizing and engineering from external collaborators and literature searches. This framework was implemented for several NREL research projects, including a biomass to hydrogen biorefinery model developed by Spath, et al in 2005. Spath's biomass to hydrogen model included conventional syngas cleanup technology of catalyzed tar reforming, syngas scrubbing and quenching, amine-based acid gas removal, and LO-CAT sulfur removal. (Spath, Aden et al. 2005) These syngas cleanup unit operations were largely duplicated in the modeling work by Phillips, et al in 2007. The basis of the research presented here is the NREL Thermochemical Ethanol via Indirect Gasification and Mixed Alcohols Synthesis of Lignocellulosic Biomass. (Phillips, Aden et al. 2007) A high-level block diagram of the NREL cleanup operations is presented in Figure 16.

Catalyzed syngas tar reforming for biomass gasification has been under investigation since the early 1980's (Mudge, Weber et al. 1981; Baker, Brown et al. 1986; Milne, Evans et al. 1998), utilizing metallic catalysts such as those used in the petrochemical industry containing Ni (Stevens 2001), and non-metallic materials such as potassium carbonate (K_2CO_3), dolomite ($CaMg(CO_3)_2$), or olivine ($(MgFe)_2SiO_4$). (Corella, Toledo et al. 2004) The NREL mixed alcohols model employs a non-metallic catalyst in tar cracking duty, based upon results from process development unit (PDU) testing at Battelle-Columbus Laboratories and pilot-scale implementation at the SilvaGas/FERCO demonstration gasifier in Burlington, VT. (Paisley and Anson 1998; Stevens 2001) Deactivated catalyst is regenerated in a combustion reactor and returned to the tar reformer. (Phillips, Aden et al. 2007)

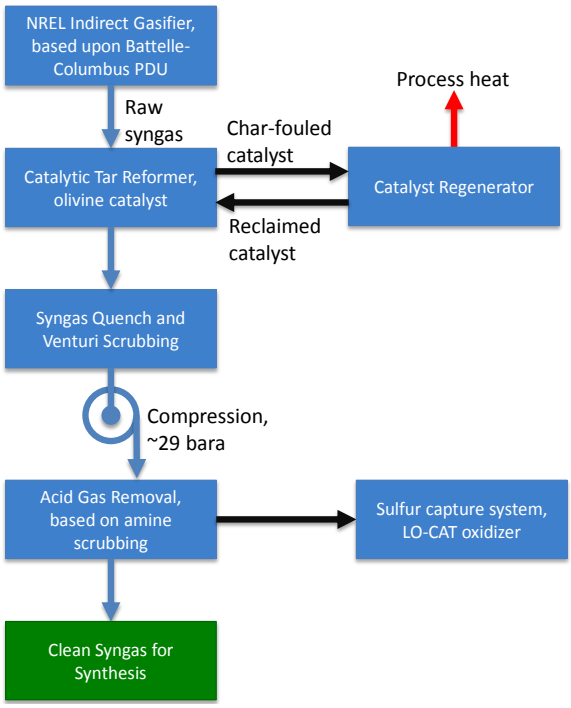

Figure 16. Simplified block diagram of NREL mixed alcohols model cleanup process area. (Phillips, Aden et al. 2007)

The scrubbing and quenching operations employed downstream of the tar reformer are straightforward, and have been widely employed for over 100 years. (Pell, Dunson et al. 2008) The venture scrubber and quench system were included in the NREL process primarily to remove tar reformer catalyst particulate carryover, but also serve as a polishing step in the removal of ammonia and tar. (Phillips, Aden et al. 2007)

Finally, CO_2 and H_2S are removed from the syngas as a preparation for fuel synthesis. The "acid gas" removal system is designed around a conventional amine scrubbing system, an industrial standard process that has been used commercially since its invention in 1930. (Bottoms 1930; Higman, van der Burgt et al. 2008) Monoethanoamine is utilized in a scrubbing tower to absorb most of the CO_2 and H_2S from the syngas, rendering it suitable for the subsequent processes of compression and catalytic mixed alcohols synthesis. (Phillips, Aden et al. 2007)

3.2.2 Overview of RTI Therminator Cleanup Technology

Integrated gasification combined cycle (IGCC) power generation systems were originally conceived as a more energy efficient improvement to conventional coal-fired Rankine cycle boiler/turbogenerator processes. (Gupta, Gangwal et al. 1992) Utilization of coal as a fuel source has the inherent issue of sulfur contamination, which poses material problems for turbine components when used in IGCC systems. (Gangwal, McMichael et al. 1992) In the early 1980's, DOE's Morgantown Energy Technology Center (METC) conducted the initial research on the use of zinc ferrite, $ZnFe_2O_4$, as reusable sorbent system

for hot-gas desulfurization (HGD). (Gupta, Gangwal et al. 1992) This research progressed to sorbent testing by Gangwal and workers at RTI in the late 1980's. (Gangwal, Stogner et al. 1989) Gangwal, et al found that while zinc ferrite was effective as a regenerable sulfur sorbent, its use in fluidized bed reactors was temperature limited to 550°C. Zinc attrition at higher temperatures lead to changes in sorbent porosity and a loss of reactivity. (Gupta, Gangwal et al. 1992) By 1995, RTI's HGD research was focused on zinc titanate, Zn_2TiO_x (where x= 3 or 4). (Gangwal, Gupta et al. 1995) Hot-gas desulfurization sorbent attrition and sintering at higher temperatures was reduced by the use of zinc titanate. (Swisher, Yang et al. 1995) Attempts to further improve the reactivity and physical properties of zinc titanate sorbents were made by RTI, accomplished by first reacting oxides of bivalent metals such as Mg, Ca, Zn, or Ni with alumina sorbent support media, and then incorporating zinc titanate. (Vierheilig, Gupta et al. 2004)

RTI has also studied the potential to combine the properties of the attrition-resistant zinc titanate sorbent with catalytic tar cracking and ammonia decomposition activity. The resultant catalyst system has been tested in the laboratory and pilot plants using a simplified bubbling-bed reactor. (Dayton 2009) The Therminator syngas cleanup process is based around this bubbling bed catalytic reactor and its accompanying catalyst regenerator/combustor, and is shown in Figure 17.

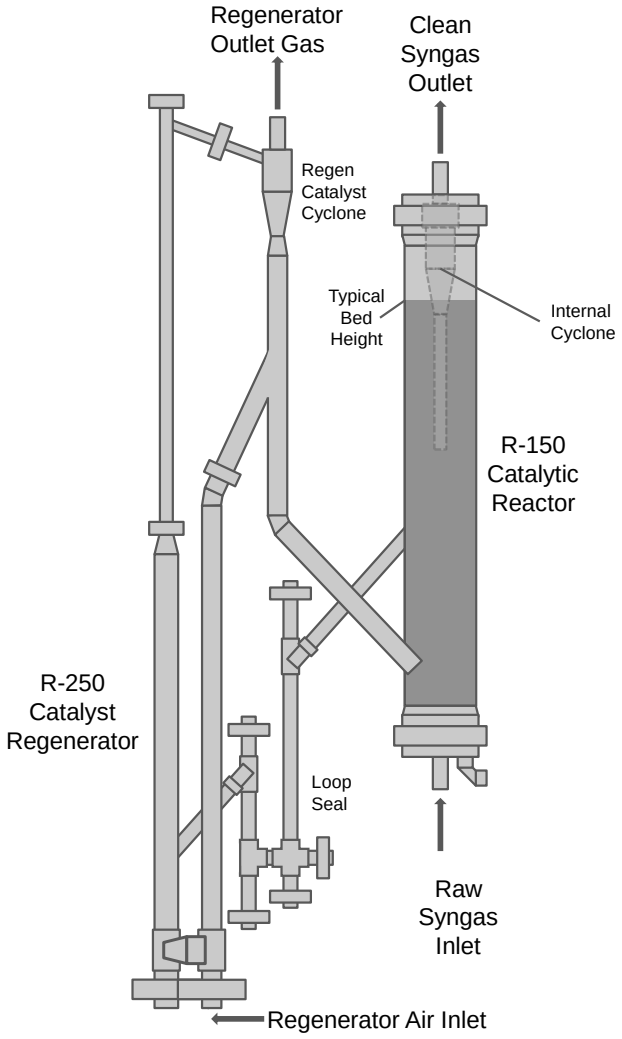

Figure 17. Therminator syngas cleanup reactor and catalyst regenerator. Figure adapted from Dayton, 2009.

3.3 Experimental

In order to quickly evaluate process comparisons between Therminator technology currently being developed and existing conventional syngas cleanup systems, computer

models for both technologies under consideration were required. RTI provided an ASPEN One V7.1 model of the Therminator system based on aspirational design specifications to serve as a research starting point. (Kalluri 2009) Therminator ASPEN model background information is outlined in Section 3.3.2. Basic model information for conventional cleanup technology as represented by the NREL mixed alcohols model follows in Section 3.3.1.

3.3.1 NREL Mixed Alcohols Model Background

Setup details of Phillip's 2007 version NREL mixed alcohols model were outlined in Chapter 2. Briefly, after the proper ASPEN environment was established, and the correct support files for the NREL model were compiled, initial model exercising was performed. Subsequent model tracing, troubleshooting, and minor alterations provided a stable platform for model exploration and manipulation. ASPEN version 2004.1 was used for the integrated NREL model; all other models were run within ASPEN One V7.1.

In the initial exercise of the complete NREL mixed alcohols model, a series of ten biomass-based gasifier feedstocks were selected as a subset of biomasses from Gaur and Reed's compendium (Gaur and Reed 1998). The selected biomass feedstocks represented the widest range ultimate carbon compositions that would allow the NREL model to reach convergence. Table 9 details the feedstocks used for gasification.

The cleanup block (A300) was isolated from overall NREL model to allow standalone operation and eliminate instabilities elsewhere in the model. All other sections

were deleted from the model, and any external recycle streams converted to input streams with appropriate values. ASPEN calculators or design specifications required for cleanup were left in the model. Where necessary, the remaining calculators and design specs referencing removed equipment or streams were modified to account for their input and output streams. Multiple passes of validation were carried out to ensure that the standalone NREL cleanup model yielded the same results as the complete model. Following the standalone cleanup validation, former model recycle stream flows such as unreacted syngas from alcohol synthesis were set to zero to make the two cleanup technologies comparable.

Table 9. Proximate, ultimate analysis, O/C, and H/C data of selected gasifier feedstocks.

	Proximate Analysis			Ultimate Analysis							
Biomass Type	FC	VM	Ash	C	H	N	S	O	Ash	O/C	H/C
Sugarcane bagasse	14.95	73.78	11.27	44.80	5.35	0.38	0.01	39.55	9.91	0.663	1.423
White Oak	17.20	81.28	1.52	49.48	5.38	0.35	0.01	43.13	1.65	0.654	1.296
Loblolly pine	12.76	86.83	0.41	50.25	5.97	0.00	0.00	43.34	0.44	0.647	1.416
Loblolly pine, 250°C torrefaction	11.80	87.70	0.50	50.73	6.21	0.12	0.00	42.44	0.50	0.628	1.459
NREL base poplar	15.29	83.84	0.87	50.88	6.04	0.17	0.09	41.90	0.92	0.618	1.415
Loblolly pine, 275°C torrefaction	16.40	83.00	0.60	52.27	6.13	0.15	0.00	40.85	0.60	0.587	1.398
Spruce	26.60	69.60	3.80	51.80	5.70	0.10	0.00	38.60	3.80	0.559	1.311
Loblolly pine, 300°C torrefaction	17.00	82.30	0.70	54.81	5.94	0.14	0.00	38.41	0.70	0.526	1.291
Peat	26.87	70.13	3.00	54.81	5.38	0.89	0.11	35.81	3.00	0.490	1.170
German Braunkole Lignite	46.03	49.47	4.50	63.89	4.97	0.57	0.48	24.54	5.55	0.288	0.927

3.3.2 RTI Therminator Model Background

An ASPEN flow sheet of the main Therminator system and the syngas quenching subsystem is presented in Figure 18 and Figure 19. The model design is centered around three ASPEN RStoic reactors, and therefore returns equilibrium product concentrations based on fractional

conversions of defined reactions. Reaction extents are based on aspirational or RTI proprietary results. Reactions carried out in each of three reactors, with their respective extents, are shown in Table 10. Tar was represented by naphthalene in the model, decompositions were catalyzed by tungsten carbide (WC), and $ZnTiO_3$ was used as a sorbent. (Kalluri 2009)

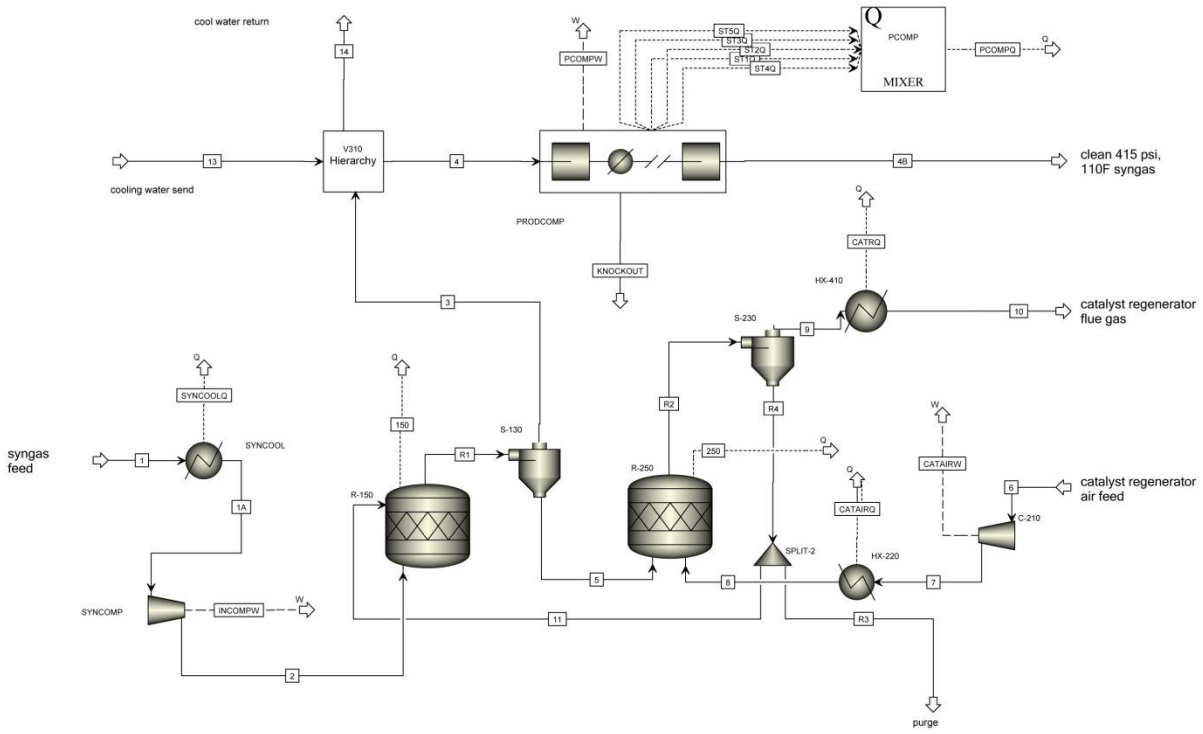

Figure 18. RTI Therminator ASPEN model flow sheet. (Kalluri 2009)

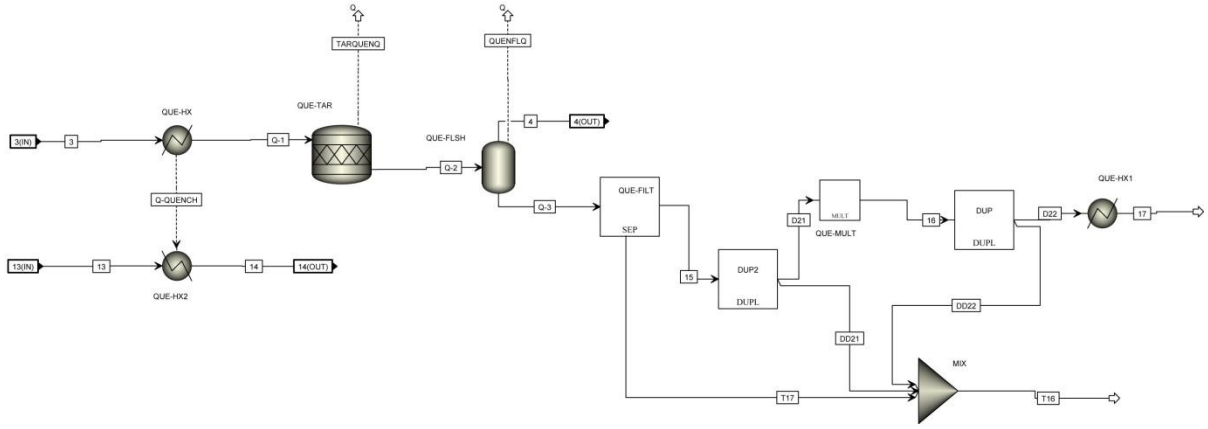

Figure 19. RTI Therminator ASPEN model quench subsystem flow sheet. (Kalluri 2009)

Table 10. Therminator model foundation reactors and their reactions and extents. (Kalluri 2009)

Equipment	Reaction	Reaction Purpose	Extent
Therminator Adsorber, R-150	Tar → $4H_2$ + 10C (char)	Tar decomposition	99% tar
	$H_2S + ZnTiO_3 \rightarrow ZnS + H_2O + TiO_2$	H_2S adsorption	>99% H_2S
	$NH_3 \rightarrow 1.5\ H_2 + 0.5N_2$	NH_3 decomposition	>99% NH_3
Catalyst Regenerator, R-250	C (char) + $O_2 \rightarrow CO_2$	Char combustion	100% C
	$ZnS + 1.5\ O_2 + TiO_2 \rightarrow ZnTiO_3 + SO_2$	Sorbent regeneration	100% ZnS
Quench Vessel, QUE-TAR	Tar (g) → Tar (s)	Tar condensation	100% tar

In this configuration the syngas stream boundary conditions were significantly different than that of the NREL model. Unit operations were added to the Therminator flow sheet to make temperature and pressure conditions comparable with the NREL model. Compressor blocks were added to the both the syngas inlet and outlet streams, and the each compressor's final internal interstage cooler configured to deliver the appropriate output gas

temperature. Table 11 describes the differences in model boundary conditions between the two models.

Table 11. Syngas stream boundary conditions for NREL cleanup and Therminator models.

Stream	NREL Cleanup	Therminator
Raw syngas inlet temp (˚C)	890	650
Raw syngas inlet pressure (MPa)	0.148	0.224
Clean syngas outlet temp (˚C)	43	46
Clean syngas outlet pressure (MPa)	2.861	0.224

3.3.3 Initial Syngas Cleanup Model Exercises

Once the conventional technology syngas cleanup section was removed from the overall NREL model, it was exercised using the 10 sample syngas stream compositions obtained from the initial gasifier tests. Table 12 presents the component syngas streams used to examine the excised NREL cleanup section response. The mixed alcohols model splits the raw syngas output from the gasifier into two section-external streams. The tar reformer catalyst regenerator utilizes a sidestream of raw syngas (stream 225F) as fuel to maintain a set flue gas exhaust temperature. This temperature was set at the default value of 1775 ˚F (968.3 °C) as was used in the original 2007 version of the Phillips model. (Phillips, Aden et al. 2007) With a uniform tar reformer catalyst regenerator temperature, the raw syngas sidestream was controlled by an existing design specification and only varied with changes in syngas fuel value. The main syngas feed stream flow to the cleanup section was held constant in all exercises.

In order to perform a similar exercise of the standalone RTI Therminator cleanup model, the raw syngas characteristics derived from each NREL model exercise feedstock were also used to define the Therminator input gas stream.

Table 12. Syngas mole fraction composition matrix used to exercise the standalone NREL and Therminator cleanup models.

Stream Comp	Sugarcane Bagasse	White Oak	Loblolly Pine	Lob Pine 250°C torr	NREL Base Poplar	Lob Pine 275°C torr	Spruce	Lob Pine 300°C torr	Peat	Lignite
H_2	0.1307	0.1375	0.1453	0.1503	0.1502	0.1610	0.1640	0.1806	0.1828	0.2876
CO	0.2345	0.2445	0.2494	0.2511	0.2506	0.2590	0.2603	0.2750	0.2761	0.3534
CO_2	0.0714	0.0743	0.0749	0.0746	0.0744	0.0757	0.0756	0.0780	0.0779	0.0803
H_2O	0.4427	0.4192	0.4088	0.4013	0.4016	0.3798	0.3761	0.3384	0.3266	0.1428
CH_4	0.0856	0.0891	0.0904	0.0905	0.0903	0.0925	0.0926	0.0964	0.0965	0.1066
C_2H_2	0.0022	0.0024	0.0025	0.0025	0.0025	0.0027	0.0027	0.0029	0.0029	0.0036
C_2H_4	0.0244	0.0253	0.0252	0.0249	0.0248	0.0248	0.0246	0.0246	0.0244	0.0156
C_2H_6	0.0017	0.0017	0.0015	0.0014	0.0014	0.0012	0.0011	0.0010	0.0009	0.0001
C_6H_6	0.0008	0.0008	0.0007	0.0007	0.0007	0.0007	0.0007	0.0006	0.0006	0.0005
Tar	0.0015	0.0014	0.0013	0.0012	0.0012	0.0012	0.0012	0.0011	0.0011	0.0009
N_2	0.0000	0.0000	0.0000	0.0000	0.0000	0.0000	0.0000	0.0000	0.0000	0.0000
O_2	0.0000	0.0000	0.0000	0.0000	0.0000	0.0000	0.0000	0.0000	0.0000	0.0000
Ar	0.0000	0.0000	0.0000	0.0000	0.0000	0.0000	0.0000	0.0000	0.0000	0.0000
NH_3	0.0045	0.0039	0.0000	0.0013	0.0018	0.0016	0.0011	0.0015	0.0097	0.0063
H_2S	0.0001	0.0000	0.0000	0.0000	0.0004	0.0000	0.0000	0.0000	0.0005	0.0023
SO_2	0.0000	0.0000	0.0000	0.0000	0.0000	0.0000	0.0000	0.0000	0.0000	0.0000

As noted in the NREL cleanup exercise, the raw gasifier syngas output is split. Where the sidestream 225F is utilized for heat and power, Stream 225A is routed through the cleanup process, ultimately used for alcohol synthesis. The molar flows and component mole fractions from NREL stream 225A were used as the flow basis for the Therminator feed syngas.

3.3.4 Cleanup Model Performance Comparisons

Following the initial model response evaluation, tests were carried out to quantify the operational results between the two cleanup technologies. The raw syngas characteristics from the default NREL hybrid poplar feedstock were used as the comparison basis (refer back to Table 12). Because the ASPEN non-conventional solid "char" present in the syngas was not included in the Therminator model component list, it was manually converted to elemental carbon and included. Additionally, the NREL catalyst regenerator and flue gas temperature post-heat exchanger were specified to reflect the temperatures used in the Therminator regenerator system, 600 and 121˚C respectively.

The difference in relative complexity of the two cleanup models was significant, and was simply addressed by only comparing streams and equipment of identical purpose. Outlet syngas compositions were compared in order to present the "bottom-line" cleanup results from the two technologies in question. Equipment energy flows, in the form of both shaft work and heat, were used to quantify the differences in the general operation of the two systems. Resultant process energy and product quality differences between the Therminator and conventional cleanup technologies as demonstrated in the NREL model were taken as indicative of relative performance of Therminator process.

3.3.5 Syngas Cleanup Technology Effects on Fuel Synthesis

The effect of this process performance on subsequent fuel synthesis was also investigated. The syngas flow and composition from the default Phillips 2007 version of the

NREL thermochemical model was used to specify the feedstock for the two cleanup sections under comparison. The resultant cleaned syngas parameters were in turn used to specify the feedstocks of two fuel synthesis processes. The MoS_2 catalyzed mixed alcohols synthesis section (denoted A400) was isolated from the integrated NREL model to allow for standalone operations. In a manner similar to the isolated evaluation of the gas cleanup section; all sections, calculators, and design specifications outside of the A400 synthesis block were deleted from the ASPEN model. Any remaining calculators and design specs that referenced deleted equipment were modified to refer to the standalone A400 input streams. A detailed explanation of the NREL synthesis section is presented in Section 2.4.4 in Chapter 2.

The second synthesis process to be tested against the two experimental cleanup technologies was the single-pass syngas to dimethyl ether (DME) process based on a $CuO/ZnO/Al_2O_3$ and γ-Al_2O_3 bifunctional catalyst. A more rigorous method of reaction modeling was desired, so a literature search of applicable reaction kinetics was conducted.

As the bifunctional nature of the catalyst implies, the conversion of syngas to DME takes place in two main sequential steps: hydrogenation of CO or CO_2 to methanol, followed by dehydration of methanol to DME. Equations 8-10 detail the reactions.

(hydrogenation) $$\mathbf{CO + 2H_2 \rightleftharpoons CH_3OH} \quad \textbf{(8)}$$

(hydrogenation) $$\mathbf{CO_2 + 3H_2 \rightleftharpoons CH_3OH + H_2O} \quad \textbf{(9)}$$

(dehydration) $$\mathbf{2CH_3OH \rightleftharpoons CH_3OCH_3 + H_2O} \quad \textbf{(10)}$$

Hydrogenation reactions are catalyzed by active copper sites supported on Zn and Al oxides. (Lee, Speight et al. 2007) The methanol dehydration to dimethyl ether is catalyzed by the acidic γ-Al_2O_3 constituent of the bifunctional catalyst. (Berčič and Levec 1992) Water-gas shift activity is also Cu-catalyzed simultaneously with methanol synthesis (Lloyd, Ridler et al. 1989; Lee, Speight et al. 2007), and is therefore considered along with the main hydrogenation and dehydration reactions.

Reaction kinetics have been estimated by many researchers for all steps. Syngas hydrogenation to methanol and water-gas shift were based upon Langmuir-Hinshelwood-Hougen-Watson (LHHW) kinetic expressions found in Luyben 2010 and Vanden Bussche 1996, converted for ASPEN use by Robinson. (Robinson 2009) The general form of a LHHW rate equation as considered by ASPEN is shown in Equations 11 and 12. (Robinson 2009) Methanol dehydration to DME was also based on LHHW kinetic expressions, derived from the research of Pyatnitskii 2009 and Mollavali, et al 2008. Equations 13-14 outline the LHHW equations for CO_2 hydrogenation and the water gas shift reaction, in the form needed to determine kinetic parameters for an ASPEN reactor. Equations 15-21 detail the van't Hoff-style temperature dependent reaction equilibrium equations utilized, and Arrhenius rate expressions used for methanol formation and water-gas shift. All temperatures and pressures are in kelvin and pascals, respectively.

General LHHW kinetic rate expression:

$$r = \text{kinetic factor}\frac{\text{driving force terms}}{\text{adsorption terms}} \quad \textbf{(11)}$$

$$r = k\frac{k_1 \prod_{i=1}^{N} C_i^{\alpha_i} - k_2 \prod_{j=1}^{N} C_j^{\beta_j}}{\left[\sum_{i=1}^{M} K_i \left(\prod_{j=1}^{N} C_j^{\alpha_j}\right)\right]^m} \quad \textbf{(12)}$$

Where:

k_1 and k_2	driving force constants for terms 1 and 2 respe ctively
N	Number of components in reaction
C_i	Concentration of i^{th} component
α_i	Component C_i concentration exponent
β_j	Component C_j concentration exponent
K_i	Adsorption constant for i^{th} term
M	Number of adsorption terms
N	Number of components
C_j	Concentration of j^{th} component
m	Adsorption term exponent

CO hydrogenation:

$$r_1 = k_4 \frac{\left[\frac{p_{CO_2} p_{H_2}}{1} - \frac{p_{CH_3OH} p_{H_2O}}{K_{E_1} {p_{H_2}}^2}\right]}{\left[1 + k_3\left(\frac{p_{H_2O}}{p_{H_2}}\right) + k_1\sqrt{p_{H_2}} + k_2 p_{H_2O}\right]^3} \quad \textbf{(13)}$$

Water-gas shift:

$$r_2 = k_5 \frac{\left[\frac{p_{CO_2}}{1} - \frac{p_{CO} p_{H_2O}}{K_{E_2} p_{H_2}}\right]}{\left[1 + k_3\left(\frac{p_{H_2O}}{p_{H_2}}\right) + k_1\sqrt{p_{H_2}} + k_2 p_{H_2O}\right]} \quad \textbf{(14)}$$

Arrhenius or van't Hoff Relationships: (Robinson 2009; Luyben 2010)

$$k_4 = 1.07\mathrm{E}^{-13} e^{\frac{36696}{RT}} \quad \frac{\mathrm{kmol}}{\mathrm{kg_{cat}}\cdot\mathrm{s}\cdot\mathrm{Pa}} \tag{15}$$

$$ln\left(\frac{1}{K_{E_1}}\right) = \frac{-7059.7}{T} + 47.41 \tag{16}$$

$$ln(k_3) = 8.1471 \tag{17}$$

$$ln(k_1) = \frac{2068.32}{T} - 6.452 \tag{18}$$

$$ln(k_2) = \frac{14928.06}{T} - 34.95 \tag{19}$$

$$k_5 = 122 e^{\frac{94765}{RT}} \quad \frac{\mathrm{kmol}}{\mathrm{kg_{cat}}\cdot\mathrm{s}\cdot\mathrm{Pa}} \tag{20}$$

$$ln\left(\frac{1}{K_{E_2}}\right) = \frac{4773}{T} - 4.672 \tag{21}$$

Note that the kinetic factor (Equations 15 and 20) are in a typical Arrhenius form, and that all other equations are in a natural log form as required by ASPEN. The general form required by ASPEN (Equation 22) for all temperature dependent driving force and adsorption constants is: (Aspen Technology 2009; Robinson 2009)

$$\ln(k) = A + \frac{B}{T} + C\ln(T) + DT \tag{22}$$

The Langmuir-Hinshelwood-Hougen-Watson kinetic rate expression for methanol dehydration to dimethyl ether is shown in Equation 23, followed by its accompanying kinetic factor, equilibrium, driving force, and adsorption constant equations (24-27). Subscript notations are taken from the source literature. (Zhang, Cao et al. 2001; Mollavali, Yaripour et al. 2008; Pyatnitskii, Strizhak et al. 2009; Shim, Lee et al. 2009)

Methanol dehydration: (Mollavali, Yaripour et al. 2008; Pyatnitskii, Strizhak et al. 2009)

$$r_3 = k_3 \frac{\left[\frac{p_{CH_3OH}}{1} - \frac{p_{DME}p_{H_2O}}{K_3 p_{CH_3OH}}\right]}{\left[1 + K_{CH_3OH}p_{CH_3OH} + \frac{p_{H_2O}}{K_{H_2O}}\right]} \quad \textbf{(23)}$$

Arrhenius or van't Hoff Relationships: (Zhang, Cao et al. 2001; Mollavali, Yaripour et al. 2008; Pyatnitskii, Strizhak et al. 2009; Shim, Lee et al. 2009)

$$k_3 = 7.833\text{E}^{-3} e^{\frac{57643.7}{RT}} \ \frac{\text{kmol}}{\text{kg}_{\text{cat}}\cdot\text{s}\cdot\text{Pa}} \quad \textbf{(24)}$$

$$ln\left(\frac{1}{K_3}\right) = \ 1.2777 - \frac{2167}{T} + 0.2258\ln T + 1.037\text{E}^{-3}T \quad \textbf{(25)}$$

$$ln\left(K_{CH_3OH}\right) = \frac{7738}{T} - 22.2374 \quad \textbf{(26)}$$

$$ln\left(K_{H_2O}\right) = \frac{-626}{T} - 8.537 \quad \textbf{(27)}$$

With reaction kinetics expressions established, an ASPEN model kinetic reactor for a simple single-pass DME plant was constructed. The reactor was configured as the core of a simple plant model, based on a design from a 5 ton/day pilot scale, single-step DME synthesis plan originally developed by the NKK Corporation (now JFE Holdings, Inc.) of Japan. (Ohno 2002; Ogawa, Inoue et al. 2003) The basic process flow diagram of the JFE plant was used as the model plant's general blueprint. The DME reactor was derived from a shell and tube plugflow syngas to methanol reactor from Luyben, and modeled as an ASPEN RPlug reactor block. Reactor and tube dimensions were taken from the Luyben design, with

the tube count modified to yield a similar residence time when using the lower feed flows from the NREL and RTI cleanup systems. The catalyst loading was controlled by an ASPEN design specification that maintained a catalyst charge to feed flow ratio (W/F ratio) as specified for the JFE plant by Ohno. Reactor operating temperature and pressure were also taken from the JFE pilot plant specifications.

Before proceeding any further with developing a complete plant model, the single ASPEN RPlug block, configured as noted, was tested against kinetic reactor results from Shim, et al. Similar syngas parameters to those of Shim were chosen, as shown in Table 13. Exercises were performed with variable pressure (fixed temperature and feed composition), variable temperature (fixed pressure and composition), and variable syngas H_2:CO ratio (fixed pressure and temperature).

Table 13. Simple kinetic DME reactor exercise parameters, based upon variable pressure, temperature and H_2:CO ratio tests from Shim, et al.

Variable Pressure Test		Variable Temp Test		Variable Syngas H_2:CO Ratio Test	
Parameter	Value	Parameter	Value	Parameter	Value
Temp	280°C	Temp	220-340°C	Temp	270°C
Pressure	15-95 kg_f/cm^2 (1.5-9.3 MPa)	Pressure	60 kg_f/cm^2 (5.88 MPa)	Pressure	60 kg_f/cm^2 (5.88 MPa)
Molar Fractions					
H_2	0.142	H_2	0.142	H_2	0.1 – 0.6
CO	0.378	CO	0.378	CO	0.2
CO_2	0.080	CO_2	0.080	CO_2	0.2
N_2	0.400	N_2	0.400	N_2	0.5 – 0.0

Following the exercises of the simple one-block DME reactor, the remainder of the model DME synthesis plant was completed, again based on the JFE pilot plant flow diagram detailed by Ohno and Ogawa. It should be noted that the JFE pilot plant is based on a slurry-phase catalytic reactor. This DME reactor model used in this study is more similar in design to one from the Korea Gas Corporation (KOGAS). KOGAS began operating 10 ton/day direct synthesis DME plant in 2008, which utilized a gaseous phase DME reactor. (Lee, Cho et al. 2009)

Both the JFE and KOGAS processes claimed a first stage of DME product purification accomplished by cryogenic separation, and the KOGAS process provided specific details that were used in this simulated DME plant. In the cryogenic separation dimethyl ether was condensed at -40°C, allowing most unused reactants to be separated from the product stream by decanting the DME-rich liquid. (Lee, Cho et al. 2009) Subsequent model CO_2 stripping and DME distillation columns as used in both the JFE and KOGAS plants were implemented with parameters specified by Cho. (Cho 2005; Cho, Lim et al. 2005) Table 14 outlines all pertinent specifications for the ASPEN single-pass DME plant. Figure 20 presents the ASPEN flow diagram of the DME plant model.

Once a stable model DME plant design was created, two versions of the model were examined, one with unreacted gas recycle from the cryo-separator (stream 4) and one without. Similarly, two versions of the standalone NREL mixed alcohols synthesis section were created. Recovered methanol from the D505 methanol distillation column first serves as molecular-sieve backflush and is then recycled back to the inlet of the R401 synthesis

reactor in order to maximize ethanol production. (Phillips, Aden et al. 2007) For the non-recycle version of the standalone mixed alcohols model, the recycle stream (513) was disconnected from the input of the synthesis reactor, allowing single-pass operation.

Table 14. ASPEN DME model specifications of selected unit operations

DME Reactor Specifications		
ASPEN Block:	RPlug	
Reactor Length:	12.2	m
Tube diameter (ID):	3.675	cm
Tube Count	~1300	
Residence time	~3.6	s
W/F	4	g_{cat}·h/mol
Temperature	260	C
Pressure	5	MPa

CO_2 Stripper Column Specifications		
ASPEN Block	RadFrac	
Column Stages	24	
Feed Stage	6	
Condenser Pressure	2.0265	MPa
Design Spec		
CO_2 target mass recovery	99	%
Vary	Boilup Ratio	

DME Distillation Column Specifications		
ASPEN Block	RadFrac	
Column Stages	20	
Feed Stage	11	
Feed Temperature	110	C
Condenser Pressure	1.8238	MPa
Design Spec		
MeOH target mass recovery	99	%
Vary	Boilup Ratio	

Energy usage in the form of both heat and shaft work was evaluated for the two synthesis models, for the recycle and non-recycle scenarios. The effects of different clean syngas compositions from the NREL conventional cleanup and the Therminator on the DME

reactor performance were investigated by comparing single-pass CO and CO_2 conversion, DME selectivity, and overall DME production. Specific model and scenario combinations will be referred to by "run number" according to Table 15. The effects mixed alcohols synthesis performance was evaluated by looking at overall alcohol production, as the synthesis reactor is non-kinetic and has a fixed product alcohol distribution.

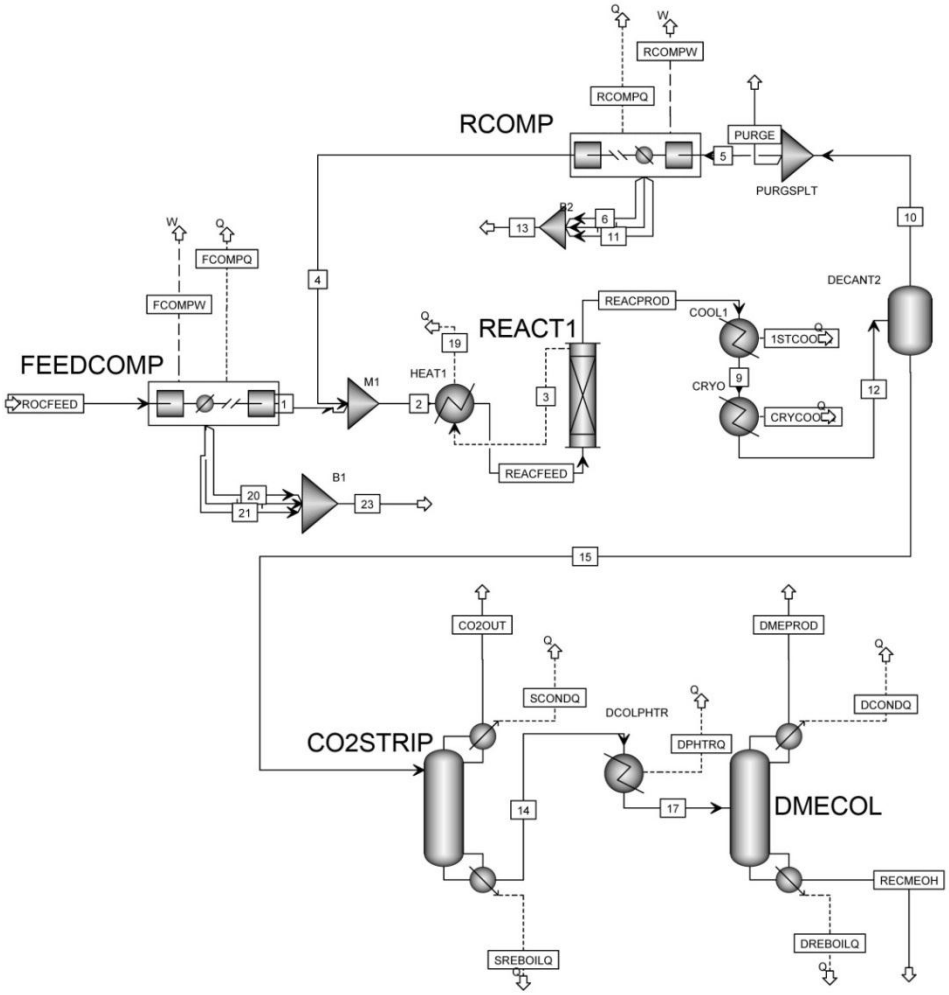

Figure 20. Test single-pass DME plant ASPEN model flow sheet

Table 15. Run numbers corresponding to specific model and scenario combinations.

Model Combination	Gas clean-up Technology	Fuel Product	Single Pass vs Gas Recycle
1	NREL	Mixed alcohols	Single pass
2	NREL	Mixed alcohols	Gas recycle
3	NREL	DME	Single pass
4	NREL	DME	Gas recycle
5	Therminator	Mixed alcohols	Single pass
6	Therminator	Mixed alcohols	Gas recycle
7	Therminator	DME	Single pass
8	Therminator	DME	Gas recycle

3.4 Results and Discussion

3.4.1 NREL Conventional Cleanup Exercise

Results from the NREL mixed alcohols cleanup process were greatly influenced by the R301 catalytic tar reformer. As noted in Chapter 2, R301 is modeled as an RStoic ASPEN reactor controlled by the calculator TARCRACK. The included water-gas shift and alcohol reforming reactions are modeled at Gibbs-energy minimized equilibrium, and hydrocarbon and ammonia reforming as stoichiometric reactions with extents taken from TARCRACK. These reactions are noted in Table 22 in Appendex A.3. The 2012 aspirational performance data used for the NREL model included the assumption that tar removals were >90%, with the exception of methane, and the tar cracking returned a significant amount of H_2 and CO to the clean syngas stream. Figure 21 and Figure 22 graphically show the contaminant reductions modeled by the tar reformer, and the accompanying percent change in molar flows of H_2 and CO across the cleanup system.

Methane made up 74-84% of the hydrocarbons in the raw gasifier syngas outlet stream, and therefore accounted for a large part of the hydrogen increase through the cleanup section. While input H_2 molar flow decreased due to lower gasification temperatures as biomass feedstock O/C ratio rises, the amount of H_2 contributed from CH_4 reforming was relatively large and consistent across the range of biomasses tested, and dominated the H_2 produced from the biomass. The ratio of these two hydrogen sources caused the significant (125-400%) increase H_2 mole flow.

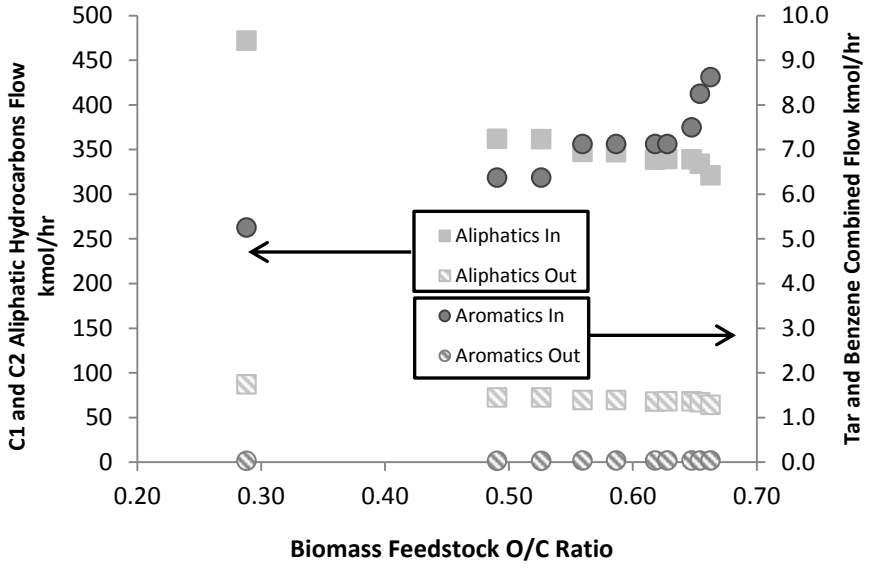

Figure 21. Syngas hydrocarbon molar flows, pre and post-catalytic tar reforming.

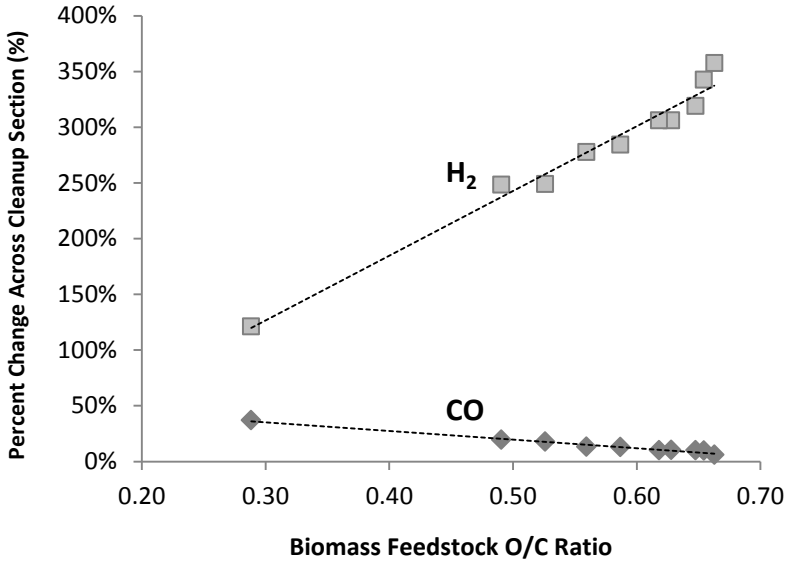

Figure 22. Change of H_2 and CO molar flow across NREL cleanup process.

On the other hand, changes in CO were less dependent on the biomass feedstock due to the relationship between the gasification temperatures and the formation of the C_1 and C_2 aliphatics. As shown in Figure 21 the syngas aromatic hydrocarbon content does increase as O/C ratio increases, but their overall contribution was small.

The CO_2 and NH_3 removal by the NREL conventional gas cleanup process was also strongly affected by the R301 tar reformer. Phillips notes that the tar reforming catalyst used in the NREL tar reformer is Ni-based, and is active for water-gas shift. (Phillips, Aden et al. 2007) Nickel based catalysts have been used extensively for reforming duty in the petrochemical industry, and researched extensively in hot gas cleanup processes for syngas. (Dayton 2002) In addition to their typical application in hydrocarbon reforming, Ni catalysts also display activity for NH_3 decomposition and water-gas shift. (Dayton 2002; Gerber 2007;

Yung, Jablonski et al. 2009) Figure 23 shows the CO_2 mole flow trend through the feedstock exercise. Since syngas H_2 concentrations rose as the biomass feedstock O/C ratio falls, the water-gas equilibrium reaction was shifted in the reverse direction by the Le Châtelier principle, and favored CO_2 production less and less strongly. Following the addition of CO_2 to the syngas stream by the tar reformer, CO_2 removal was accomplished in the amine scrubbing section, modeled as a simple split controlled by the design spec CO2SPEC. Syngas CO_2 mole fraction was set to 5% by the CO2SPEC design specification.

Ammonia decomposition across the catalytic tar reformer was set at the aspirational target of 90%, as controlled by the TARCRACK calculator. Additional ammonia reduction noted in Figure 24 was attributable to NH_3 solubilized in the quench system and lost in knockout water in post-quench syngas compression.

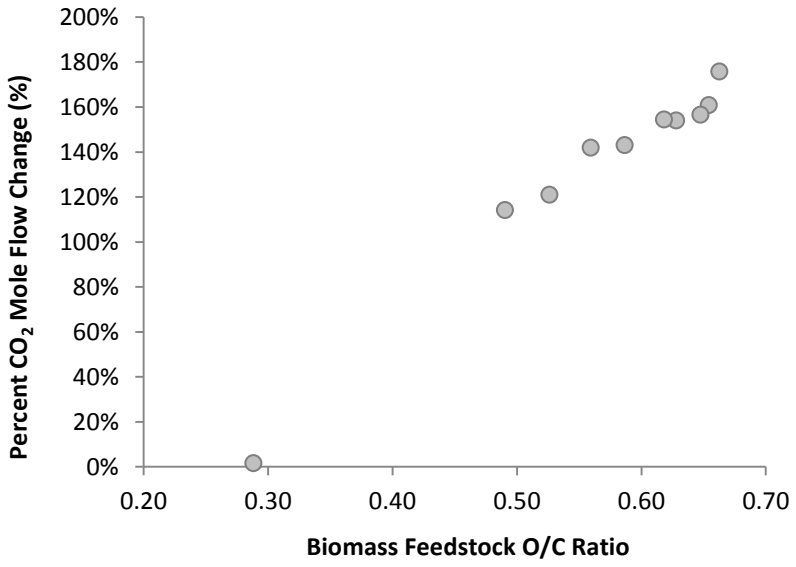

Figure 23. Percent change of CO2 mole flow across NREL tar reformer reactor.

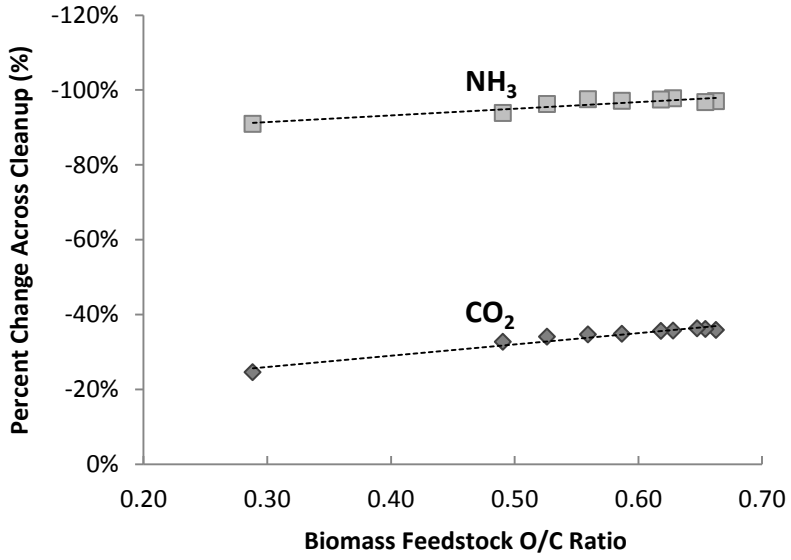

Figure 24. NH_3 and CO_2 mole flow change across NREL cleanup system

The remaining constituents to be removed in the cleanup section were hydrocarbons, water, and hydrogen sulfide. The hydrocarbons ethane, ethylene, acetylene, benzene, and tar were reduced in the tar reformer to the level specified by the TARCRACK calculator (99, 90, 90, 99, 99% respectively). Further reductions of benzene into the ppm range and tar into the ppb range were accomplished by tar precipitation in the quench system. Greater than 99% of the water carried in the syngas and added during tar reforming was removed primarily as knockout liquid during the syngas compression prior to amine scrubbing, and to a lesser extent by condensation during quenching.

Hydrogen sulfide removal is designed to be accomplished with a conventional monoethanoamine scrubbing unit. Phillips specifies an H_2S removal of 99.6% in the NREL model report. (Phillips, Aden et al. 2007) Actual modeled H_2S reduction is affected by a

simple split block, with a fixed H_2S split fraction of 84.287%. Model exercise results confirm this value.

3.4.2 RTI Therminator Cleanup Exercise

The RTI Therminator ASPEN model was designed based on laboratory results since Therminator performance and process validation work for biomass catalytic tar cracking and H_2S adsorption activity is underway. (Kalluri 2009) Model runs with a range of raw syngas feed compositions (refer back to Table 12 for composition matrix) confirmed the equilibrium reactions and split parameters as shown previously in Table 10 and designed into the Therminator model. Table 16 shows the average removal results from the exercised Therminator cleanup model. There was a decrease in the concentration of all syngas components except hydrogen. In contrast to the NREL clean-up system H_2 was only added to the syngas stream in the catalytic ammonia decomposition. Figure 25 shows the change in H_2 gas mole flow across the Therminator cleanup and its relationship to inlet NH_3 concentration.

Table 16. Average syngas component removals across the Therminator cleanup model from ten selected feedstocks. Negative removal is an addition.

Component	$\bar{x}$	Σ	Component	$\bar{x}$	σ
CO	0.16%	0.035%	CH_4	0.37%	0.080%
H_2	-5.76%	2.604%	C_2H_6	2.67%	0.573%
CO_2	1.68%	0.364%	C_2H_4	1.68%	0.361%
H_2O	99.41%	0.414%	C_2H_2	2.21%	0.476%
H_2S	99.91%	0.002%	Benzene	93.58%	3.106%
NH_3	99.77%	0.005%	Tar	100%	0.000%

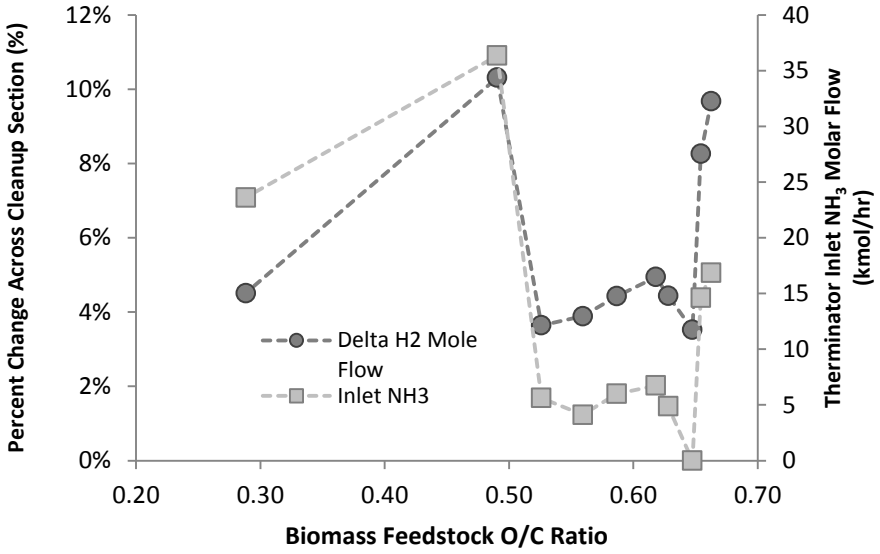

Figure 25. H_2 mole flow change across Therminator cleanup. NH_3 decomposition is only additional source of H_2 in the Therminator model beyond inlet H_2.

The catalyst/sorbent system employed in the Therminator was modeled as only active in tar reforming, NH_3 decomposition, and H_2S removal by adsorption. Water-gas shift activity was not designed into the ASPEN R-150 catalytic reactor, so no modifications in syngas CO and CO_2 composition were made within that unit operation. No reforming

beyond that of syngas tars was included either, so aliphatic hydrocarbons are minimally removed from by the Therminator cleanup system.

The quench reactor was modeled with three blocks, QUE-HX, QUE-TAR, and QUE-FLASH. QUE-HX and QUE-TAR served to cool the syngas to 46°C and condense and precipitate any residual tar vapor to CISOLID (ASPEN solid phase). QUE-FLASH flashed the syngas from 0.224 MPa to 0.138 MPa absolute, with the clean product syngas flashed off and the quench water reclaimed for recycling and wastewater treatment. (Kalluri 2009) As the O/C ratio increased, the cleanup inlet syngas water and benzene composition also increased. When the syngas was flashed in the quench system, higher water and benzene concentrations equated to a higher fraction of condensed and recovered liquids. The condensed liquids served to partly solubilize many of the syngas components, including CO, CO_2, methane, ethane, ethylene, acetylene, H_2S, and NH_3. The net result was that the minimal removal of gaseous syngas components by solubilization in the quench water was further reduced as the O/C ratio increased. Contaminant removals "hardwired" into the model yielded the smallest standard deviations shown in Table 16, whereas the removal of all other components varied with water and benzene concentrations. It is noteworthy that while not intentional, benzene removal was affected with the quench flash and subsequent syngas compression. Approximately 75% of the benzene reduction occurred in the quench section of the Therminator model, with the balance being removed by liquids knockout during syngas compression to 2.86 MPa.

3.4.3 Cleanup Models Composition and Energy Comparison

One of the primary goals of examining both the NREL cleanup and RTI Therminator models in detail was to comparisons virtual operational results. Differences in clean syngas composition and energy usage between the two technologies were studied. Ultimately, any differences in clean syngas composition would be evaluated in terms of potential synthesis impacts.

The two models were evaluated with syngas derived from the NREL mixed alcohols model gasifier, with hybrid poplar as the feedstock. The cleanup compositional results were tabulated for main syngas input/output stream in each model, and are presented in Table 17.

Mass flows were used to present stream flows for consistency with previous RTI documentation. (Kalluri 2009) Important differences to note were around the mass ratios of the primary syngas components (H_2, CO, CO_2). The NREL cleanup section yielded a mass ratio of 1:6.2 H_2:CO (2.2:1 molar ratio), while the Therminator gave a syngas with a mass ratio of 1:22 H_2:CO (0.67:1 molar ratio). These differences in primary syngas constituents were attributable to the steam-reforming and water-gas shift activities that were included in the NREL catalytic tar reformer. Methane, C_2 and higher aliphatic hydrocarbons, and aromatic hydrocarbons including tar were reformed to additional CO and H_2 in the NREL cleanup system. Modeled water-gas shift activity generated additional CO_2 and H_2, further altering the syngas CO and H_2O concentrations.

While the exact specifications for the RTI catalytic tar cracker and sulfur adsorber were not available due to their proprietary nature, examples of tar cracking catalysts include

well-known supported Ni-based materials, tungsten carbides (WC), and tungstenated zirconia (WZ). (Dayton 2009)

Ni-based catalysts are established alkane and tar reformers (Ross 2005; Gerber 2007; Navarro, Pena et al. 2007; Torres, Pansare et al. 2007), utilized as methane-reforming catalysts in the petrochemical industry. Tungsten carbide and tungsten-zirconium catalysts are known to a lesser extent to be capable of tar decomposition (cracking). (Levy and Boudart 1973; Pansare, Goodwin et al. 2008)

Alkane steam-reforming is also considered possible over WC and WZ catalysts (Claridge, York et al. 1998). Water-gas activity should be possible over tungsten-based catalysts given the similarity in chemical activity between molybdenum and tungsten (Levy and Boudart 1973), and the capability of Mo-based catalysts to facilitate the WGS reaction. (Ranhotra, Bell et al. 1987; Patt, Moon et al. 2000; Alexander and Hargreaves 2010) Despite the potential for the Therminator's catalytic reactor to yield tar and alkane reforming, as well as water-gas shift effects, the ASPEN model was not designed to include these capabilities. The minimal reduction of CH_4, C_2H_6, C_2H_4, and C_2H_2 across the Therminator cleanup system as shown in Table 16 confirms this point. However, excellent tar and ammonia decomposition reactivity was specifically designed into the model, and was evident from the results.

The $ZnTiO_3$ sulfur sorbent included in the Therminator model is quite capable of sulfur removal, with proper attention to sorbent attrition. (Gangwal, McMichael et al. 1992;

Gupta, Gangwal et al. 1992; Gupta, Gangwal et al. 1993; Swisher, Yang et al. 1995; Gupta and O'Brien 2000; Jung, Park et al. 2010)

Table 17. Cleanup technologies comparison for overall input/output streams. Syngas is derived from the NREL gasifier model, with hybrid poplar feedstock at 2000 tonnes/day, 50% moisture.

		Syngas feed	Syngas, pre-compression	Clean syngas	Catalyst regen flue gas	Syngas feed	Syngas, Pre-compression	Clean syngas	Catalyst regen flue gas
	UNITS	RTI1	RTI4	RTI4B	RTI10	NREL225A	NREL315	NREL362	NREL335
Temperature	°F	1633	115	110	250	1633	137	110	250
Temperature	°C	890	46.1	43.3	121.1	890	58.4	43.3	121.1
Pressure	psia	21.4	32.5	415	32.5	21.4	15.0	415	16.5
Pressure	bar	1.5	2.2	28.6	2.2	1.5	1.0	28.6	1.1
Total Mass Flow	lb/hr	1.68E+05	1.10E+05	1.06E+05	2.42E+04	1.68E+05	1.75E+05	9.52E+04	1.17E+05
Total Act. Vol. Flow	ACFH	8.66E+06	9.87E+05	7.32E+04	1.87E+05	8.67E+06	4.55E+06	1.18E+05	1.91E+06
Enthalpy Flow	MMBtu/hr	-444	-241	-218	-20	-444	-539	-180	-194
Component Mass Flow									
H2	lb/hr	2502	2629	2629	0.00	2502	10172	10172	0.00
CO	lb/hr	57990	57919	57887	0.00	57991	63941	63941	0.00
CO2	lb/hr	27070	26718	26571	4566	27070	68788	17445	26443
H2O	lb/hr	59782	4213	254	447	59782	28764	392	16928
CH4	lb/hr	11970	11936	11921	0.00	11970	2386	2386	0.00
C2H2	lb/hr	544	535	531	0.00	544	54	54	0.00
C2H4	lb/hr	5756	5681	5650	0.00	5756	571	571	0.00
C2H6	lb/hr	342	335	332	0.00	342	3.4	3.4	0.00
Aromatics (C_6H_6)	lb/hr	438	82	22	0.00	438	2.6	2.6	0.00
Tar ($C_{10}H_8$)	lb/hr	1315	0.00	0.00	0.00	1315	0.00	0.00	0.00
N2	lb/hr	0.00	210	210	16969	0.00	190	190	69954
O2	lb/hr	0.00	0.00	0.00	1724	0.00	0.00	0.00	2819
Ar	lb/hr	0.00	0.00	0.00	289	0.00	0.00	0.00	1193
NH_3	lb/hr	256	0.60	0.58	0.00	256	8.8	6.7	0.00
H_2S		116	0.10	0.10	0.00	116	116	18.3	0.00
SO_2		0.00	0.00	0.00	218	0.00	0.00	0.00	32
Mole Fraction									
H_2		0.1502	0.2508	0.2623		0.1502	0.4729	0.6367	
CO		0.2506	0.3977	0.4156		0.2506	0.2139	0.2880	
CO_2		0.0744	0.1168	0.1214	0.1299	0.0744	0.1465	0.0500	0.1445
H_2O		0.4016	0.0450	0.0028	0.0311	0.4016	0.1496	0.0027	0.2260
CH_4		0.0903	0.1431	0.1494		0.0903	0.0139	0.0188	
C_2H_2		0.0025	0.0039	0.0041		0.0025	0.0002	0.0003	
C_2H_4		0.0248	0.0389	0.0405		0.0248	0.0019	0.0026	
C_2H_6		0.0014	0.0021	0.0022		0.0014	11PPM	14PPM	
Aromatics (C_6H_6)		0.0007	203PPM	58PPM		0.0007	3PPM	4PPM	
Tar ($C_{10}H_8$)		0.0012				0.0012	10PPB	13PPB	
N_2			0.0014	0.0015	0.7583		0.0006	0.0009	0.6005
O_2					0.0674				0.0212
Ar					0.0091				0.0072
NH_3		0.0018	7PPM	7PPM		0.0018			
H_2S		413PPM	580PPB	596PPB		413PPM	320PPM	68PPM	
SO_2					0.0043				119PPM

The amine scrubbing system utilized in the NREL model is industry-proven H_2S removal technology. (Rochelle 2009) Both cleanup models were effect at reducing H_2S and NH_3 into the ppm and ppb range.

Work and energy comparisons were also made between the two cleanup models for Runs 1-8. The same NREL gasifier syngas derived from hybrid poplar feedstock was the raw feed syngas for the Therminator and NREL cleanup. The aforementioned difference in model complexity necessitated comparing only similar basic unit operations, with the simpler Therminator model as the basis. Table 18 presents selected energy and shaft work results for the two models.

The primary differences in energy and work between the two cleanup systems are contained in the tar-reforming unit in the NREL model. A substantial amount of energy was required for the hydrocarbon reforming reactions, and this energy was derived from combustion of a raw syngas sidestream in the catalyst regenerator. The large difference in flue gas flow (a factor of 5) equated to a greater amount of reclaimable heat in the NREL regenerator flue gas that can be used for boiler feedwater preheating and biomass drying. An order-of-magnitude energy discrepancy between the two models around syngas quenching was because the NREL model cools the syngas before quenching by heat exchanging against the raw synthesis alcohol stream. The modeled Therminator process accomplishes its syngas cooling entirely by quenching the stream.

Shaft work required for post-cleanup syngas compression was 2.6 times greater for the NREL cleanup system than for the Therminator, despite having a mass flow only 1.6

times larger. The operating pressure differential between the two cleanup reactors and the subsequent syngas compression stage was approximately 4.5% higher for the NREL reforming reactor. That greater pressure differential and a 4.6 times greater syngas volumetric flow rate yielded the significantly larger syngas compression shaft work.

Table 18. Selected heat and work flows from NREL conventional cleanup and Therminator cleanup systems.

RTI Therminator Model				**NREL Mixed Alcohols Model, Cleanup Section Only**			
Block	Description	Value	Units	Block	Description	Value	Units
SYNCOOL	inlet syngas cooler	(52,331,453)	BTU/hr	NA			
SYNCOMP	inlet syngas compressor	5,861	hp	NA			
R150	Therminator reactor	(7,641,652)	BTU/hr	R303A	tar reformer	106,753,688	BTU/hr
R250	catalyst regen	(18,901,514)	BTU/hr	R301A, R301B	catalyst regen	(106,753,688)	BTU/hr
HX220	cat regen air preheat	5,354,721	BTU/hr	H330	cat regen air preheat	6,280,989	BTU/hr
C210	cat regen air compressor	554	hp	K305	cat regen air compressor	372	hp
HX410	cat regen flue gas cooler	(5,420,110)	BTU/hr	H311	cat regen flue gas cooler	(29,370,392)	BTU/hr
QUE-HX2	quench cooling	(130,453,828)	BTU/hr	M301	quench cooling	(13,848,766)	BTU/hr
QUE-TAR	quench tar precip	-	BTU/hr	NA			
QUE-FLSH	quench syngas sep	-	BTU/hr	S301	quench syngas sep	-	BTU/hr
PRODCOMP	product syngas compressor	8,898	hp	K301	pre-amine syngas compressor	23,292	hp
NA				P300AM	amine feed pump	514	hp
NA				H300RB	amine column reboiler steam	113,600	lb/hr
NA				H300D	amine column preheater	(736,000)	BTU/hr
NA				R304	LOCAT oxidizer	(347,000)	BTU/hr

3.4.4 Cleanup Model Impacts on Mixed Alcohols Synthesis: Runs 1, 2 vs. 5, 6

The evaluation of mixed alcohols synthesis from the two cleaned syngas test streams yielded unexpected results, and provided additional insight into the NREL model's construction. As alluded to the in Section 3.4.3, the cleaned syngas derived from the Therminator contained roughly 25% of the H_2 available from the NREL cleanup process, and approximately 90% of the CO. These contrasts, in conjunction with 50% higher CO_2 and 10 times the aliphatic hydrocarbon load in the Therminator syngas, manifested themselves in

significant differences in mixed alcohol production. Table 19 details the results of mixed alcohols. Non-recycle results (Run 1 vs. 5) were intuitive in that a lower amount CO and H_2 fed to the synthesis reactor by the Therminator resulted in less production for each alcohol. Of interest was the observation that percent product alcohol distributions were subtly different between the two tested syngases. It was noted in section 2.4.4 that for the most part the product distribution of alcohols is fixed, defined by a series of non-kinetic reactions. When synthesized from NREL cleaned syngas, the product alcohols in stream 592 had a composition of 0.5%, 99.35%, and 0.15% of methanol, ethanol, and propanol respectively. The Therminator syngas resulted in an almost identical synthesis product composition of 0.5% methanol, 99.35% ethanol, and 0.15% propanol, but with an overall alcohol production rate only 67% of that from the NREL syngas.

Impacts due to cleanup technology were also manifested in the synthesis process model with default methanol recycling scheme. With methanol recycle, the Therminator-based ethanol production was 102% greater than that of the NREL syngas. A detailed examination of the ASPEN run results showed that the mixed alcohol synthesis model could not proceed through its sequential synthesis reactions because of low input hydrogen flow rate. ASPEN adjusted the reaction extents as necessary, but only the first seven synthesis reactions received enough hydrogen to proceed to completion.

The incomplete reactions include the water-gas shift, CO hydrogenation to methanol, and methanol chain-growth to ethanol. When taken together, the hydrogen deficiency shifts the mixed alcohol production towards C_1 and C_2 alcohols.

Table 19. Mixed alcohols synthesis material and energy results for NREL and Therminator derived clean syngas.

	With Methanol Recycle		Without Methanol Recycle		
Input Syngas	Conventional	Therminator	Conventional	Therminator	Units
H2	10173	2630	10173	2630	lb/hr
CO	63939	57884	63939	57884	lb/hr
CO2	17441	26567	17441	26567	lb/hr
H2O	385.5	254.4	385.5	254.4	lb/hr
N2	189.6	209.8	189.6	209.8	lb/hr
H2S	18.4	0.1	18.4	0.1	lb/hr
Aliphatic hydrocarbons	3026	18430	3026	18430	lb/hr
Benzene	2.5	22.5	2.5	22.5	lb/hr
Tar	4.06E-03	0.00	4.06E-03	0.00	lb/hr
Higher Alcohols Stream					
Methanol	0.04	0.16	0.04	0.18	lb/hr
Ethanol	139.5	142.8	137.1	89.6	lb/hr
Propanol	1994	2023	1815	1255	lb/hr
Butanol	250.9	253.3	228.4	157.0	lb/hr
Pentanol	33.3	33.5	30.3	20.8	lb/hr
Product Ethanol Stream					
Methanol	69.0	70.7	67.9	47.4	lb/hr
Ethanol	13669	14001	13460	9375	lb/hr
Propanol	20.1	20.4	17.9	10.0	lb/hr
Butanol	0.0	0.0	0.0	0.0	lb/hr
Pentanol	0.0	0.0	0.0	0.0	lb/hr
Selected Heat and Work Flows					
High Pressure Feed Compression	4471	2740	4471	2740	HP
Unreacted Syngas Decomp	-17926	-10176	-17490	-10542	HP
R410 Synth Reactor Preheat	23.9	18.9	21.3	16.0	MMBTU/hr
R410 Synthesis Reactor	-61.5	-52.5	-60.9	-42.8	MMBTU/hr
Product Alcohol Cooling	-33.3	-26.8	-32.2	-24.3	MMBTU/hr
Higher Alcohol Column Cond	-6.5	-7.4	-6.4	-5.5	MMBTU/hr
Higher Alcohol Column Reboil	5.7	6.5	5.6	4.9	MMBTU/hr
Ethanol Column Cond	-12.9	-17.0	-12.9	-14.0	MMBTU/hr
Ethanol Column Reboil	8.1	12.0	8.1	10.6	MMBTU/hr

With post-distillation methanol recycle and lower H_2 Therminator syngas this scenario was amplified, producing alcohols methanol through propanol at the expense of butanol and pentanol. The mixed alcohol model results for Therminator syngas were primarily an artifact of the manner in which the synthesis reactor was modeled: with sequential, non-kinetic equations. As a check, a test syngas stream was devised based on the

Therminator syngas composition, with the same CO mole flow, and an H_2:CO molar ratio adjusted to 1:1 by increasing H_2 flow and reducing inerts methane and ethylene. The result of feeding this modified Therminator syngas through the standard methanol-recycling synthesis model was a more reasonable 5.6% less ethanol production than that of the NREL syngas.

Energy results were consistent with the magnitude of the syngas and heat flows (Runs 1–4). Model scenarios involving methanol recycle have greater energy requirements and recovery demands than those without, excluding pre-synthesis syngas compression. Energy requirements between cleanup technologies followed the same relationship.

3.4.5 Dimethyl Ether Kinetic Reactor Exercise

The basic validation of the ASPEN RPlug DME reactor were deemed reliable enough to allow study of the performance of the NREL and Therminator cleanup technologies for DME synthesis. Elements of the single-step DME process model developed by Shim and coworkers were used to develop the DME reactor in question, and therefore their model exercises were used as a testing template. Figure 26-Figure 31 present the single-step DME kinetic reactor exercise results. The DME kinetic model developed by Shim includes an additional methanol generation reaction for CO and H_2 reactants, and uses the forward water-gas shift reaction. This is in contrast to the DME model used in the study, which is based upon the work of Vanden Bussche and Froment, Luyben and Robinson, and Pyatnitskii, et al.

These DME model only considers the CO_2/H_2 reaction path, and utilize a reverse water gas shift reaction.

Model temperature sensitivity response differed from that noted by Shim and coworkers, where their model predicted a maximum at about 260°C for DME yield, CO conversion, and DME, methanol, and CO_2 production. The model used here exhibited a DME yield inversely proportional to reactor temperature across the entire test range, similar to results noted by others in literature. (Ogawa, Inoue et al. 2003; Ereña, Garoña et al. 2005; Aguayo, Ereña et al. 2007) The model results found also showed a slight increase in methanol production with an increase in temperature, and a gradual reduction in DME production over the same range. The small increase in methanol production was likely due to the endothermic nature of the modeled reverse water-gas shift reaction. At increased temperatures the reaction rate will slow, leaving more CO_2 to serve as a methanol formation reactant.

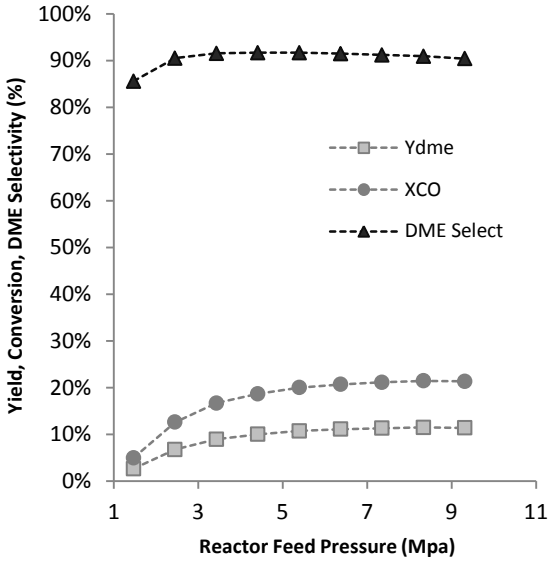

Figure 26. DME yield and selectivity, and CO conversion sensitivity to reactor pressure with fixed temperature and syngas composition.

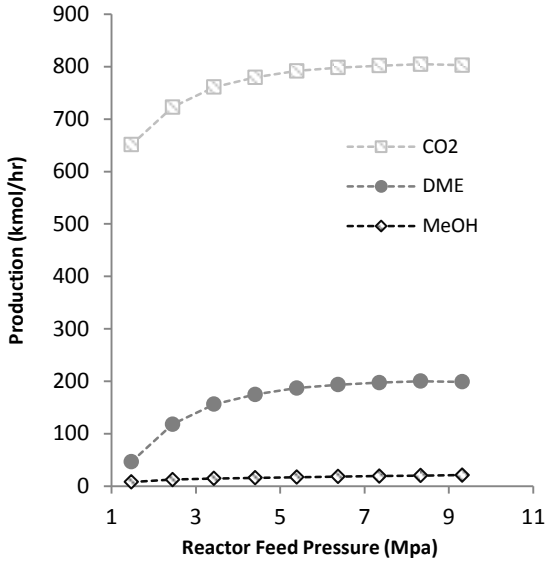

Figure 27. DME, methanol, and CO_2 production sensitivity to reactor pressure with fixed temperature and syngas composition.

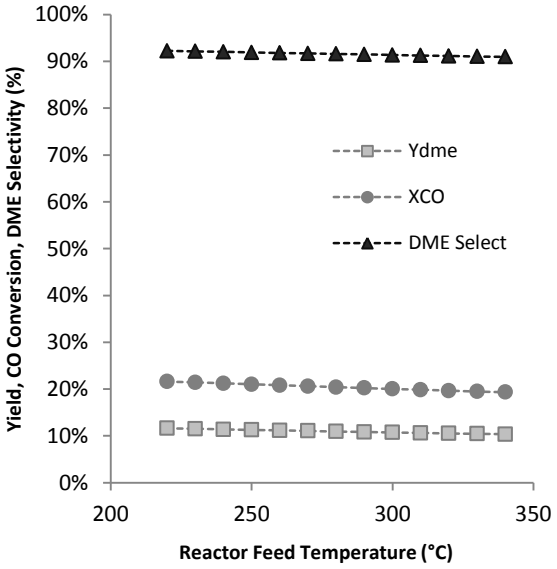

Figure 28. DME yield and selectivity, and CO conversion sensitivity to reactor temperature with fixed pressure and syngas composition.

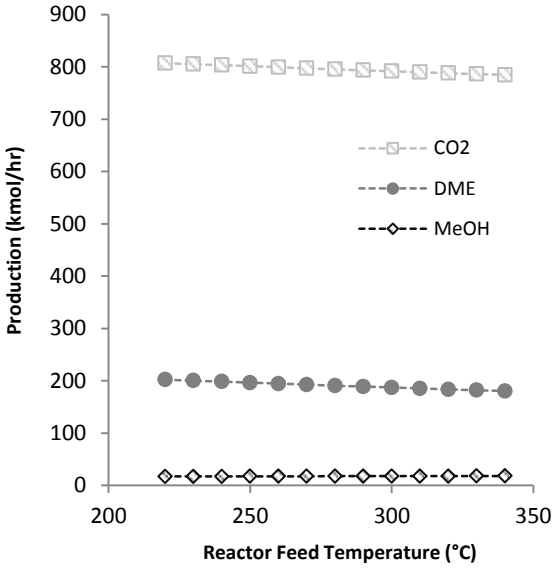

Figure 29. DME, methanol, and CO_2 production sensitivity to reactor temperature with fixed pressure and syngas composition.

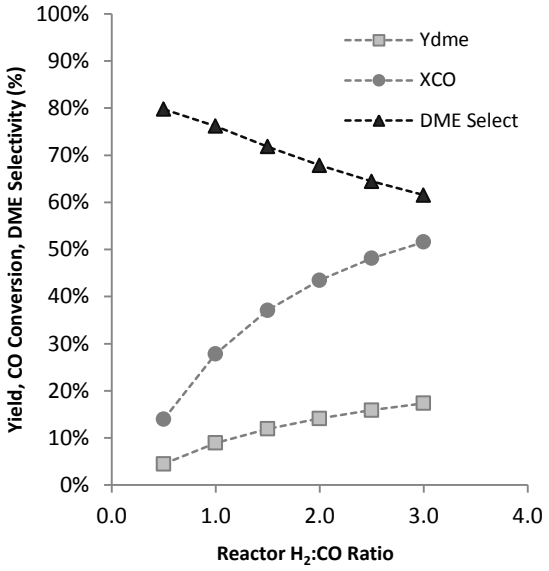

Figure 30. DME yield and selectivity, and CO conversion sensitivity to feed syngas H2:CO ratio at constant temperature and pressure.

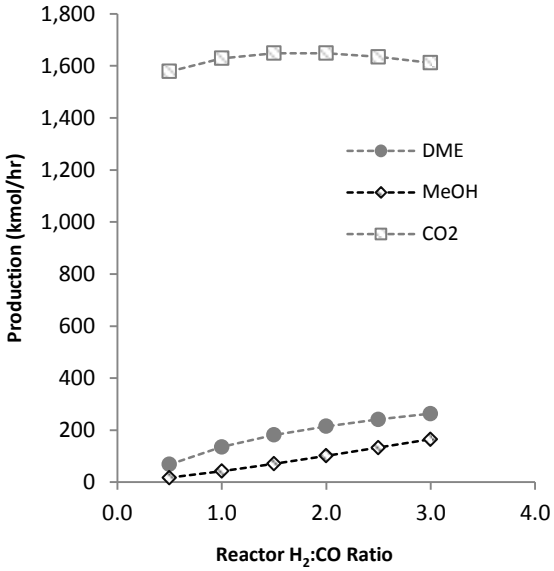

Figure 31. DME, methanol, and CO_2 production sensitivity to feed syngas H2:CO ratio at constant temperature and pressure.

Pressure response from the experimental kinetic ASPEN DME reactor was similar to that found by Shim, et al, although all yields, conversions, and production rates were lower. Aguayo also notes a directly proportional relationship between methanol and DME production and reactor pressure, citing that a decrease in the number of moles from reactants to products tends to favor the forward reactions.

Syngas compositional effects on single-step DME synthesis were addressed by Shim, et al, as well as other researchers found in literature. Shim notes that DME production reaches a maximum at a H_2:CO ratio of approximately 1:1, with a gradual decrease as the ratio and accompanying methanol production increases. Conversely, both Ogawa and Ng, found the maximum DME production at a H_2:CO ratio of approximately 2:1. (Ng, Chadwick

et al. 1999; Ogawa, Inoue et al. 2003) The model DME reactor in question yielded results most similar to those of Erena, et al, who found an increasing DME yield through a maxima at an H_2:CO ratio of 6:1. In a manner similar to the temperature sensitivity results, the H_2:CO ratio results showed lower productions, yields, and conversions across the entire test range, a result also noted by Aguayo.

Our DME model includes kinetics expressions from several researchers, and was not validated against experimental data, so the general response to varied operating conditions, rather than the absolute value of the flows, was used to judge the overall utility of the model. The temperature response generally trended down with temperature as noted by Ogawa, et al. The pressure response trended upward in manner also seen by Shim, et al and Aguayo and coworkers. Finally, the H_2:CO response had a general sensitivity trend like that found by Erena, et al; Ng, et al; and Ogawa, et al.

3.4.6 Cleanup Model Impacts on Dimethyl Ether Synthesis

With a reasonable kinetic DME reactor constructed in ASPEN, and a simple DME processing plant model built around it, the impacts of the two cleanup technologies under investigation were evaluated. The results of using syngas feedstock derived from the NREL and Therminator processes with the model DME plant, both with and without internal recycle, are presented in Table 20.

Generally, the NREL process-cleaned syngas resulted in a greater yield of all desirable products, for both the recycle and non-recycle cases, as H_2 was not a limiting

reagent. This was the same basic scenario noted in the mixed alcohols synthesis Section 2.4.4. While the Therminator syngas contained a greater concentration of CO_2, which was the primary methanol reactant for the synthesis pathway modeled, it also contained only 25% of the H_2 available from the conventional process. The preliminary evaluation of the DME model (Figure 30 and Figure 31) demonstrated the sensitivity of reactor to its feed syngas H_2:CO_x ratio, where additional DME yield could be achieved with ratios as high as 6:1. (Ereña, Garoña et al. 2005) For this reason, the lower hydrogen present in the Therminator cleaned syngas limited the amounts of DME and methanol produced in the synthesis model.

Table 20. Model DME plant results when utilizing clean syngas from the conventional NREL cleanup and the Therminator process.

	With Flash Recycle		Without Flash Recycle		
Input Syngas	Conventional	Therminator	Conventional	Therminator	Units
H2	10173	2630	10173	2630	lb/hr
CO	63939	57884	63939	57884	lb/hr
CO2	17441	26567	17441	26567	lb/hr
H2O	385.5	254.4	385.5	254.4	lb/hr
N2	189.6	209.8	189.6	209.8	lb/hr
H2S	18.4	0.10	18.4	0.10	lb/hr
Aliphatic hydrocarbons	3026	18430	3026	18430	lb/hr
Benzene	2.5	22.5	2.5	22.5	lb/hr
Tar	4.06E-03	0.00	4.06E-03	0.00	lb/hr
DME Product Stream					
Dimethyl ether (DME)	29690	15795	25609	13104	lb/hr
Methanol	139	13.3	80.1	5.5	lb/hr
CO_2	3892	535	2407	418	lb/hr
H_2S	16.1	0.1	18.7	0.1	lb/hr
Aliphatic hydrocarbons	11.4	120.8	10.1	99.3	lb/hr
Methanol Product Stream					
Dimethyl ether (DME)	0.49	79.4	0.29	0.0	lb/hr
Methanol	13794	1318	7927	1104	lb/hr
CO_2	0.0	0.0	0.0	0.0	lb/hr
H_2S	0.0	0.0	0.0	0.0	lb/hr
Aliphatic hydrocarbons	0.0	0.0	0.0	0.0	lb/hr
Selected Heat and Work Flows					
High Pressure Feed Comp	2499	1531	2499	1531	HP
Recycle Compressor	5974	5229			HP
DME Synth Reactor Preheat	67.3	65.78	23.5	17.1	MMBTU/hr
DME Synthesis Reactor	-80.8	-40.0	-71.6	-35.1	MMBTU/hr
Post Reactor Cooling	-115.9	-96.2	-40.5	-27.1	MMBTU/hr
CO_2 Stripper Column Cond	-1.9	-4.2	-2.0	-3.1	MMBTU/hr
CO_2 Stripper Column Reboil	12.3	11.3	9.3	8.4	MMBTU/hr
DME Column Cond	-5.4	-1.6	-4.3	-2.0	MMBTU/hr
DME Column Reboil	4.5	0.5	2.0	1.2	MMBTU/hr

The unreacted gas recycle based on both the KOGAS process (Cho, Lim et al. 2005) and the JFE process (Ohno 2002) increased the DME production for both test syngases (Runs 4 and 8). As the DME reactor was modeled with only the CO_2 to methanol to DME reaction pathway, and the reactor outlet stream was approximately 75% unused reactants, the DME yield improvement was predictable and amounted to increases of 15.9% and 20.5% for

NREL and RTI cleanup derived syngas respectively. The disparity between the recycle yield improvements was likely due to the H_2-limited nature of the DME production model with Therminator-cleaned syngas. A similar H_2 limiting reactant effect was also noted for the Therminator-derived clean syngas for mixed alcohols synthesis. Manipulation of the Therminator syngas to a 1:1 H_2:CO ratio by reducing inert components methane and ethylene showed an increase of approximately 26% for DME production in overall yield of DME.

As was noted in the evaluation of the modeled cleanup technologies on mixed alcohols synthesis, process energy requirements indicated in the DME models vary proportionally with material flow magnitudes. High-pressure compression work for the DME process syngas feed was 63% higher with NREL derived syngas than with that from the Therminator, as the conventionally cleaned syngas feed had approximately 1.5 times the volumetric flow rate. The remaining energy flow differences between the two feedstock model runs shown in Table 20 were related to the reduced DME production for Therminator-cleaned syngas. Reduced DME production was directly manifested in lower exothermic synthesis reaction energy and lower ejected heat from product gas cooling, with approximately double the available heat generated from the DME reactions on NREL syngas.

Energy usage patterns for once-through DME synthesis were identical between the CO_2 recycle and non-recycle cases, and tied to DME production. Of note for the recycle cases are the reactor preheater energy and the necessary inclusion of a recycle compressor. The recycled gas stream required about three times the synthesis reactor preheater energy to bring its temperature to the required 260°C. Between 5,200 and 6,000 HP of compressor

work was also required to bring the refrigeration-recovered, unreacted CO_2 back to the proper pressure for the DME reactor feed. The discrepancy between the recycle compressor horsepower requirements is primarily due to greater volumetric flow rate of the NREL-derived syngas.

3.5 Conclusions

A novel catalyst and zinc titanate sorbent based syngas cleanup technology (RTI Therminator) was evaluated against a conventional catalytic syngas tar reformer and amine scrubbing system (NREL model). In order to perform the comparisons, two ASPEN models were prepared and independently tested with a series of model syngases. Comparison between the baseline cleanup technology excised from the overall NREL mixed alcohols model and an interfaced Therminator model confirmed that as modeled the Therminator technology will break down tars and ammonia in a manner similar to that of the baseline system. Lower molecular weight aliphatic hydrocarbons that were catalytically reformed in the NREL system were not "cracked" or reformed based on the current parameters used in the Therminator model. As a consequence, these hydrocarbons represented a non-reactive burden for the Therminator-derived syngas application in any subsequent synthesis processes. Furthermore, any non-reformed hydrocarbons equate to a significant reduction of desirable CO and H_2 in the product syngas.

More favorable comparison results were observed with sulfur removal affected by the zinc titanate sorbent material within the Therminator model. As modeled, the Therminator

sulfur sorbent removed more of the primary sulfur species, H_2S than the baseline quench/amine scrubbing technology of the NREL model.

Synthesis process impacts of the Therminator and baseline NREL cleanup systems were investigated. A single-step dimethyl ether (DME) reactor was modeled with literature derived Langmuir-Hinshelwood-Hougen-Watson (LHHW) kinetics. The single step DME reactor model was tested for sensitivities around reactor pressure, temperature, and feed H_2:CO ratio, yielding reasonable results when evaluated against literature model results.

The resulting model kinetic reactor was used as the basis for a simulated synthesis process, along with the mixed alcohols synthesis model sections from the NREL model. When fed with a representative syngas, the resultant project syngases from each cleanup technology were used as the feedstock for both the single-step DME and NREL mixed alcohols synthesis processes. Relative to the Therminator the baseline NREL cleanup system yielded a greater amount of synthesis product in almost every case, due to the increased amount of CO and H_2 in the NREL syngas. Pilot-scale validation of the Therminator cleanup technology and associated ASPEN model will demonstrate whether the Therminator catalysts are capable of aliphatic hydrocarbon reforming and if a fuel synthesis yield penalty would occur.

Energy requirement comparisons were drawn between the two cleanup technologies and the two synthesis processes. The need for finding corresponding unit operation energy requirements between the cleanup and synthesis systems was made more difficult by the

greater model complexity of the cleanup and synthesis systems derived from the NREL mixed alcohols model.

Overall Conclusions and Future Work

The application of the NREL thermochemical mixed alcohols model as a tool to explore process effects from feedstock variation was examined. This work shows that the that the NREL model has considerable limitations as a predictive tool, in particular for evaluation of the impacts of varying biomass feedstock composition. Model limitations include non-kinetic empirical correlation based gasifier and a non-kinetic, user define mixed alcohols product ratios in the synthesis section. Addressing the design of the gasifier model is among several items to be considered for future work. Indeed, NREL has already attempted to update the original Battelle-Columbus Laboratory correlations, basing new empirical relationships on an updated PDU. (Kinchin and Bain 2009)

Operational differences between the RTI Therminator cleanup process and the more traditional cleanup system employed in the NREL mixed alcohols model were evaluated. The Therminator model was based on laboratory data for tar, ammonia, and H_2S reduction, limiting the detailed insights in the operating differences between the two cleanup technologies. Of note were syngas contaminants not decomposed or reformed by the Therminator. More research work needs to be performed around evaluating the activity of the Therminator catalyst for these contaminants, as they represented lost CO and H_2 for the cleaned syngas and reduced fuel production in modeled synthesis systems.

A kinetic single-step DME synthesis model was constructed as part of an evaluation of synthesis implications from processing syngas with Therminator or NREL systems. The model performed reasonably well when compared against literature results, and should be

useful as a tool in future process modeling work. Particularly instructive was the identification of the correct construction methods for a LHHW-kinetics based reactor in the ASPEN environment. Future modeling work in this area should take these construction methods and apply them towards creating kinetic synthesis models for Fischer-Tropsch liquids and an update to the NREL mixed alcohols synthesis model.

References

Aguayo, A. T., J. Ereña, et al. (2007). "Kinetic modeling of dimethyl ether synthesis in a single step on a CuO-ZnO-Al2O3/gamma-Al2O3 catalyst." Industrial & Engineering Chemistry Research **46**(17): 5522-5530.

Ahrenfeldt, J. and H. Knoef (2005). Handbook biomass gasification. Netherlands, BTG Biomass Technology Group.

Alexander, A. M. and J. S. J. Hargreaves (2010). "Alternative catalytic materials: carbides, nitrides, phosphides and amorphous boron alloys." Chemical Society Reviews **39**(11): 4388-4401.

Anderson, R. B. (1984). The Fischer-Tropsch Synthesis. New York, Academic Press, Inc.

Aspen Technology, I. (2009). EAP101 AspenPlus: Process Modeling. Burlington, MA, Aspen Technology, Inc.

Babu, S. P. (2005). Observations on the Current Status of Biomass Gasification. Paris, International Energy Agency (IEA)**:** 14.

Bain, R. (2006). Biomass Gasification. USDA Thermochemical Conversion Workshop, Richland, WA, NETL/DOE.

Bain, R. L. (1992). Material and Energy Balances for Methanol from Biomass Using Biomass Gasifiers. Golden, CO, National Renewable Energy Lab.

Baker, E. G., M. D. Brown, et al. (1986). Engineering analysis of biomass gasifier product gas cleaning technology. Richland, WA, Pacific Northwest National Laboratory (PNNL)**:** Medium: ED; Size: Pages: 100.

Basu, P. (2006). Combustion and gasification in fluidized beds. Boca Raton, CRC/Taylor & Francis.

Bergman, P. C. A., A. R. Boersma, et al. (2005). Torrefaction for biomass co-firing in existing coal-fired power stations. Petten, Energy Research Centre of the Netherlands**:** 71.

Berčič, G. and J. Levec (1992). "Intrinsic and Global Reaction Rate of Methanol Dehydration Over Gamma-AL2O3 Pellets." Industrial & Engineering Chemistry Research **31**(4): 1035-1040.

Bottoms, R. R. (1930). Process for Separating Acidic Gases. U. P. a. T. Office. United States, Girdler Corporation**:** 5.

Breckenridge, W., A. Holiday, et al. (2000). Use of SELEXOL(R) Process in Coke Gasification to Ammonia Project. Laurance Reid Gas Conditioning Conference. Norman, OK, Dow Chemical, Inc.**:** 17.

Bridgwater, A. V. and M. A. Bolhàr-Nordenkampf (2005). Economics of biomass gasification. Handbook Biomass Gasification. H. A. M. Knoef. Enschede, The Netherlands, Biomass Technology Group (BTG)**:** 321-343.

Bögner, F. and K. Wintrup (1984). The Fluidized-Bed Coal Gasification Process (Winkler Type). The Handbook of Synfuels Technology. R. A. Meyers. New York, McGraw-Hill**:** 14.

Channiwala, S. A. and P. P. Parikh (2002). "A unified correlation for estimating HHV of solid, liquid and gaseous fuels." FUEL **81**(8): 1051-1063.

Childress, A. (2007). Gasification World Database 2007. Pittsburgh, PA, US Department of Energy, National Energy Technology Laboratory. **2010:** 32.

Cho, J. (2005). DME (10 TPD) Process Simulation Using Aspen Plus Release 12.1. Yeongju, South Korea, Dong Yang University**:** 25.

Cho, J., K. Lim, et al. (2005). "Simulation of DME Separation Process as Diesel Alternative Fuel." Applied Chemistry **9**(2): 4.

Ciferno, J. P. and J. J. Marano (2002). Benchmarking Biomass Gasification Technologies for Fuels, Chemicals and Hydrogen Production. Morgantown, US Department of Energy (DOE)**:** 65.

Claridge, J. B., A. P. E. York, et al. (1998). "New catalysts for the conversion of methane to synthesis gas: Molybdenum and tungsten carbide." Journal of Catalysis **180**(1): 85-100.

Company, E. C. and A. P. a. Chemicals (2003). Project Data on Eastman Chemical Company's Chemicals-from-Coal Complex in Kingsport, TN**:** 35.

ConocoPhillips. (2010). "E-Gas Gasification." Retrieved Oct 14, 2010, from http://www.conocophillips.com/EN/tech/downstream/e-gas/Pages/index.aspx.

Corella, J. and A. Sanz (2005). "Modeling circulating fluidized bed biomass gasifiers. A pseudo-rigorous model for stationary state." Fuel Processing Technology **86**(9): 1021-1053.

Corella, J., J. M. Toledo, et al. (2004). "Olivine or dolomite as in-bed additive in biomass gasification with air in a fluidized bed: Which is better?" Energy & Fuels **18**(3): 713-720.

Corella, J., J. M. Toledo, et al. (2005). "Catalytic Hot Gas Cleaning with Monoliths in Biomass Gasification in Fluidized Beds. 3. Their Effectiveness for Ammonia Elimination." Industrial & Engineering Chemistry Research **44**(7): 2036-2045.

Craig, K. (1993). Wood Devolatilazation and Pyrolysis. Golden, CO, NREL**:** ASPEN BATYD5.for fortran subroutine, written by K.R.Craig,1993. User routine to model fixed-bed gasification wood devolatilization based on the ultimate analysis of the wood, ash, and char. As noted, based on the NYLD routine written by MIT for Conoco study (1981).

Davis, B. H. and M. L. Occelli (2007). Fischer-Tropsch synthesis, catalysts and catalysis. Amsterdam ; Boston, Elsevier.

Dayton, D. (2002). Review of the Literature on Catalytic Biomass Tar Destruction: Milestone Completion Report. Golden, CO, National Renewable Energy Laboratory (NREL)**:** Medium: ED; Size: 33 pages.

Dayton, D. (2009). Biomass Gasification and Tar Cracking Process Development. Gasification 2009 - Gas Cleanup and Gas Treatment. Stockholm, Research Triangle Institute International (RTI)**:** 34.

Demirbaş, A. (2005). "Relationship between Initial Moisture Content and the Liquid Yield from Pyrolysis of Sawdust." Energy Sources **27**(9): 823-830.

Desrosiers, R. (2002). Thermodynamics of Gas-Char Reactions. Encyclopedia of biomass thermal conversion: the principles and technology of pyrolysis, gasification, and combustion. T. B. Reed. Golden, CO, Biomass Energy Foundation Press. **2:** 133-176.

DOE. (2008). "Clean Coal Technology: From Research to Reality." 2010, from http://www.fossil.energy.gov/aboutus/fe_cleancoal_brochure_web2.pdf.

Dominicis, D. P. and C. K. Holt (1984). The Westinghouse Coal-Gasification Process. The Handbook of Synfuels Technology. R. A. Meyers. New York, McGraw-Hill**:** 38.

E4Tech (2009). Review of Technologies for Gasification of Biomass and Wastes. Heslington, UK, National Non-Food Crops Centre**:** 130.

Egloff, G. and P. Van Arsdell (1943). Motor Vehicles Propelled by Producer Gas. The Petroleum Engineer. Dallas, Petroleum Engineer Pub. Co. **15:** 65-144.

EIA. (2010). "OPEC Revenues Fact Sheet Energy Data, Statistics and Analysis - Oil, Gas, Electricity, Coal." Retrieved May 2010, 2010, from http://www.eia.doe.gov/emeu/cabs/OPEC_Revenues/Factsheet.html.

Ereña, J., R. Garoña, et al. (2005). "Direct synthesis of dimethyl ether from (H2+CO) and (H2+CO2) feeds. Effect of feed composition." International journal of chemical reactor engineering **3**.

Feldmann, H. F., M. A. Paisley, et al. (1988). Conversion of Forest Residues to a Methane-Rich Gas in a High-Throughput Gasifier. Columbus, OH, Columbus Battelle Division, Pacific Northwest Laboratory (PNL). **PNL-6570**.

Gangwal, S. K., R. Gupta, et al. (1995). "Hot-Gas Cleanup - Sulfur Recovery Technical, Environmental, and Economic Issues." Heat Recovery Systems & Chp **15**(2): 205-214.

Gangwal, S. K., W. J. McMichael, et al. (1992). Bench-scale testing and evaluation of the Direct Sulfur Recovery Process. Morgantown, WV, Morgantown Energy Technology Center (METC/DOE)**:** 44.

Gangwal, S. K., J. M. Stogner, et al. (1989). "Testing of novel sorbents for H2S removal from coal gas." Environmental Progress **8**(1): 26-34.

Gaur, S. and T. B. Reed (1998). Thermal data for natural and synthetic fuels. New York, Marcel Dekker.

Geosits, R. F. and L. A. Schmoe (2005). IGCC - The Challenges of Integration. ASME Turbo Expo 2005: Power for Land, Sea and Air, Reno, Nevada, ASME.

Gerber, M. A. (2007). Review of Novel Catalysts for Biomass Tar Cracking and Methane Reforming. Richland, WA, Pacific Northwest National Laboratory (PNNL)**:** Medium: ED; Size: PDFN.

Golumbic, N. R. (1946). Review of Fischer-Tropsch and related processes for synthetic liquid fuel production. [Washington], U.S. Bureau of Mines.

Griel, C., H. Hirschfelder, et al. (2002). Operational Results from Gasification of Waste Material and Biomass in Fixed Bed and Circulating Fluidized Bed Gasifiers. Noordwijk, Netherlands, IChemE**:** 10.

Groeneveld, M. J. and W. P. M. van Swaaij (1979). "Gasification of solid waste--Potential and application of co-current moving bed gasifiers." Applied Energy **5**(3): 165-178.

Gupta, R., S. K. Gangwal, et al. (1992). "Development of zinc ferrite sorbents for desulfurization of hot coal gas in a fluid-bed reactor." Energy & Fuels **6**(1): 21-27.

Gupta, R. P., S. K. Gangwal, et al. (1993). NH3/H2S Advances. Coal-Fired Power Systems 93 - Advances in IGCC and PFBC Review Meeting. Morgantown, WV, Morgantown Energy Technology Center (METC/DOE)**:** 18.

Gupta, R. P. and W. S. O'Brien (2000). "Desulfurization of Hot Syngas Containing Hydrogen Chloride Vapors Using Zinc Titanate Sorbents." Industrial & Engineering Chemistry Research **39**(3): 610-619.

Hanping, C., L. Bin, et al. (2008). "Experimental Investigation of Biomass Gasification in a Fluidized Bed Reactor." Energy & Fuels **22**(5): 3493-3498.

Higman, C., M. van der Burgt, et al. (2008). Gasification. Amsterdam ; Boston, Gulf Professional Pub./Elsevier Science**:** 435.

Hochgesand, G. (1970). "Rectisol and Purisol." Industrial engineering chemistry **62**(7): 37.

Jennings, J. R. and S. A. Ward (1989). Ammonia Synthesis. Catalyst Handbook. M. V. Twigg. London, Wolfe Publishing, Ltd.**:** 384-440.

Jung, S. Y., J. J. Park, et al. (2010). "A study of the sulfidation and regeneration reaction cycles of Zn-Ti-based sorbents with different crystal structures." Korean Journal of Chemical Engineering **27**(5): 1428-1434.

Kalluri, R. (2009). RTI Therminator Model. Research Triangle Park, NC, Research Triangle Institute (RTI).

Kinchin, C. M. and R. L. Bain (2009). Hydrogen Production from Biomass via Indirect Gasification: The Impact of NREL Process Development Unit Gasifier Correlations. Golden, CO, National Renewable Energy Laboratory (NREL)**:** 1-27.

Kinoshita, C. M., Y. Wang, et al. (1994). "Tar formation under different biomass gasification conditions." Journal of Analytical and Applied Pyrolysis **29**(2): 169-181.

Kinoshita, C. M., W. Yue, et al. (1991). "Chemical-Equilibrium Computations for Gasification of Biomass to Produce Methanol." Energy Sources **13**(3): 361-368.

Kohl, A. L. and R. Nielsen (1997). Gas purification. Houston, Tex., Gulf Pub.

Kumar, A., D. Jones, et al. (2009). "Thermochemical Biomass Gasification: A Review of the Current Status of the Technology." Energies **2**(3): 556-581.

Kwant, K. W. and H. Knoef (2004). Status of Gasification in Countries Participating in the IEA and GasNet Activity, August 2004**:** 167.

LaFontaine, H. and F. P. Zimmerman (1989). Construction of a Simplified Wood Gas Generator for Fueling Internal Combustion Engines in a Petroleum Emergency. Washington, DC, Federal Emergency Management Agency (FEMA).

Lee, S., J. G. Speight, et al. (2007). Handbook of alternative fuel technologies. Boca Raton, CRC Press.

Lee, S.-H., W. Cho, et al. (2009). Scale Up Study of DME Direct Synthesis Technology. 24th World Gas Conference. Buenos Aires, Argentina, International Gas Union.

Lee, S. Y., M. R. Gogate, et al. (1992). "A NOVEL SINGLE-STEP DIMETHYL ETHER (DME) SYNTHESIS IN A 3-PHASE SLURRY REACTOR FROM CO-RICH SYNGAS." CHEMICAL ENGINEERING SCIENCE **47**(13-14): 3769-3776.

Levy, R. B. and M. Boudart (1973). "Platinum-Like Behavior of Tungsten Carbide in Suface Catalysis." Science **181**(4099): 547-549.

Li, X. T., J. R. Grace, et al. (2004). "Biomass gasification in a circulating fluidized bed." Biomass and Bioenergy **26**(2): 171-193.

Lloyd, L., D. E. Ridler, et al. (1989). The Water-gas Shift Reaction. Catalyst Handbook. M. V. Twigg. London, Wolfe Publishing, Ltd**:** 283-339.

Ludewig, W. (1966). "Highlights in History of BASF." Transactions of the Institution of Chemical Engineers and the Chemical Engineer **44**(6): T237.

Luxmore, C. (2007) "Risky Business." Waste management world. **8**.

Luyben, W. L. (2010). "Design and Control of a Methanol Reactor/Column Process." Industrial & Engineering Chemistry Research **49**(13): 6150-6163.

Lv, P., J. Chang, et al. (2003). "Biomass Air-Steam Gasification in a Fluidized Bed to Produce Hydrogen-Rich Gas." Energy & Fuels **17**(3): 677-682.

Mako, P. F. (1984). The SASOL Approach to Liquid Fuels from Coal Via the Fischer-Tropsch Reaction. The Handbook of Synfuels Technology. R. A. Meyers. New York, McGraw-Hill**:** 38.

Maniatis, K. (2008). Progress in Biomass Gasification: An Overview. Progress in Thermochemical Biomass Conversion. A. V. Bridgwater. Hoboken, NJ, Wiley-Blackwell**:** 31.

Mann, M. K. (1995). Technical and Economic Assessment of Producing Hydrogen by Reforming Syngas from the Battelle Indirectly Heated Biomass Gasifier. Golden, CO, National Renewable Energy Laboratory (NREL). **NREL/TP-431-8143**.

Mason, J. (2010). "About << Gasifier Experimenters Kit." Retrieved Oct 16, 2010, 2010, from http://www.gekgasifier.com.

Mattusch, C. (2008). Metalworking and Tools. Oxford handbook of engineering and technology in the Classical world. J. P. Oleson. Oxford ; New York, Oxford University Press**:** 418-438.

Meyers, R. A. (1984). Handbook of synfuels technology. New York, McGraw-Hill.

Milne, T. (2002). Pyrolysis - The Thermal Behavior of Biomass Below 600 C. Encyclopedia of biomass thermal conversion: the principles and technology of pyrolysis, gasification, and combustion. T. B. Reed. Golden, CO, Biomass Energy Foundation Press. **2:** 95-132.

Milne, T. A., R. J. Evans, et al. (1998). Biomass Gasifier "Tars": Their Nature, Formation, and Conversion. Golden, CO, National Renewable Energy Laboratory (NREL)**:** Medium: ED; Size: vp.

Mollavali, M., F. Yaripour, et al. (2008). "Intrinsic kinetics study of dimethyl ether synthesis from methanol on gamma-Al-2 O-3 catalysts." Industrial & Engineering Chemistry Research **47**(9): 3265-3273.

Mudge, L. K., S. L. Weber, et al. (1981). Investigations on catalyzed steam gasification of biomass. Richmond, WA, Battelle Pacific Northwest Labs**:** 162.

Navarro, R. M., M. A. Pena, et al. (2007). "Hydrogen production reactions from carbon feedstocks: Fossils fuels and biomass." Chemical Reviews **107**(10): 3952-3991.

NETL. (2009). "NETL: Gasifipedia." Retrieved October 20, 2010, 2010, from http://www.netl.doe.gov/technologies/coalpower/gasification/gasifipedia/4-gasifiers/4-1-2-6_eagle.html.

NETL, W. Shelton, et al. (2000). British Gas / Lurgi Gasifier IGCC Base Cases. Morgantown, US Department of Energy**:** 47.

Ng, K. L., D. Chadwick, et al. (1999). "Kinetics and modelling of dimethyl ether synthesis from synthesis gas." CHEMICAL ENGINEERING SCIENCE **54**(15-16): 3587-3592.

Ogawa, T., N. Inoue, et al. (2003). "Direct Dimethyl Ether Synthesis." Journal of Natural Gas Chemistry **12**: 9.

Ohno, Y. (2002). Recent Situation and Future Development of DME Direct Synthesis Technology. Japan DME Forum Workshop 2002. Tokyo, NKK Corporation**:** 9.

Paisley, M. A. and D. Anson (1998). "Biomass Gasification for Gas Turbine-Based Power Generation." Journal of Engineering for Gas Turbines and Power **120**(2): 284-288.

Paisley, M. A., R. P. Overend, et al. (2004). FERCO's SilvaGas(R) Biomass Gasification Process Commercialization Opportunities for Power, Fuels, and Chemicals.

Pansare, S. S., J. G. Goodwin, et al. (2008). "Simultaneous Ammonia and Toluene Decomposition on Tungsten-Based Catalysts for Hot Gas Cleanup." Industrial & Engineering Chemistry Research **47**(22): 8602-8611.

Patt, J., D. J. Moon, et al. (2000). "Molybdenum carbide catalysts for water-gas shift." Catalysis Letters **65**(4): 193-195.

Pell, M., J. B. Dunson, et al. (2008). Gas-Solid Operations and Equipment. Perry's Chemical Engineers' Handbook. D. W. Green and R. H. Perry. New York, McGraw-Hill**:** 17-36.

Phillips, J. (2006). Different Types of Gasifiers and Their Integration with Gas Turbines. The Gas Turbine Handbook. S. T. Services. Washington, DC, US DOE/NETL**:** 556.

Phillips, S., A. Aden, et al. (2007). Thermochemical Ethanol via Indirect Gasification and Mixed Alcohol Synthesis of Lignocellulosic Biomass. Golden, CO, NREL**:** 132.

Pyatnitskii, Y. I., P. E. Strizhak, et al. (2009). "Kinetic modeling for the conversion of synthesis gas to dimethyl ether on a mixed Cu-ZnO-Al2O3 catalyst with gamma-Al2O3." Theoretical and Experimental Chemistry **45**(5): 325-330.

Quaak, P., H. Knoef, et al. (1999). "Energy from biomass a review of combustion and gasification technologies." from http://www.worldbank.icebox.ingenta.com/content/wb/324.

RangeFuels. (2011). Retrieved Feb 8, 2011, from http://www.rangefuels.com/our-plants.html.

Ranhotra, G. S., A. T. Bell, et al. (1987). "Catalysis Over Molybdenum Carbides and Nitrides - 2. Studies of CO Hydrogenation and C2H6 Hydrogenolysis." Journal of Catalysis **108**(1): 40-49.

Reed, T. B. (2002). Encyclopedia of biomass thermal conversion : the principles and technology of pyrolysis, gasification & combustion. Golden, Colo., Biomass Energy Foundation Press.

Reed, T. B. (2002). Types of Gasifiers and Gasifier Design Considerations. Encyclopedia of biomass thermal conversion : the principles and technology of pyrolysis, gasification & combustion. T. B. Reed. Golden, Colo., Biomass Energy Foundation Press. **3:** 1-25.

Rensfelt, E. (2005). State of the Art of Biomass Gasification and Pyrolysis Technologies 2005. SYNBIOS - The Syngas Route to Automotive Biofuels. Stockholm**:** 48.

Rentech. (2009, 2009). "Rentech - Rialto Project." Retrieved October 26, 2010, from http://rentechinc.com/rialto.php.

Rezaiyan, J. and N. P. Cheremisinoff. (2005). "Gasification technologies a primer for engineers and scientists." from http://public.eblib.com/EBLPublic/PublicView.do?ptiID=263392.

Robinson, P. J. (2009). Langmuir-Hinshelwood-Hougen-Watson (LHHW) Kinetics in Aplus Plus: An Example using Water-Gas Shift and Methanation Kinetics. Bethlehem, PA, Lehigh University**:** 12.

Rochelle, G. T. (2009). "Amine Scrubbing for CO2 Capture." Science **325**(5948): 1652-1654.

Rollins, M. L., L. Reardon, et al. (2002). Economic Evaluation of CO2 Sequestration Technologies Task 4, Biomass Gasification-Based Processing, US Department of Energy**:** 87.

Ross, J. R. H. (2005). "Natural gas reforming and CO2 mitigation." Catalysis Today **100**(1-2): 151-158.

Rubin, E., M. B. Berkenpas, et al. (2007). Technical Documentation: Integrated Gasification Combined Cycle System (IGCC) with Carbon Capture and Storage (CCS). Pittsburgh, PA, Carnegie Mellon University**:** 209.

Salo, K. and A. Horvath (2008). Biomass Gasification in Skive: Opening Doors in Denmark. Renewable Energy World. Tusla, OK, PennWell Publishing Co. **11:** 4.

Sasol (2009). annual review and summarised financial information 2009. Johannesburg, South Africa, Sasol Limited**:** 37.

Schlinger, W. G. (1984). The Texaco Coal Gasification Process. Handbook of Synfuels Technology. R. A. Meyers. New York, McGraw-Hill**:** 22.

Shadle, L. J., D. A. Berry, et al. (2000). Coal Conversion Processes, Gasification. Hoboken, NJ, John Wiley & Sons, Inc.

Shim, H. M., S. J. Lee, et al. (2009). "Simulation of DME synthesis from coal syngas by kinetics model." Korean Journal of Chemical Engineering **26**(3): 641-648.

Spath, P., A. Aden, et al. (2005). Biomass to Hydrogen Production Detailed Design and Economics Utilizing the Battelle Columbus Laboratory Indirectly-Heated Gasifier. Golden, CO, NREL**:** Medium: ED; Size: 161 pages.

Stefano, J. M. (1985). Evaluation and modification of ASPEN fixed-bed gasifier models for inclusion in an integrated gasification combined-cycle power plant simulation. Morgantown, WV, U.S. Department of Energy**:** 61.

Stevens, D. J. (2001). Hot Gas Conditioning: Recent Progress with Larger-Scale Biomass Gasification Systems; Update and Summary of Recent Progress. Golden, CO, National Renewable Energy Laboratory (NREL)**:** Medium: ED; Size: vp.

Steynberg, A. and M. Dry (2004). Fischer-Tropsch technology. Amsterdam ; Boston, Elsevier.

Stone, K. R. (1984). Coal Decomposition Unit Operation Block. Morgantown, WV, Morgantown Energy Technology Center**:** ASPEN fortran subroutine to decompose attributed components to their constituent elements on component's ultimate analysis.

Swisher, J. H., J. Yang, et al. (1995). "Attrition-Resistant Zinc Titanate Sorbent for Sulfur." Industrial & Engineering Chemistry Research **34**(12): 4463-4471.

Torres, W., S. S. Pansare, et al. (2007). "Hot Gas Removal of Tars, Ammonia, and Hydrogen Sulfide from Biomass Gasification Gas." Catalysis Reviews: Science & Engineering **49**(4): 407-456.

Uhde. (2009, Dec 12, 2009). "Uhde GmbH - Technology Profile: PRENFLO." Retrieved Oct 20, 2010, 2010, from http://www.uhde.eu/competence/technologies/gas/techprofile.en.epl?profile=10000003&pagetype=2.

van der Drift, A., H. Boerrigter, et al. (2004). Entrained Flow Gasification of Biomass: Ash behavior, feeding issues, and system analyses. Petten, Energy Research Centre of the Netherlands**:** 58.

van Krevelen, D. W. (1950). "Graphical-statistical method for the study of structure and reaction processes of coal." Fuel **29**(12): 15.

Van Loo, S. and J. Koppejan. (2008). "The handbook of biomass combustion and co-firing." from http://www.netlibrary.com/urlapi.asp?action=summary&v=1&bookid=208922.

Vierheilig, A. A., R. P. Gupta, et al. (2004). Attrition Resistant, Zinc Titanate-Containing, Reduced Sulfur Sorbents. U. S. P. a. T. Office. United States, Research Triangle Institute
Intercat, Inc. **B1:** 17.

Wang, U. (2011). "Report: Range Fuels to Shut Down Plant." Retrieved Feb 8, 2011, from http://www.reuters.com/article/2011/01/14/idUS154341571120110114.

Wang, Y. and C. M. Kinoshita (1992). "Experimental analysis of biomass gasification with steam and oxygen." Solar Energy **49**(3): 153-158.

Warnecke, R. (2000). "Gasification of biomass: comparison of fixed bed and fluidized bed gasifier." Biomass & Bioenergy **18**(6): 489-497.

Weil, B. H. and J. C. Lane (1948). Synthetic petroleum from the synthine process. Brooklyn, Remsen Press Division, Chemical Pub. Co.

Weiss, M. M. (1997). Selection of the Acid Gas Removal Process for IGCC Applications. Second European Gasification Conference: Gasification Technology in Practice. Milan, IChemE**:** 12.

Xylowatt. (2008, April 15, 2008). "XYLOWATT sa - the Belgian manufacturer of wood gasification power plants." Retrieved October 26, 2010, from http://www.xylowatt.com/RadermeckerEN.htm.

Yung, M. M., W. S. Jablonski, et al. (2009). "Review of Catalytic Conditioning of Biomass-Derived Syngas." Energy & Fuels **23**: 1874-1887.

Zhang, H.-t., F.-h. Cao, et al. (2001). "Thermodynamic Analysis for Synthesis of Dimethyl Ether and Methanol from Synthesis Gas." Journal of East China University of Science and Technology **27**(2): 4.

Zhou, J., S. M. Masutani, et al. (2000). "Release of Fuel-Bound Nitrogen during Biomass Gasification." Industrial & Engineering Chemistry Research **39**(3): 626-634.

Zoeller, J. R. (2009). "Eastman Chemical Company's "Chemicals from Coal" program: The first quarter century." Catalysis Today **140**(3-4): 118-126.

Zoeller, J. R., V. H. Agreda, et al. (1992). "Eastman chemical company acetic anhydride process." Catalysis Today **13**(1): 73-91.

Zwart, R. W. R., A. Bos, et al. (2008). Principle of OLGA tar removal system. ECN. E. R. C. o. t. N. (ECN). Petten, ECN. **b-08-022**.

APPENDIX

Appendix A – NREL Thermochemical Mixed Alcohols Model Design Details

A.1 Model Area A100, Feedstock Preparation

The A100 process area is straightforward in concept, where feedstock at a user-defined moisture is dried by direct contact with tar reformer and char combustor flue gas. Moisture removal is accomplished by the use of a FLASH2 block, specified with an atmospheric pressure and an outlet vapor fraction of 0.89, to flash the water from the biomass. The heat stream of the flash block is tied to HEATER block which removes heat from a combined flue gas stream. The dry feedstock moisture is defined in the ASPEN model at 5%, and maintained by the control of a design spec on the HEATER block (QM104B) and a calculator (DRYER). The A100 process area passes the dry biomass feedstock to area A200.

A.2 Model Area A200, Gasification

Area A200 primarily contains the model blocks that define the double-circulating bed indirectly heated BCL gasifier. Figure 32 provides a simplified overview of A200. The gasifier is modeled by reactor block R201, an ASPEN RYield reactor with yield controlled by the Fortran user subroutine BATYD5. This configuration is identical to the one used in the Spath hydrogen plant model. (Spath, Aden et al. 2005)

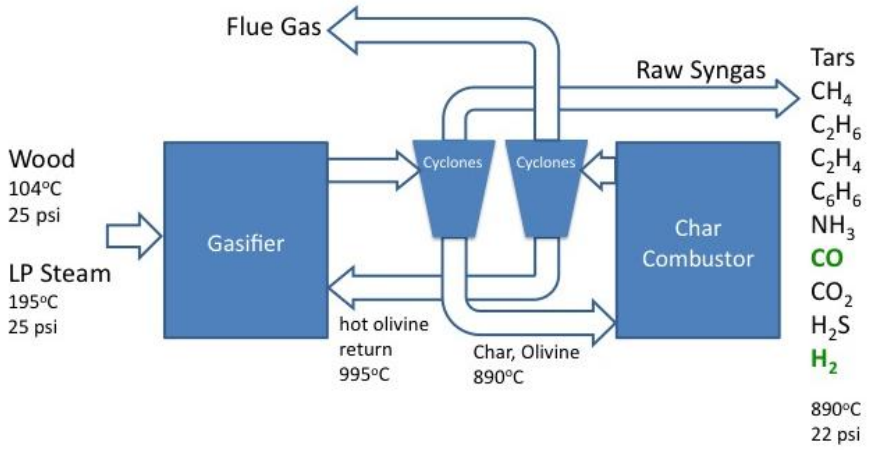

Figure 32. Area A200 gasifier section flow diagram

In order for the R201 RYield block to interface with the BATYD5, eight real number parameters are fed to the user routine. (Table 21)

Table 21. Required parameters passed from R201 to BATYD5. (Craig 1993)

Parameter	Function
1	Gasifier outlet temperature
2	Gasifier outlet pressure
3	Percent of nitrogen in wood going to the char
4	Percent of sulfur in the wood going to the char
5	H/C mass ratio in the char
6	Percent of oxygen in the wood going to the char
7	Fraction reduction CH4 in favor of CO
8	Fraction reduction CH4 in favor of CO2

The BATYD5 is the most current iteration of Craig's wood devolatilization and pyrolysis routine. The routine consists of Aspen interface calls, an implementation of the Bain BCL correlations, an elemental balance to calculate char characteristics, error checking subroutines, and stream/block bookkeeping. The Aspen interface calls allow the BATYD5

user routine to have access to model data stored in a matrix called *the plex*. The flow basis for the syngas is calculated first, and composition versus temperature correlations are generated next.

DGAS = (XDGAS(1) + T1*XDGAS(2) + T2*XDGAS(3)) * ZLBMAF **(28)**

Where XDGAS(n) are the correlation coefficients against temperature, T1 the stream temperature in degrees F, T2 = $T1^2$, and ZLBMAF the pounds of dry, ash-free wood. DGAS is in SCF.

Each syngas component is computed in a similar manner, following the form $\boldsymbol{x = A + BT + CT^2}$, multiplying the result by DGAS from Equation 28. Final char molar flow is arrived at with the same procedure, using temperature correlations and finally multiplying by the computed bone dry wood feed. With final syngas compositions calculated, a set of material balances are carried out to determine the ultimate analysis of the char, along with energy bookkeeping around the gasifier. Figure 33 outlines the FORTRAN logic of the BATYD5 user subroutine.

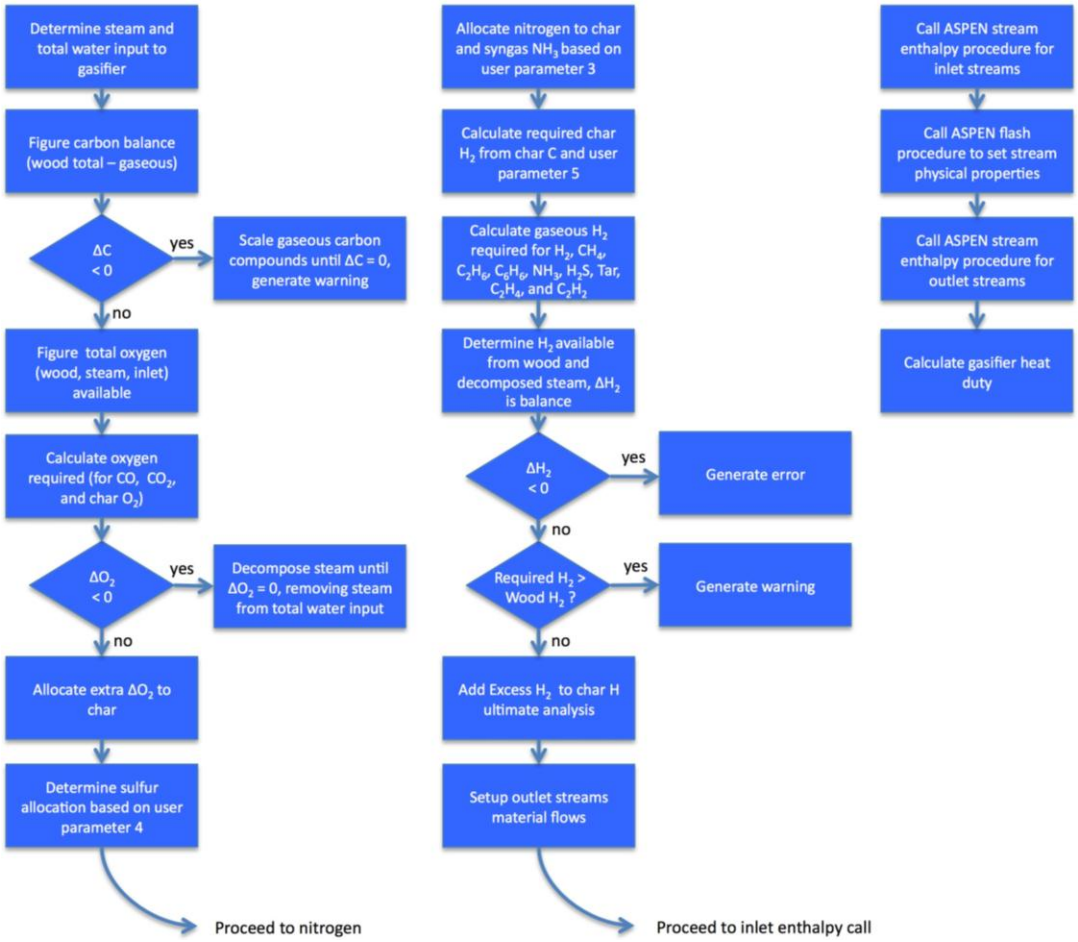

Figure 33. Logic flowchart for BATYD5 user subroutine material balances and energy bookkeeping.

The R201 reactor is controlled to approximately adiabatic conditions through the use of the design spec ADIABAT and the Aspen calculator routine GSTEMP. GSTEMP makes a model connection between the R201 reactor temperature parameter and the temperature parameter passed to the BATYD5 subroutine. The ADIABAT design spec controls the heat duty of R201 to approximately zero by varying the reactor temperature.

However, R201 represents only half of the two-reactor indirectly heated Battelle-style gasifier unit. The combustor unit is modeled by a user-defined Aspen block, USER200A, and a RStoic reactor , R202. USER200A allows USRDC1 user subroutine to convert the non-conventional char stream component to Mixed or CISolid components. The USRDC1 user subroutine calculates the mass flow for each component of the char's ultimate analysis, assigns those values to the appropriate conventional components, and zeroes out the non-conventional char flow. Just as was done in the BATYD5 subroutine, Aspen stream enthalpy calls are made for the input and output streams, and the heat duty for the block derived. After USER200A, the R202 RStoic reactor carries out standard combustion reactions on the conventional input stream components. An Aspen design spec COMBCTL1 sets the combustion airflow, attempting to maintain 20% excess air. Heat required by the USER200A conversion block is taken from the R202 combustion reactor. The Aspen design spec COMBCTL2 attempts to maintain the R202 heat duty at approximately zero by varying the reactor temperature. Cyclone separators for the first pass of syngas cleaning and for char combustor flue gas are simply modeled with standard Aspen Sep blocks. Syngas flow leaving Area A200 is split into a syngas stream ultimately used for mixed alcohols synthesis, and one for heat and power.

A.3 Model Area A300, Gas cleanup

Area 300 encompasses the syngas cleanup systems of the mixed alcohols model. Tar generated in the pyrolysis and gasification process from Area A200 is treated with a catalyzed tar reformer. The tar reformer is designed to crack hydrocarbons to carbon monoxide and hydrogen, and ammonia to nitrogen and hydrogen. Aspirational conversion values are used in the model. (Phillips, Aden et al. 2007) Table 22 shows the hydrocarbon and ammonia conversion values used.

Table 22. Tar reformer aspirational hydrocarbon and ammonia conversion. (Phillips, Aden et al. 2007)

Compound	Aspirational Conversion
Methane	80%
Ethane	99%
Ethylene	90%
Tar	99.9%
Benzene	99%
Ammonia	90%

An Aspen REquil reactor (R303A) is used to simulate the tar reformer. Reaction extent for reforming the compounds listed in Table 22 is controlled by the TARCRACK calculator. The tar reformer catalyst is modeled with equilibrium water-gas shift activity, setup using a temperature approach reaction specification type with 0˚F differential.

Recovered waste alcohols from the alcohol separation process are cracked in the tar reformer to help improve the CO conversion rate. R303A alcohol reforming reactions are also modeled using the temp approach. Reforming steam is controlled by the REFSTM

calculator, which attempts to set the steam ratio to 3.0 mol H_2O to 1 mol C. (Phillips, Aden et al. 2007)

Energy to drive the reforming reactions is derived from the tar reformer catalyst regenerator, R301A. The catalyst regenerator is modeled in two parts, using an adiabatic RStoic reactor with default Aspen combustion reactions and an outboard heat exchanger (R301B) to tie back to the tar reformer. Unconverted syngas from the fuel synthesis area is supplied to the catalyst regenerator for base loading fuel value. Raw syngas from area A200 is variably allocated to R301A to allow control of the R301B reactor outlet temperature. Manual control of the flue gas temperature from R301B can be accomplished with design spec R301BTEM.

An important consequence of this feedback loop is that the overall heat balance for the model can be adjusted by varying the design spec target temperature, and that this adjustment has ramifications in mixed alcohols product yield. The NREL mixed alcohols model was conceived as a system needing no additional energy input. Area A900 calculates the overall plant energy balance in horsepower, which can be manually set to zero by trial-and-error adjustment of the R301B outlet temperature. The post-R301B flue gas heater block H311 cools the flue gas further, and is tied to the Aspen design spec QBALANCE. QBALANCE examines all major model heat sources and sinks and attempts to reconcile them by altering the makeup of high-pressure steam to the turbine section of Area A600. Changes in turbine shaft work (W_{gen}) in turn affect the overall plant energy balance. Additionally, the cooled regenerator flue gas following H311 is used as a heat source for the

direct contact biomass dryer in area A100, controlled by the QM104B design spec. QM104B attempts to hold the heat duty of the biomass dryer to zero by adjusting the cooling temperature parameter of the H311. In this way, biomass feedstock moisture will have a direct influence of the overall heat and work balance of the model, wetter material requiring higher temperature flue gas to meet the moisture removal specifications called for the in DRYER calculator (default 5% moisture). High temperature flue gas leaves less ejected heat at H311 for the QBALANCE calculator.

Tar reformed syngas is further cleaned with a simulated quench followed by an acid gas scrubber. Syngas quenching is simply modeled with an Aspen two outlet flash block and heater block, reducing the syngas temperature and removing all solid components such as ash and olivine. Quench water flow is controlled by the design spec QUENCHFL and quench captured solids moisture content is set by the SLUDGE calculator. Post-quench syngas is compressed through a shaft driven five-stage polytropic compressor block, with fixed outlet discharge and interstage coolers. Acid gas removal is accomplished with a conventional amine scrubber system, whose model consists of two simple Sep blocks, the AMREBOIL, CO2SPEC, and SULFAD design specs, and the AMFLOW calculator. The amine reboiler steam flow is controlled with the AMREBOIL spec, the synthesis feed syngas CO2 fraction by CO2SPEC, and H_2S fraction by SULFAD. Monoethanolamine flow to the scrubber is calculated by AMFLOW.

The acid gas waste stream that is stripped from the syngas is reduced in pressure from 415 to 35 psia and heated slightly ahead of the A300S sulfur removal area implemented in

the model. The sulfur removal system chosen by Phillips et al was a standard LO-CAT iron catalyzed conversion of H_2S to elemental sulfur. The LO-CAT process was modeled simply as a system of three splits (Sep blocks), an RStoic reactor block, a design spec and two calculators. The initial split is controlled by the calculator H2SSPLIT and selectively removes all H_2S from the acid gas waste stream. The resultant sulfur-free gas is sent back to the tar reformer to recapture the CO_2 carbon for the process. The RStoic reactor converts all of the H_2S to water and elemental sulfur, with the reaction air controlled by the calculator DESULF. The final split captures all the element sulfur as a waste/product stream, with the balance of the split stream to be exhausted to the atmosphere.

A.4 Model Area A400, Mixed Alcohol Synthesis

Area A400 comprises the mixed alcohols model synthesis section. Clean, sulfur-free syngas is further pressurized in A400 to 1000 psia, using a shaft-driven three-stage polytropic compressor block with integral intercoolers. Shaft work "streams" from the high pressure syngas compressor are brought to the plant work balance blocks of area A900. Intercooler heat load streams are similarly added to the model's QBALANCE calculator. High pressure syngas is preheated by heat exchange with char combustor (R202) flue gas to 300˚C and reacted in the synthesis reactor blocks. The model design for synthesis is based on an alkali-modified MoS_2 Fischer-Tropsch catalyst, chosen for sulfur and CO_2 tolerance. (Phillips, Aden et al. 2007) The synthesis reactions are carried out with two reactor blocks, R410 and

R410WG. R410 is an RStoic reactor block and accomplishes alcohol synthesis with a set of series-run reactions that have specified fractional conversions, chosen to give a fixed, prescribed product alcohol distribution. R410WG water-gas shifts any remaining CO and H_2O after the primary synthesis reaction. Table 23 details the aspirational alcohol distribution that guided the setup of reaction conversions used in R410 (shown in Table 24). Because the reactions are run sequentially, water-gas shift reactions are repeated at Equations 1, 5, 9, and 14, limited by the water available at that point in reaction list. Reactions 2 – 4 model the catalyzed chain growth of alcohols recycled from the A500 alcohol separation and purification area. The fractional conversion of Reaction 6 provides the means to control the single pass CO conversion to 60% as specified in the project model design. Reaction 8 allows the model to approximate the catalytic methanol degradation activity that is attributed to the MoS_2 catalyst used in the project. Likewise, reactions 11, 13, 16, and 17 model catalytic dehydration of alcohols to alkanes. Finally, the overall alcohol distribution is affected by the fractional conversions from reactions 7, 10, 12, and 15.

Table 23. Aspirational mixed alcohols product distribution used in the NREL model, before purification and methanol recycle. (Phillips, Aden et al. 2007)

Alcohol	Weight %
Methanol	5.01
Ethanol	70.66
Propanol	10.07
Butanol	1.25
Pentanol ≥	0.17
Others	10.98
Water	1.86
Total	100.00

The R401WG REquil equilibrium reactor block simulating water-gas shift activity follows the R401 primary synthesis reactor to round out the catalyzed synthesis reactions. The product gas from the water-gas shift section of the synthesis reactor pair is cooled with a series of heat exchangers for process heat recycle, and the raw alcohols condensed out from the unreacted syngas. Unreacted syngas is decompressed through an Aspen turbine/ compressor block to capture shaft work, and sent to the catalyst regenerator in the tar reformer system to offset raw syngas required to maintain the R301B reactor temperature.

Table 24. NREL alcohol synthesis reactor (R401) fractional conversion parameters. RStoic Reactions are carried out sequentially. (Phillips, Aden et al. 2007)

R401 Reaction ID	Chemical Reaction	Fractional
1	$CO + H_2O \rightarrow H_2 + CO_2$	0.98 of H_2O
2	$CO + 2H_2 + C_3H_7OH \rightarrow C_4H_9OH + H_2O$	0.98 of C_3H_7OH
3	$CO + 2H_2 + C_2H_5OH \rightarrow C_3H_7OH + H_2O$	0.98 of C_2H_5OH
4	$CO + 2H_2 + CH_3OH \rightarrow C_2H_5OH + H_2O$	0.999 of CH_3OH
5	$CO + H_2O \rightarrow H_2 + CO_2$	0.98 of H_2O
6	$CO + 2H_2 \rightarrow CH_3OH$	0.205 of CO
7	$CO + 2H_2 + CH_3OH \rightarrow C_2H_5OH + H_2O$	0.75 of CH_3OH
8	$CH_3OH + H_2 \rightarrow CH_4 + H_2O$	0.7 of CH_3OH
9	$CO + H_2O \rightarrow H_2 + CO_2$	0.98 of H_2O
10	$CO + 2H_2 + C_2H_5OH \rightarrow C_3H_7OH + H_2O$	0.1 of C_2H_5OH
11	$C_2H_5OH + H_2 \rightarrow C_2H_6 + H_2O$	0.98 of H_2
12	$CO + 2H_2 + C_3H_7OH \rightarrow C_4H_9OH + H_2O$	0.1 of C_3H_7OH
13	$C_3H_7OH + H_2 \rightarrow C_3H_8 + H_2O$	0.1 of C_3H_7OH
14	$CO + H_2O \rightarrow H_2 + CO_2$	0.98 of H_2O
15	$CO + 2H_2 + C_4H_9OH \rightarrow C_5H_{11}OH + H_2O$	0.1 of C_4H_9OH
16	$C_3H_7OH + H_2 \rightarrow C_4H_{10} + H_2O$	0.01 of C_3H_7OH
17	$C_5H_{11}OH + H_2 \rightarrow C_5H_{12}^{+1} + H_2O$	0.01 of $C_5H_{11}OH$

A.5 Model Area A500, Alcohol distillation and dehydration

Area A500 comprises the model systems that remove most of the water from the synthesis product stream, and that separate the mixed alcohol distribution into methanol, ethanol, and higher alcohols. Condensed raw alcohols from the synthesis section are treated with a molecular sieve system to remove 99.5% of the water. (Phillips, Aden et al. 2007) The molecular sieve trains are modeled with the C-MSWAT1 calculator controlling the water split on a Sep block. A side stream of methanol recovered from subsequent distillation is used to flush the mole sieve system, and is recycled to the R301 tar reformer catalyst

regenerator for fuel. Two Aspen RADFRAC blocks (rigorous distillation column models) simulate a distillation column that separates out alcohols greater than ethanol and a column that splits methanol from the final product ethanol. Methanol recovered from the second distillation column is recycled back to the inlet of the synthesis reactor to optimize ethanol production.

A.6 Model Area A600, Steam System

The NREL mixed alcohols model integrates a steam generation, turbine, and condensate recovery system to simulate the heat and power requirements of the biorefinery plant. The A600 Steam System Area is composed of several subsystems, one for boiler feedwater, steam generation, steam turbines, and water recycle (condensate recovery). (Phillips, Aden et al. 2007)

The boiler feedwater system is modeled in a straightforward manner, utilizing Aspen tank, pump, and heater blocks to allow for later equipment sizing and to account for steam system power requirements. Deaerator-heating is accomplished with a heater and a two-outlet flash block. On the other end of the steam cycle is the condensate recovery system, which is comprised of basic mixing and pumping unit operations. Boiler feedwater makeup is controlled by the STMMAKE calculator.

Steam generation is also a simple model subsystem, utilizing a series of heater blocks to the boiler feedwater heating and superheating that takes place during heat exchange with syngas and the synthesis reactor in the process. Rather than make direct “heat stream”

connections between the model boiler feedwater heat sources and their respective process counterparts, the required heat input is added to the heat sink side of the QBALANCE energy-closure calculator. Boiler feedwater high pressure pumping is modeled with one single stage Aspen pump block, with a fixed discharge pressure of 930 psi. Boiler feedwater chemical makeup is also handled by the STMMAKE calculator. A formal steam drum is not modeled, and generated steam is not directly connected to the rest of the model. Blowdown from the steam drum uses a simple split (SEP) block.

Overall process heat closure is controlled by the QBALANCE design spec, which performs a heat balance on all major heat sources and sinks, and varies a virtual high pressure steam flow input accordingly. The QBALANCE design spec effectively separates the model-generated high pressure steam from the rest of the process by providing an isolated steam source. This was undoubtedly done to simplify model convergence issues.

The final subsystem of the A600 area simulates the process' turbo-generator. The turbine is modeled as two-extraction condensing turbine, using three Aspen turbine blocks tied together with a shaft work "stream." The first extraction is 176 psia, the second at 50 psig, and the remainder of the steam is sent to a heater block serving as a model condenser. Low pressure steam is routed directly to individual process users with a split block controlled by the STMDEM calculator.

A.7 Model Areas A700 and A900, Ancillary systems

Cooling tower service for process cooling water is processed in area A700, primarily comprised of Aspen Sep and heater blocks that allow the cooling water system model to be controlled by the design spec CWTEMP, and the calculators CWAIRI, CWBAL, and CWDUTY. Area A900 provides a means for performing a work balance across the entire biorefinery plant model. Motor, fan, and pump work requirements are summed in each process area with an Aspen calculator, the total of which is balanced against the shaft work generated in the steam turbines and the unreacted syngas expander from area A400. The overall work balance for the plant is calculated in A900 as the work "stream" W_{net}. As mentioned previously, W_{net} is manually adjusted to approximately zero by setting the tar reformer catalyst regenerator flue gas temperature in the R301BTEM design spec.